THE LEIDENFROST PHENOMENON FOR BINARY LIQUID SOLUTIONS

By

EDWARD S. GODLESKI

Bachelor of Science in Chemical Engineering
Lehigh University
Bethlehem, Pennsylvania
June, 1958

Master of Science
Cornell University
Ithaca, New York
February, 1961

Submitted to the Faculty of the Graduate College of
the Oklahoma State University
in partial fulfillment of the requirements
for the degree of
DOCTOR OF PHILOSOPHY
July, 1967

THE LEIDENFROST PHENOMENON FOR

BINARY LIQUID SOLUTIONS

Thesis Approved:

Kenneth J Bell
Thesis Adviser

John B West

Jerald D Parker

Wayne C Edmister

N N Durham
Dean of the Graduate College

PREFACE

The study of film boiling of discontinuous masses on a flat plate has largely been confined to pure liquids. This work extends the analysis to binary solutions and proposes a theoretical model by which the rate of evaporation and the change in composition of binary liquid drops can be computed. A technique was developed for determining the lower limit of stable film boiling which resulted in Leidenfrost temperatures lower than were previously obtained.

Many people aided me in both my graduate studies and thesis. Yet it was largely due to the help given me by two persons that I was able to accomplish this work. The first is Dr. Kenneth J. Bell who served as my thesis advisor. He possesses the ability to know when to push and when to let one coast. But most important is his patience, a virtue I have put to the test many times. The other is Dale Scott, Director of the Computer Center, Bobbie Brooks, Inc. Dale was more than willing to spend the time necessary to convert their IBM 1410 computer to handle my program and then spent several weekends testing the program and then running data.

I am grateful to the Ford Foundation and the Phillips Petroleum Company for the financial support they gave me. It was because of the Forgivable Loan Program of the Ford Foundation that I was able to take a leave of absence from teaching to

pursue my graduate studies on a full-time basis. The Phillips Petroleum Company extended additional financial support to me through a fellowship.

The Bobbie Brooks, Inc. generously allowed me the use of their computer facilities for debugging and running my computer program.

My graduate committee consisted of Dr. Kenneth J. Bell, Chairman, Dr. John B. West, and Prof. Wayne C. Edmister, all in Chemical Engineering, and Dr. Jerald D. Parker from Mechanical Engineering. I thank them for their wise counsel and pleasant nature.

TABLE OF CONTENTS

LIST OF TABLES

LIST OF FIGURES

CHAPTER I

INTRODUCTION

The Leidenfrost Phenomenon is the film boiling of discontinuous liquid masses on a flat surface. Analysis of this type of boiling has gone on for many years, though in a somewhat haphazard manner. Only recently has a significant effort been made to investigate fully all aspects of the Phenomenon. This activity has resulted in a better understanding of the mechanisms involved and an elimination of some of the ambiguity resulting from different names being used to describe the same phenomena.

Boiling can be divided into three regions depending upon the manner in which heat transfer occurs and the way vaporization takes place: film, transition, and nucleate boiling. Film boiling is that region in which the liquid is separated from the heating surface by a film of its own vapor. Solid-liquid contact rarely if ever occurs and vapor generation takes place at the vapor-liquid interface. In transition boiling liquid jets periodically but only momentarily touch the heating surface. These contacts are a result of disturbances on the liquid surface caused by the instability of the liquid-vapor interface. In nucleate boiling liquid continually adheres or wets the surface except at the sites of bubbly formation. During stable film boiling the surface temperature remains fairly constant.

while in transition boiling the local surface temperature will drop suddenly where the liquid comes in contact with the heated surface.

Small liquid masses (usually of volumes less than about 0.05 ml) evaporating in film boiling assume a nearly spheroidal shape. These liquid drops float above the hot surface or plate on their vapor film The most common example of this behavior occurs when drops of water are sprayed on a hot frying pan, and they bounce and glide about the surface. Masses of volumes greater than about 0.05 ml are noticeably flattened out on the plate; for volumes greater than about 0.4 ml for most ordinary liquids or greater than about 1.5 ml for water, vapor bubbles start breaking through the center of the mass. For sufficiently large masses, the mechanism becomes essentially identical to film boiling from a completely submerged surface. The surface temperature at which the vapor film breaks down at least occasionally and the liquid touches the hot surface is termed the Leidenfrost point.

Experimental studies of the evaporation rate for both drops and extended masses have been done by Gottfried (12), Lee (19), and Patel (21). Their work was limited to pure liquids. A theoretical model describing the evaporation process of spherical drops on a hot surface was proposed by Gottfried and Bell (13), and later expanded and modified by Lee and Bell (14).

The purpose of this investigation was to extend the analysis of the Leidenfrost Phenomenon to binary liquid solutions. Total evaporation times for initial liquid volumes ranging from 0.006 to 8 cm^3

were measured for various plate temperatures. The Leidenfrost point and the smallest liquid volume for which vapor bubbles break through the mass were determined. Liquid composition changes during evaporation were measured. A theoretical model is presented for the evaporation of binary liquid drops.

CHAPTER II

LITERATURE SURVEY

Many studies of the Leidenfrost Phenomenon for pure liquids have appeared in the literature and a brief review of only the most recent is presented. Gottfried, et al. (14) have presented evaporation time data for small droplets of five ordinary liquids and have proposed an analytical model which is in fair agreement with the data. The model postulates that heat is transferred to the droplet by conduction from the plate below the drop through the supporting vapor film and by radiation from the plate; mass is removed by diffusion from the upper surface and by bulk evaporation from the lower surface; the drop is supported by the excess pressure above atmospheric in the flowing vapor film under the droplet. This paper also contains a brief historical survey of the Leidenfrost Phenomenon starting with the work of J. G. Leidenfrost in 1756.

Baumeister, et al. (2) analyzed the evaporation rate of larger masses, expecially those smaller than the critical size for bubble breakthrough and obtained good agreement between theory and experiment. Patel and Bell (22) obtained evaporation rate data for masses up to 10 ml; they also studied bubble dynamics in the 10 ml masses photographically and found that the results were consistent with the submerged surface film boiling studies of Hosler and Westwater (15) and with the predictions of the Taylor instability theory.

The recent works of Baumeister, et al. (3) and Wachters, et al. (32) substantiate the conclusions reached in this study regarding the results obtained by decreasing the heating surface temperature during evaporation. This "transition" plate temperature technique results in an extension of the film boiling regime to a plate temperature near the liquid saturation temperature, and therefore a shortening of the transition boiling region.

Apparently the only study to date of the Leidenfrost Phenomenon for liquid mixtures is that by Tamura and Tanasawa (26) who studied the total evaporation time of liquid drops on a hot surface at temperatures up to 900°C. Ten liquids were used including the pure substances ethanol, benzene, and water and the mixtures, gasoline, kerosine, and a heavy oil. Their apparatus consisted of a 16 cm diameter stainless steel plate with a concave surface. Small drops were placed on the plate and the evaporation process was observed and photographed. Plate temperatures starting about 50°C below the liquid boiling point and ranging beyond the point where the combustible liquids ignited resulted in evaporation curves that covered all regions of boiling. Since the initial drop sizes in all but one case were smaller than those used in this investigation, it is not possible to compare actual evaporation data. But the general shape of the curves is the same. For the one case, benzene, where the drop sizes were in the same range, the total evaporation time as a function of plate temperature agrees well with the present work.

CHAPTER III

EXPERIMENTAL APPARATUS

The basic components of the apparatus used in this investigation were a stainless steel plate resting on ceramic heating elements, a potentiometer and a Variac. The apparatus is shown schematically in Figure 1.

Two plates were used in the evaporation studies. Each plate had five thermocouples imbedded below the top surface to measure the plate surface temperature. A 4-inch diameter plate shown in Figure 2 was used for the experiments with drops and a 7-inch diameter plate with a 3° slope of the sides shown in Figure 3 was used for the extended masses. The smaller plate was type 304 stainless steel, 3/16 inch thick in the center test region, while the larger plate was type 316 stainless steel with a center test region about 1/2 inch thick. The sloping sides of the smaller plate kept the liquid drops on the flat center portion of the plate where the thermocouples were imbedded. Because the largest drops studied on this plate were about 0.03 ml, they approximated a sphere and the sides of the plate had little effect other than to keep the drop confined to the center portion of the plate. The liquid masses studied with the larger plate varied from 0.1 to 8 ml. For these large volumes the liquid often covered a third of the flat

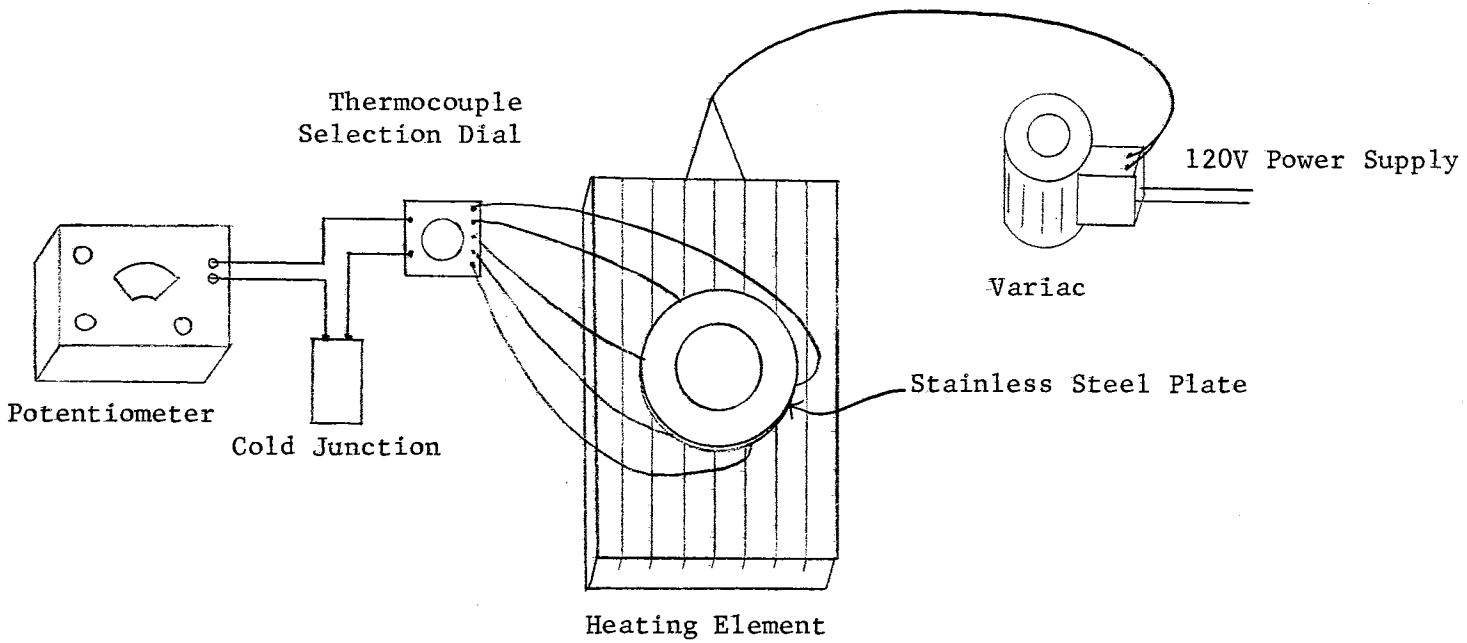

Figure 1. Schematic Diagram of Apparatus

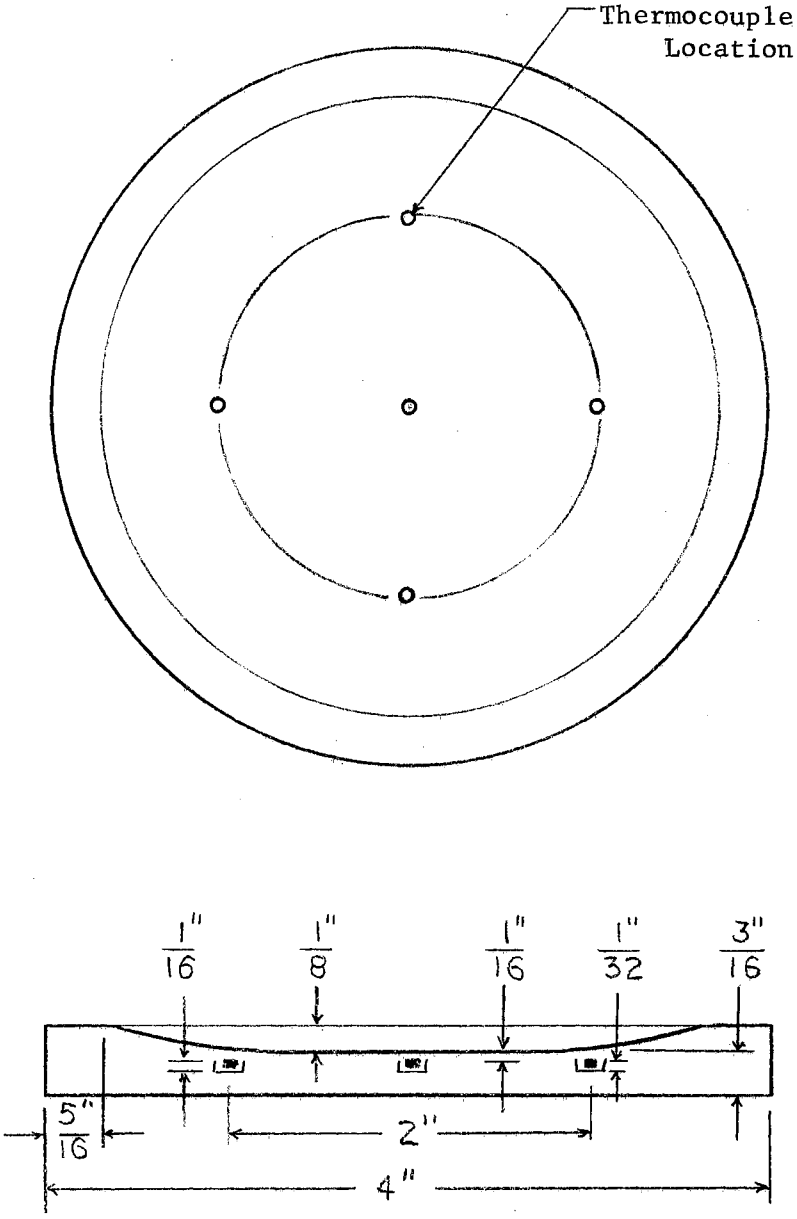

Figure 2. Diagram of 4-inch Stainless Steel Plate

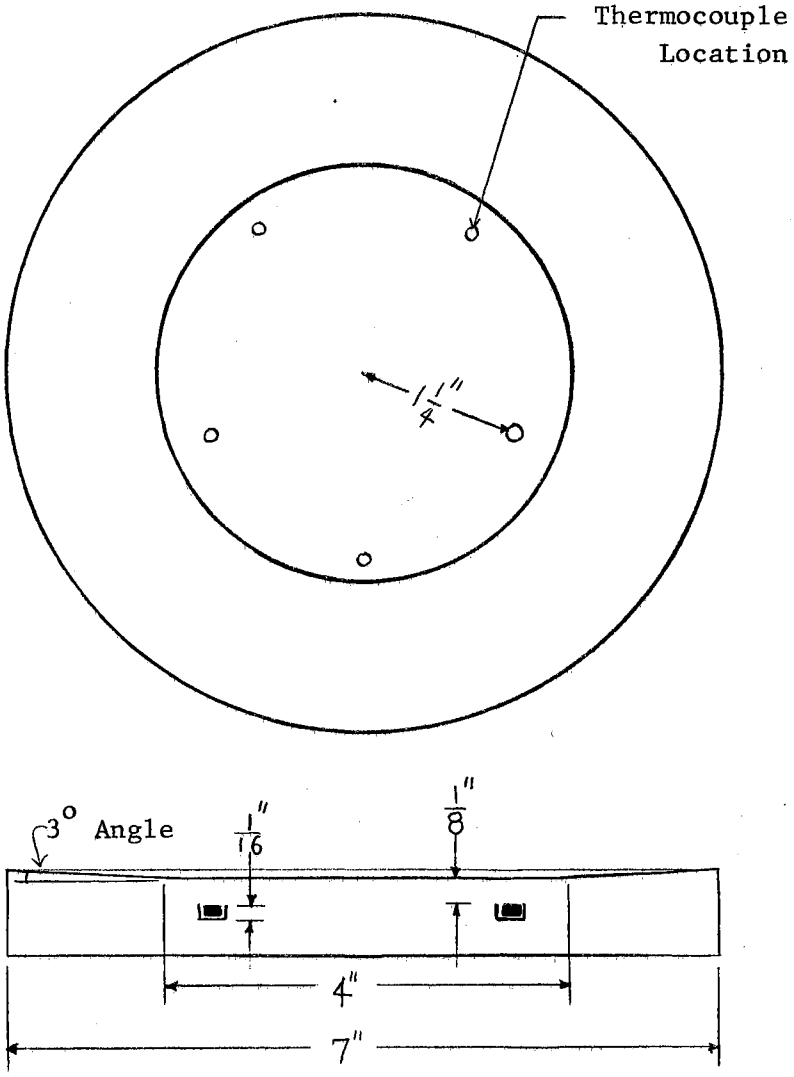

Figure 3. Diagram of 7-inch Stainless Steel Plate

test surface of the plate. From experiments with plates of steep sloping sides, it was found that both the total evaporation time and the maximum volume of liquid stable against bubble breakthrough are affected if the liquid is not allowed to assume its unconstrained shape. The 3^{o} slope for the sides of the larger plate was adequate for retaining the liquid on the plate, and the deformation of the peripheral outline of the liquid was minimal.

The thermocouples used for both plates were chromel-alumel (24 gauge). The potential developed by the heated thermocouple bead was read with a millivolt potentiometer (Leeds and Northrup Company, Philadelphia, Pennsylvania, Cat. No. 8690) that gave readings to $\pm$ 0.01 millivolts or one-fourth of a degree Centigrade. An ice-water bath was used as the reference junction. The thermocouples were sealed to the thermocouple wells with a cement of high thermal conductivity, Alundum Cement RA172 (Central Scientific, No. 11460B). The lead wires were encased in ceramic insulating ducts that were then sealed to the grooves beneath the plate with the Alundum Cement.

The four-inch, stainless steel plate rested on top of a 550 watt cermaic heating unit (Hevi-Duty Electric Company, Watertown, Wisconsin, Model 54 KTS). The seven-inch plate was heated by two, 650 watt Model 54-KSS heating elements connected in parallel and placed side by side. The temperature was controlled with an alternating current transformer (Variac). The surfaces of the plates were given a high polish and heated to 500^{o}C for several hours to allow the bronze-colored oxide film to form. This film is stable and very smooth and required no further polishing.

Masses of 0.1 to 0.9 ml were produced by a calibrated microliter syringe, while masses from 1 to 8 ml were produced by a calibrated 10 ml pipette. The initial liquid volumes produced in this manner were reproducible to within an average of $\pm$ 3 percent for the pipette and within an average of $\pm$ 1 percent for the microsyringe (21).

The liquids used to prepare the mixtures were reagent grade benzene, ethanol, and toluene, and distilled water.

CHAPTER IV

EXPERIMENTAL PROCEDURE

Adjusting The Plate Temperature

Before beginning a series of experiments and while the plate was at room temperature, the surface was polished with Metallographic Emery Paper, fineness #410 (Fisher Scientific Company, Cat. No. 90545). If experimentation lasted several hours periodic cleaning of the plate surface was necessary to remove any dust that might settle there. This was accomplished with fine steel wool and compressed air.

At the start of a run, the Variac was turned on full and a metal cover was placed over the plate. This allowed the plate to reach the desired operating temperature in fifteen to thirty minutes. When the plate temperature was within ten or twenty degrees of the desired value, the cover was removed and the Variac turned down to the correct value for that operating temperature. No further power adjustment was required for the 4-inch plate once the desired plate temperature was attained. The control of the heat flux to the 7-inch plate was more complicated.

The 7-inch plate was used with liquid volumes up to 8 ml. The heat loss from the plate due to the evaporating fluid would often lower the plate temperature ten or fifteen degrees. The

greatest loss of heat from the plate occurred when the liquid was first placed on the plate. There was a sudden drop in plate temperature followed by a slow, steady decrease. The temperature would reach a minimum and then increase. The initial plate temperature would not be attained until after all the liquid had evaporated. To compensate for this effect, the plate was kept in a state of dynamic heating. By adjusting the Variac so that the plate temperature was continually increasing and placing the liquid on the plate at a plate temperature slightly above the desired value, the initial temperature drop which usually occurred in less than five seconds would decrease the temperature to the desired level. The decreasing plate temperature was then compensated for by the increasing heat flux to the plate. This technique required constant adjustment of the Variac but was relatively simple once sufficient experience had been acquired. By this method the plate temperature range during the entire evaporation process, including the initial plate temperature, never varied more than six Centigrade degrees. The variation in plate temperature during all but the first few seconds of the run was less than two Centigrade degrees.

The plates were heated from the bottom and lost heat from the top. Therefore, a temperature gradient existed within the plate. The upper surface of the plate was cooler than the center. With the thermocouples below the surface, their readings were probably higher than the actual plate surface. However, a rough calculation of rate of heat loss from the plate surface to

the air indicates that at the most the surface temperature should not be more than five degrees below the thermocouple readings.

Placing the Liquid on the Plate

The 4-inch plate was used for drops of various sizes, placed on the plate with a hypodermic needle and syringe assembly. In the case of the 7-inch plate, liquid volumes of 1 ml and larger were placed on the plate with a 10 ml differential pipette; and for volumes below 1 ml, a microliter syringe with an adjustable plunger was used.

Five hypodermic needles of various diameters were used to obtain a range of drop sizes. The total evaporation time recorded was the time measured from when the drop first touched the plate to when the last bit of liquid vaporized.

With the microliter syringe the plunger could be set to deliver a predetermined amount of liquid. One of the larger size needles was used with this syringe. Its size was unimportant since volumes of 0.1 ml and larger were used. In the case of the 10 ml pipette, a propipette was attached to the top of the pipette to control the amount and rate of liquid delivery. Because the discharge time of the liquid from the 10 ml pipette was several seconds, the measurements of total evaporation time started when half of the liquid had been discharged from the pipette. If the drop shattered upon hitting the plate or picked up dirt at any time during the evaporation, the run was rejected. The total

evaporation time for drops was determined from the average of five runs; the individual evpaoration times were usually within $\pm$ 0.3 seconds independent of drop size and plate temperature, with a maximum variation of $\pm$ 0.5 seconds. For extended masses, the total evaporation time was reported as the average of three runs, and the individual values were within $\pm$ 2 seconds. If bubble breakthrough occurred during the evaporation, then the time required for the volume of liquid to evaporate to a size where bubble breakthrough no longer occurred was noted. For large liquid volumes the total evaporation time was somewhat insensitive to the initial liquid volume. For the 8 ml volumes, a range of $\pm$ 0.1 ml in initial liquid volume resulted in no perceptible change in total evaporation time.

The highest plate temperatures were near the upper limit of the heating coils beneath the plate. This was about 450°C for the 7-inch plate and about 410°C for the 4-inch plate. The lower temperature limit depended upon the composition of the liquid. Runs were made at progressively lower plate temperatures until the liquid evaporated in the transition or nucleate boiling regime. This lower limit was easily recognized and reproducible. The liquids sizzled or splattered or visibly wet the plate surface. Whereas the total evaporation time had been increasing as the plate temperature was lowered, the evaporation time now dropped to a fraction of the previous value. The plate temperature that resulted in the highest liquid evaporation time was considered the Leidenfrost point for that liquid.

The total evaporation time versus plate temperature data are presented in Appendix C for drops and Appendix D for extended masses.

Determination of the Composition of the Evaporating Solutions

The determination of the liquid composition during a run required the sampling of the liquid while it was evaporating on the plate. For a given initial liquid mass, composition, and plate temperature, samples were obtained at various time intervals during the evaporation. A new liquid mass was used for each sampling. A sample was obtained by inserting the tip of the needle of a microliter syringe into the evaporating liquid and withdrawing some of the liquid. For drops, all the liquid was drawn into the syringe and the sample was analyzed in a gas chromatograph. Because only binary solutions were used, the chromatographic analysis was simple. Peak heights were measured and the ratio of the two peak heights was compared to those obtained from the solutions of known composition used to calibrate the chromatograph, as in Figure 4. The data then consisted of the liquid mole fraction at a given fraction of the total evaporation time. The mole fractions reported in Appendix E represent the average of three liquid samples, the separate peak height ratios being averaged to obtain the mole fraction. The separate ratios were within $\pm$ 2 mole percent and usually $\pm$ 1 mole percent.

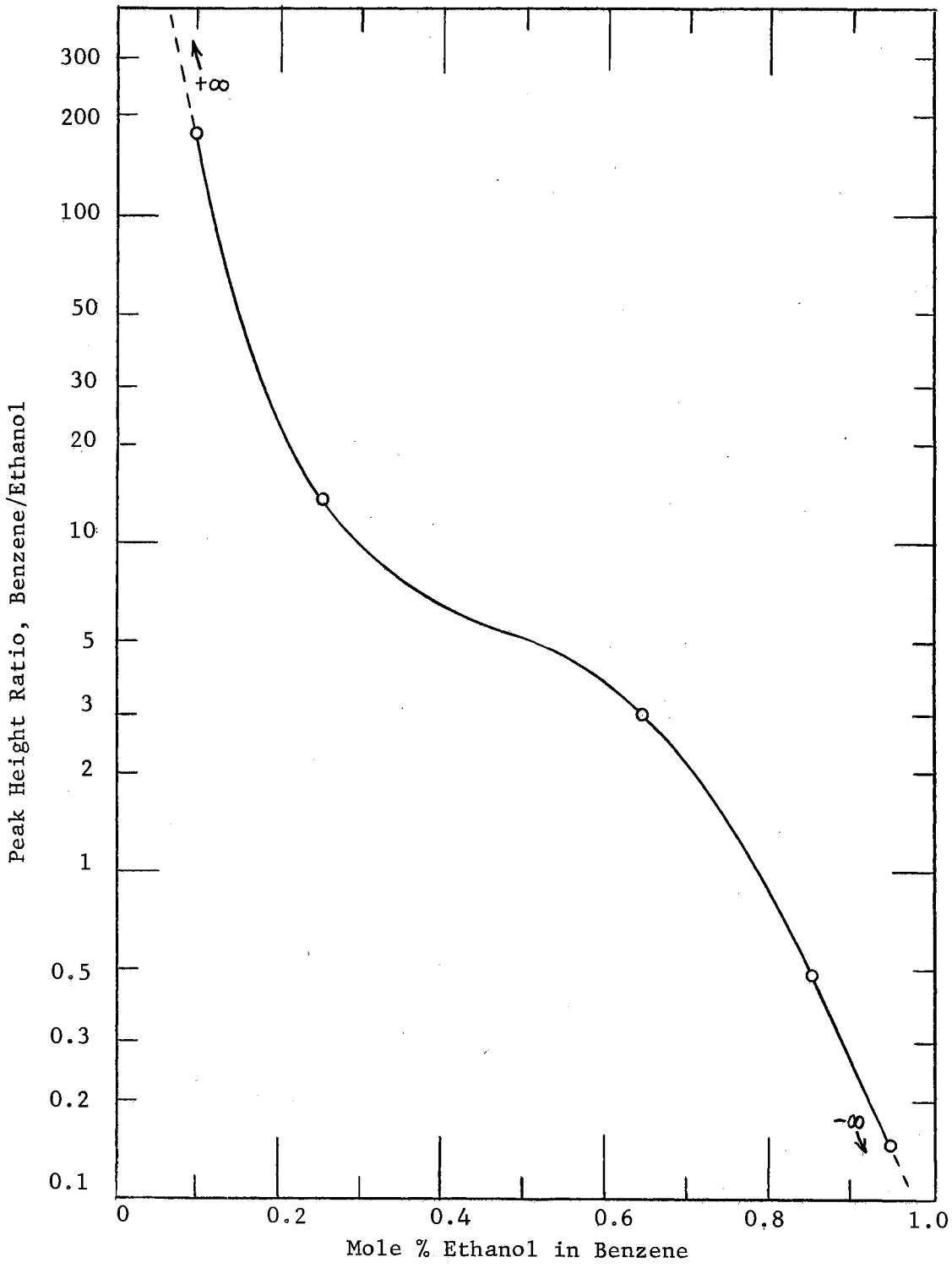

Figure 4. Chromatographic Calibration Curve for Ethanol-Benzene Solutions

To analyze the effect of evaporation on liquid composition, the liquid mole fraction as a function of the mass fraction of liquid evaporated was required. This was obtained from a plot of the initial liquid mass versus the time for the mass to completely evaporate for a given initial liquid composition and plate temperature. An example of such a plot is shown in Figure 5 (the experimental data are plotted on log-log paper since this gives a relatively straight curve). A plot of instantaneous liquid composition as a function of the time after deposition is drawn from the data obtained by sampling the liquid during evaporation. This is shown in Figure 6. From this plot, the difference in time between total evaporation and a given time after deposition is chosen (the line A in Figure 6). This time increment, plotted on Figure 5 (the triangle), gives the liquid mass for that evaporation time and liquid composition. The mass fraction of liquid evaporated can then be determined.

Leidenfrost Point Determination by the Transient Plate Temperature Method

The usual procedure for obtaining the Leidenfrost point of a liquid was to determine the lowest plate temperature at which a liquid could be placed on the plate and still evaporate in film boiling. A great deal of difficulty was encountered in determining this temperature for some of the liquids investigated. To circumvent the problem, a technique was used whereby

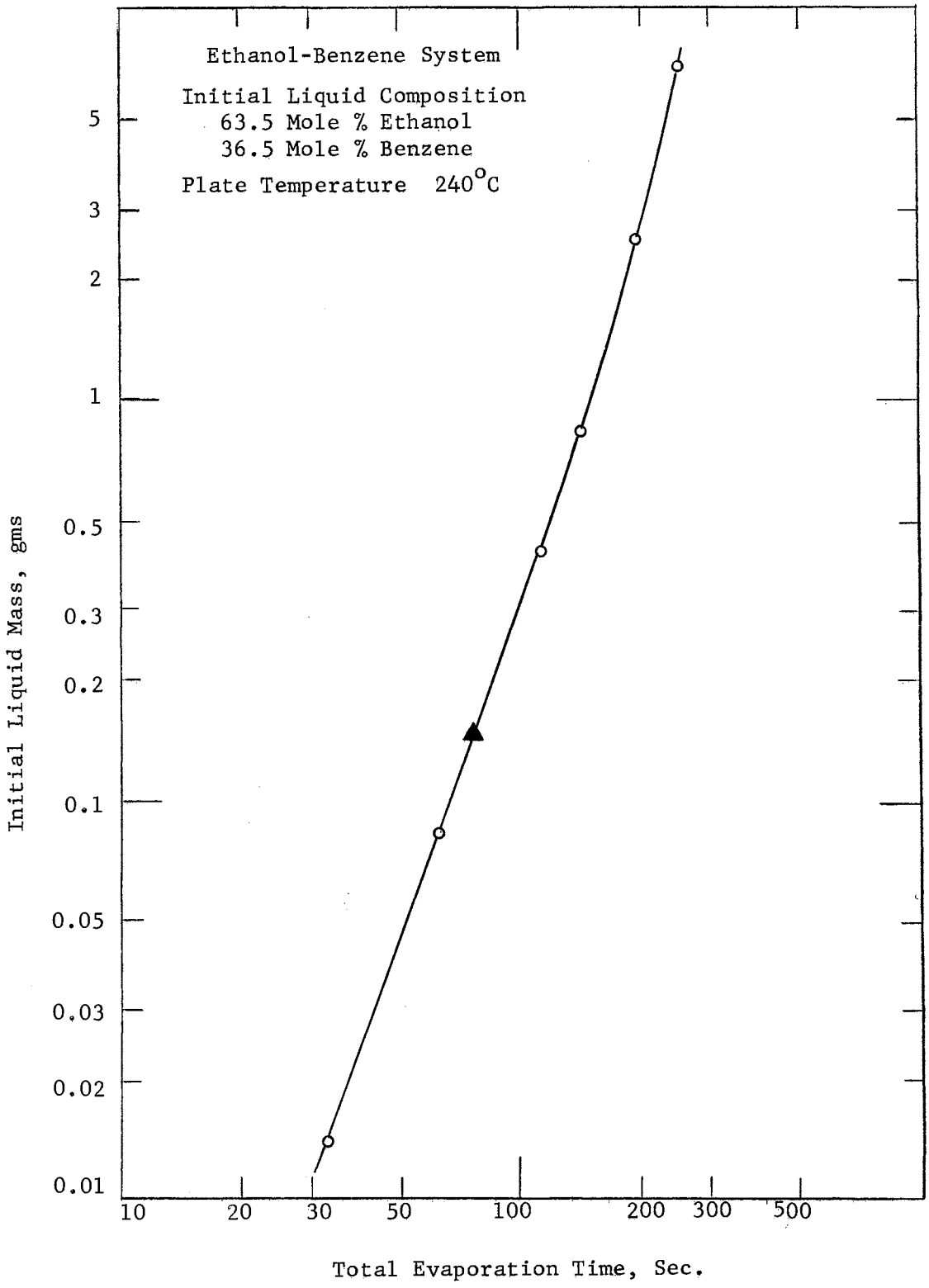

Figure 5. Initial Liquid Mass vs. Total Evaporation Time

Ethanol-Benzene System

Initial Liquid Composition : 63.5 Mole % Ethanol
36.5 Mole % Benzene

Plate Temperature : 240°C

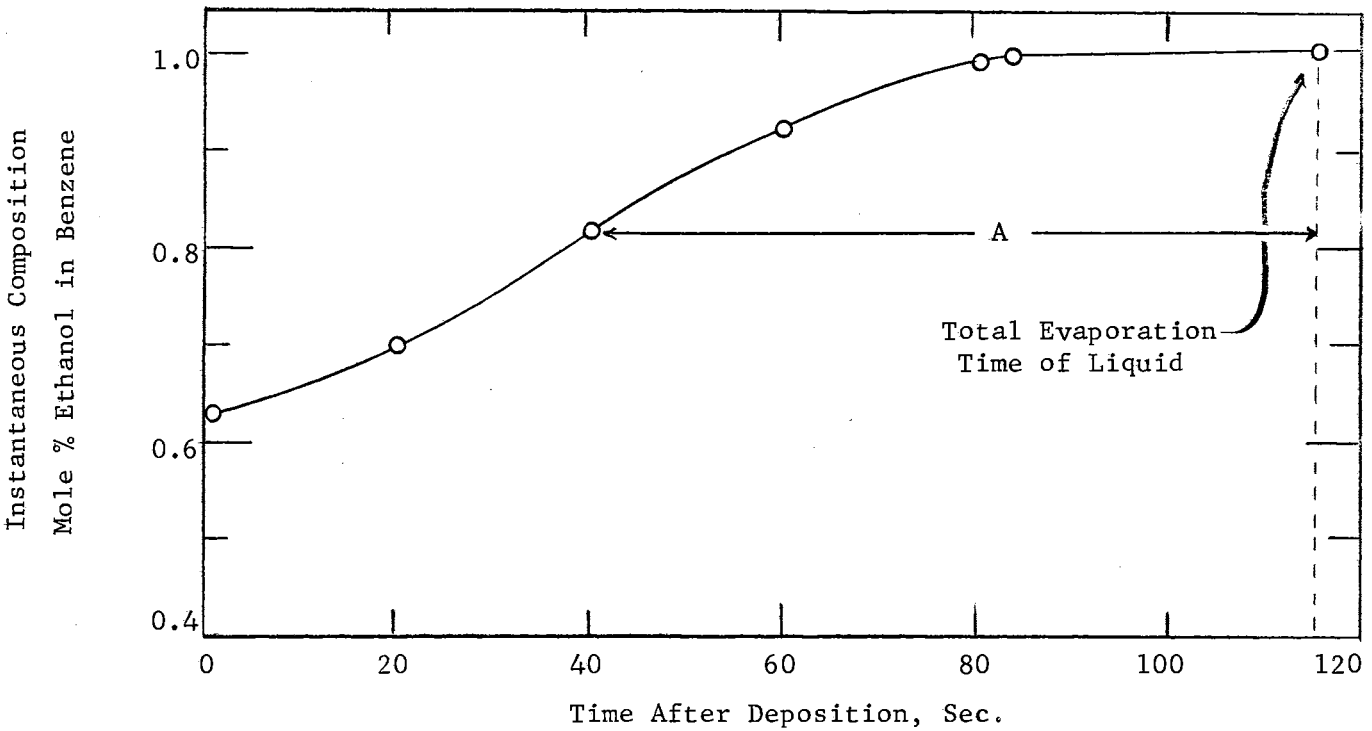

Figure 6. Instantaneous Liquid Composition vs. Time After Deposition

the Leidenfrost point could be determined by unsteady state plate temperatures. The liquid was poured onto the plate from a beaker. The temperature of the plate was high enough to have the liquid in film boiling. The plate was then cooled. The plate temperature at which the liquid collapsed onto the plate (went into nucleate boiling) was considered the Leidenfrost point.

The plate was heated to a point well above that temperature at which the liquid could be placed on it and still be in film boiling. The heat supplied to the plate was reduced and the plate was allowed to cool. The liquid at its boiling point was then poured onto the plate from a 15 ml beaker. The heat to the plate was sometimes increased near the Leidenfrost temperature to slow down the rate of cooling. The average rate of cooling of the plate was 0.1°C per second or six degrees per minute. The rate of cooling was higher when the liquid was first placed on the plate and lower near the Leidenfrost temperature.

This method was used only with pure liquids and the ethanol-benzene azeotrope, so that composition did not change during evaporation.

CHAPTER V

THEORETICAL ANALYSIS

Theoretical Development

The theoretical analysis resulting in an analytical model describing the film boiling of pure liquid drops on a flat heated surface has been developed by Gottfried, Lee, and Bell, (14), and is described in detail by Lee (19). Since this analysis is the basis for the expanded model of binary liquid evaporation it is outlined below.

The drop is postulated to be spherical and well mixed so that no thermal gradients exist inside the drop. The drop temperature is at the liquid normal boiling point and the drop floats above the heated surface on a cushion of its own vapor. Three physical processes must be considered: (1) Vaporization of the liquid followed by transport of the vapor from the drop surface, (2) Energy transfer to the drop from the hot surface by conduction-convection, and radiation, (3) Momentum transfer in or through the flowing vapor beneath the drop. In addition, a force balance between the mass of the drop and the pressure above atmospheric in the vapor film between the drop and the heated surface is required.

MASS BALANCE

The rate of change of volume of the drop is proportional to the rate of evaporation from the lower surface W_1 and the upper surface W_2 of the drop.

$$\rho_L \frac{dV}{dt} = -(W_1 + W_2) \tag{1}$$

Liquid evaporates into the vapor film beneath the drop replenishing the vapor that flows away from this region. A material balance for this vapor flow through the walls of a hypothetical cylinder of height δ and radius x' gives W_1 as a function of position beneath the drop, θ and average vapor velocity through the cylinder walls (see Figure 7).

$$W_1(\theta) = \rho_v 2\pi x' \delta \bar{u} \tag{2}$$

Liquid is evaporated from the upper surface by molecular diffusion

$$W_2 = \frac{DMP_t}{RT_s r} A_2 \tag{3}$$

where P_t is the external pressure on the system (1 atm for the present work).

ENERGY BALANCE

Energy is supplied to the lower half of the drop by conduction through the vapor film Q_c , and by radiation Q_{R1} , and to the upper half of the drop by radiation Q_{R2} . This energy results in vaporization from the upper and lower surfaces of the drop plus the superheating of the vapor film beneath the drop

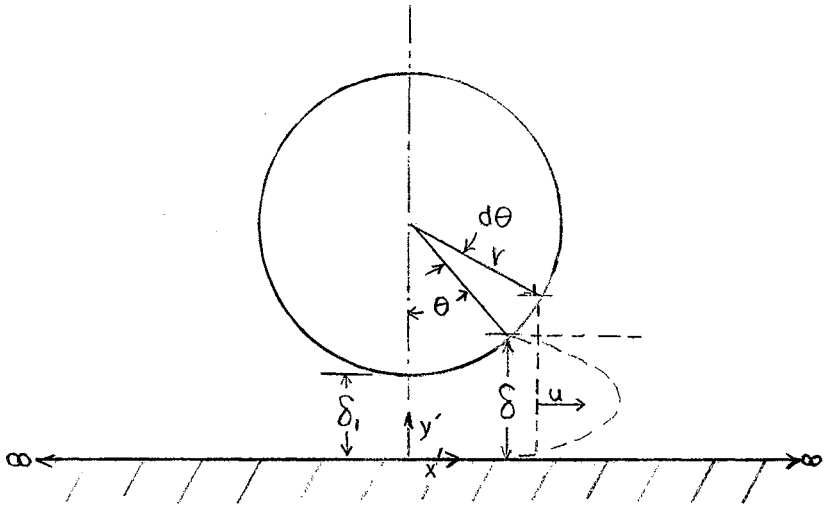

Some Geometric Relationships:

$$\delta = \delta_1 + r(1 - \cos\theta)$$

$$x' = r\sin\theta$$

$$dx' = r\cos\theta\, d\theta$$

$$dA_p = 2\pi x'dx' = 2\pi r^2 \sin\theta\cos\theta\, d\theta$$

Figure 7. Geometric Configuration for the Spherical Drop Model

to an average temperature between the drop T_s and the surface T_p.

$$Q_C + Q_{R1} + Q_{R2} = W_1 \left[\lambda + 1/2\ C_p(T_p - T_s)\right] + W_2\lambda$$
$$= QW_1 + QW_2 \qquad (4)$$

where $$QW_1 = W_1 \left[\lambda + 1/2\ C_p(T_p - T_s)\right] = W_1\lambda' \qquad (4\text{-A})$$

$$QW_2 = W_2\lambda \qquad (4\text{-B})$$

The thermal transfer rate across the vapor film between the heated surface and the lower half of the drop, assuming transfer perpendicular to the surface is

$$Q_c = \frac{k(T_p - T_s)}{\bar{\delta}} A_p \qquad (5)$$

where A_p is the projected area of the drop and $\bar{\delta}$ is the mean vapor film thickness.

$$\bar{\delta} = \left[\frac{2(\delta_1 + r)}{r^2} \ln\frac{\delta_1 + r}{\delta_1} - \frac{2}{r}\right]^{-1} \qquad (6)$$

δ_1 is the distance between the bottommost part of the drop and the heating surface.

Radiant energy transferred between the surface and the lower half of the drop is given by

$$Q_{R1} = \frac{A_1\sigma\,(T_p^4 - T_s^4)}{(\frac{1}{\epsilon_L} - 1) + \frac{1}{0.682}} \qquad (7)$$

while the transfer between the surface and the upper half is

$$Q_{R2} = \frac{A_2 \sigma (T_p^4 - T_s^4)}{(\frac{1}{\epsilon_L} - 1) + \frac{1}{0.318}} \tag{8}$$

MOMENTUM BALANCE

Vaporization on the lower half of the drop causes flow in the film supporting the drop above the surface. For laminar flow this can be represented by

$$g_c \frac{\partial P}{\partial x'} = \mu \frac{\partial^2 u}{\partial y'^2} \tag{9}$$

From this equation, assuming no slip at the vapor boundaries, the average radial velocity of vapor is found to be

$$\bar{u} = \frac{g_c \delta^2}{12 \mu} \left(-\frac{\partial P}{\partial x'} \right) \tag{10}$$

with δ being the vertical distance between the drop and the surface at angle θ.

FORCE BALANCE

The mass of the drop is supported by the excess pressure of the vapor film beneath the drop.

$$\frac{4}{3} \pi r^3 (\rho_L - \rho_v) \frac{g}{g_c} = \int_{A_p} P(\theta') \, dA_p \tag{11}$$

SOLUTION OF MASS, ENERGY, MOMENTUM, AND FORCE BALANCES

Introducing Equation (10) into Equation (2) results in the pressure gradient as a function of the evaporation rate W_1.

$$W_1(\theta) = \frac{2\pi \rho_v g_c x' \delta^3}{12 \mu} \left(-\frac{\partial P}{\partial x'} \right) \tag{12}$$

Substituting Equation (12) into Equation (11) and rearranging with the use of the geometric relationships from Figure 7

$$r = \frac{9}{\pi} \frac{\mu}{g\rho_v(\rho_L - \rho_v)} \int_0^{\pi/2} \sin\theta' \cos\theta' \, d\theta \int_\theta^{\pi/2} \frac{W_1(\theta) \cos\theta \, d\theta}{\sin\theta \left[\delta_1 + r - r\cos\theta\right]^3} \qquad (13)$$

The rate of vapor generation from the lower surface of the drop $W_1(\theta)$ appears implicility in Equation (13). The solution of this equation therefore requires hypothesizing the mechanisms of heat and mass transfer taking place on the lower portion of the drop.

Assume QW_1 can be approximated by an effective thermal conductivity, k_e, that takes into account the conductive and radiative heat transfer.

$$\lambda' W = QW = \frac{k_e (T_p - T_s)}{\bar{\delta}} A_p \qquad (14)$$

It may also be assumed that

$$QW_1 = Q_c + Q_{R1} \qquad (15)$$

This assumption is too restrictive since it limits the amount of energy supplied to the lower portion of the drop and allows no interchange of heat inside the drop due to internal mixing. However, it serves as an initial approximation for k_e. From Equations (5), (14), and (15),

$$\frac{k_e (T_p - T_s)}{\bar{\delta}} A_p = \frac{k (T_p - T_s)}{\bar{\delta}} A_p + Q_{R1}. \qquad (16)$$

This rearranges to

$$k_e = k \left(1 + \frac{Q_{R1}}{Q_c}\right) = k (1 + K) \qquad (17)$$

where K is a correction factor between the actual thermal conductivity of the vapor film, k and the effective thermal conductivity. In computation, K is first set equal to 0 and then approximated by $K = Q_{R1}/Q_c$. The convergence of K is checked by a rearrangement of Equation (4).

$$QW_1 = \frac{k_e (T_p - T_s)}{\bar{S}} A_p = Q_{R1} + Q_{R2} + Q_c - QW_2 \qquad (18)$$

This equation removes the assumption of Equation (15).

It is now possible to solve Equation (13) by initially setting K = 0. This yields a value for δ_1 which allows the evaluation of Q_c from Equation (5) and (6) and therefore the checking of k_e with Equation (18). If Equation (18) doesn't balance within prescribed limits, K is adjusted by the relationship

$$K = \frac{(QW_1)_{ave}}{Q_c} - 1 \qquad (19)$$

where $(QW_1)_{ave}$ is the arithmetic average of the value of QW_1 calculated from the heat balance and the value computed from the effective thermal conductivity.

It is now possible to find the rate of change in mass of the drop by Equation (1). But because of the complexity in evaluating the terms in this equation, an analytical solution is not possible. The rate of change of volume

$$\frac{dV}{dt} = -\frac{1}{\rho_L} (W_1 + W_2) = f(V,t) \qquad (1\text{-A})$$

is therefore solved by the iterative procedure of stepwise integration (18).

For an initial volume, V_i, W_1 and W_2 values are obtained (satisfying the necessary heat, momentum, and force balances). The volume at the end of a time increment, Δt is

$$V_{i+1} = V_i - \Delta t\, f(V_i,t) = V_i - \Delta t\, f_i \tag{20}$$

Evaluation of W_1 and W_2 is made for this new volume V_{i+1}. This permits the modification of V_{i+1} as follows:

$$V'_{i+1} = V_i - \Delta t\, f_{i+1} \tag{21}$$

Successive values of V_{i+1} are modified using an average of the rate of evaporation over the time interval Δt.

$$V_{i+1}^{(1)} = V_i - 1/2\ \Delta t\ (f_{i+1} + f'_{i+1}) \tag{22}$$

$$V_{i+1}^{(2)} = V_i - 1/2\ \Delta t\ (f_{i+1} + f_{i+1}^{(1)}) \tag{23}$$

$$\vdots \qquad\qquad \vdots$$

$$V_{i+1}^{(j-1)} = V_i - 1/2\ \Delta t\ (f_{i+1} + f_{i+1}^{(j-2)}) \tag{24}$$

$$V_{i+1}^{(j)} = V_i - 1/2\ \Delta t\ (f_{i+1} + f_{i+1}^{(j-1)}) \tag{25}$$

These equations are solved by iteration until the following convergence is obtained:

$$\left| \frac{V_{i+1}^{(j)} - V_i^{(j-1)}}{V_{i+1}^{(j)}} \right| \leq 10^{-5} \tag{26}$$

Analytical Model for Binary Liquid Solutions

The evaporation of binary liquids requires an additional postulation to the assumptions already incorporated in the pure component evaporation model. This postulation involves the manner in which the liquid composition changes during vaporization. If vaporization is very fast, the liquid could evaporate under non-equilibrium conditions such that the vapor and liquid are of nearly the same composition. This can be visualized as the outer layers of the drop being vaporized as a whole with no change in composition of the underlying layers. Diffusion may also play a predominant role as is often the case with vaporization without ebullition (20). The transport of the vapors away from the liquid-vapor interface is controlled by their diffusion rate through an inert gas. Also, diffusion may not influence vaporization; for example, it may be assumed that the vapor is always in equilibrium with the liquid as when the vapor is bubbled through the liquid.

From the experimental results to be explained in the following chapter, vaporization appears to follow the path of Rayleigh vaporization, that is, equilibrium always exists between liquid and vapor phases. The instantaneous composition of the vapor produced is in equilibrium with the mixed liquid composition remaining in the drop.

The saturation temperature of the drop is determined from its composition and activity coefficients (γ) by a bubble point

calculation. The sum of the partial pressures is compared to the external pressure on the system by the equation:

$$P_T = \gamma_1 (VP)_1 x_1 + \gamma_2 (VP)_2 x_2 \qquad (27)$$

where the activity coefficients are calculated as a function of the drop composition from the Van Laar equation. The solution of the equation involves a trial and error procedure. The vapor composition in equilibrium with the liquid is found from

$$y_i = \frac{\gamma_i (VP)_i x_i}{P_T} \qquad (28)$$

The drop is supported by a vapor film which flows between the drop and the heated surface and consists of vapor whose composition is in equilibrium with the drop liquid. The upper boundary of the film is at the drop saturation temperature and the lower boundary is at the heated surface temperature. The physical properties of this film-viscosity, thermal conductivity, specific heat, and density-are expressed as functions of temperature and composition and evaluated at the arithmetic average of the drop and heated surface temperatures and at the vapor composition in equilibrium with the liquid drop. The drop physical properties such as density and latent heat of vaproziation are expressed as functions of drop compositions.

The vapor film in contact with the upper surface of the drop is assumed to be at the drop saturation temperature and equilibrium vapor composition. The diffusivity for the vapor

mixture is therefore calculated at these conditions as explained in Appendix A.

The change in liquid composition is calculated in the following manner. The mass of liquid vaporized during a differential time interval is assumed to be at the equilibrium vapor composition existing at the start of the time interval. The decrease in mass of a component of the liquid during the time interval is then equal to the total mass evaporated times the mass fraction of that component in the vapor. The amount of a component remaining in the liquid is then the difference between the amount present at the start of the time interval minus the mass of that component vaporized. Repeating this procedure for all liquid components results in a new liquid composition which is then used for the next time interval.

Overall Computational Procedure

An outline of the computational procedure follows:

A. Calculation of Physical Properties

(1) Drop saturation temperature is calculated by trial and error procedure from Equation (27).

(2) Vapor composition is obtained from Equation (28).

(3) Viscosity, thermal conductivity, specific heat, and vapor density are evaluated at the average temperature of the vapor film beneath the drop and at the equilibrium vapor composition.

(4) Liquid density and latent heat of vaporization are evaluated at the liquid composition.

(5) Diffusivity is evaluated at the equilibrium vapor composition and liquid temperature.

B. Convergence of Energy Balance

(1) Radius and area of drop are calculated.

(2) Values for W_2, QW_2, Q_{R1}, and Q_{R2} are calculated from Equations (3), (4-B), (7), and (8).

(3) The radiative heat transfer is ignored for the first iteration by taking $K = 0$ in Equation (17). For all other iterations the corrected value of K or the value of K calculated from the previous volume convergence is used.

(4) The rate of evaporation beneath the drop is obtained from Equation (14).

(5) The vapor film thickness beneath the drop is obtained from Equation (13).

(6) QW_1, $\overline{\delta}$, and Q_c are calculated from Equations (4-A), (6), and (5).

(6-A) For only the first iteration in which K was taken as zero, K is calculated from $K = Q_{R1}/Q_c$ and the computation switches to step (B-4) to re-evaluate W_1.

(7) The heat balance is now checked with Equation (4). If it is satisfied to within an allowable error, the computation then moves to the evaluation of the change

in volume. If Equation (4) is not satisfied, K is recalculated using Equation (19) and the computation switches to step (B-3).

C. Convergence of Volume

(1) The energy, momentum, and force balances have been satisfied. The rate of change of volume can therefore be calculated from Equation (1-A).

(2) The volume at the end of the time increment is obtained from Equation (20). The computation switches to step (B-1) to satisfy the energy, momentum, and force balances for this new volume.

(3) This procedure is repeated until Equation (26) is satisfied.

D. Calculation of Composition Change

(1) The new liquid composition is calculated assuming equilibrium vaporization.

(2) The computation then moves on to the next time increment.

The above procedure is repeated until the drop volume equals zero. A simplified flow diagram of this computational procedure is presented in Figure 8. The FORTRAN program for the digital computation with a sample of the program output appears in Appendix F.

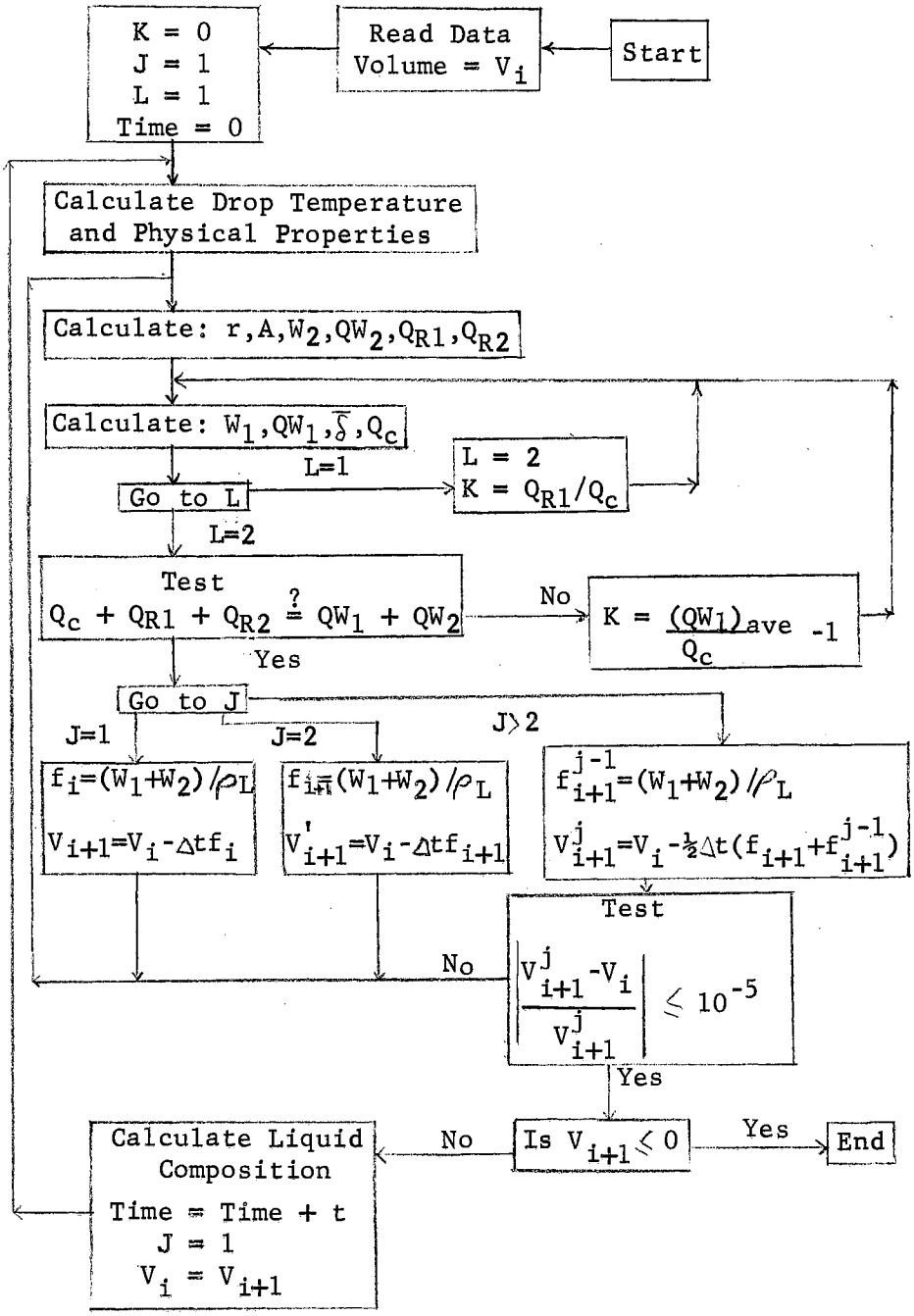

Figure 8. Flow Diagram of Computational Procedure for Evaporation of Binary Liquid Drops

CHAPTER VI

RESULTS AND DISCUSSION

The experimental data consist of the total evaporation time of a liquid mass on a heated stainless steel plate at various plate temperatures, and the change in composition of the mass during evaporation. The initial masses varied from 0.0045 to 7.0 grams and plate temperatures ranged from 150 to 450°C. The larger masses covered a considerable area of the plate and had vapor bubbles breaking through the liquid surface. The smaller masses are drops approaching a sphere in shape. The temperature ranges extends from temperatures high enough to allow evaporation by film boiling to those substantially below the Leidenfrost point. Composition changes for both large and small masses during evaporation were found at several plate temperatures, all above the Leidenfrost point.

Total Evaporation Time

The total evaporation time results for pure ethanol, benzene, toluene, and water, are presented in Figures 9, 13, 16 and 17. Results for ethanol-benzene appear in Figures 10-12, and for benzene-toluene in Figures 14 and 15. It is interesting to note the relative smoothness of the curves drawn through the data points, considering that they represent over a thousand-fold

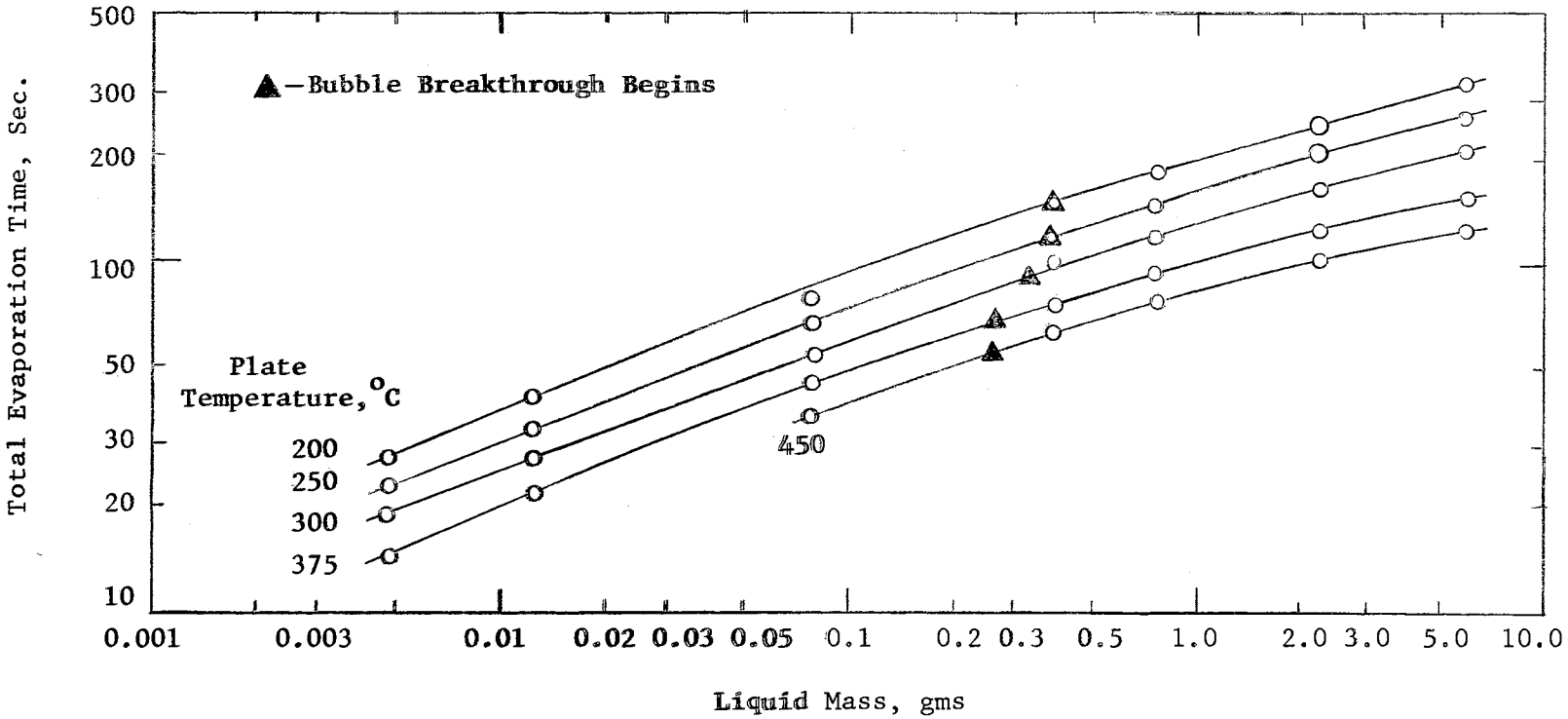

Figure 9. Total Evaporation Time vs. Initial Liquid Mass for Ethanol

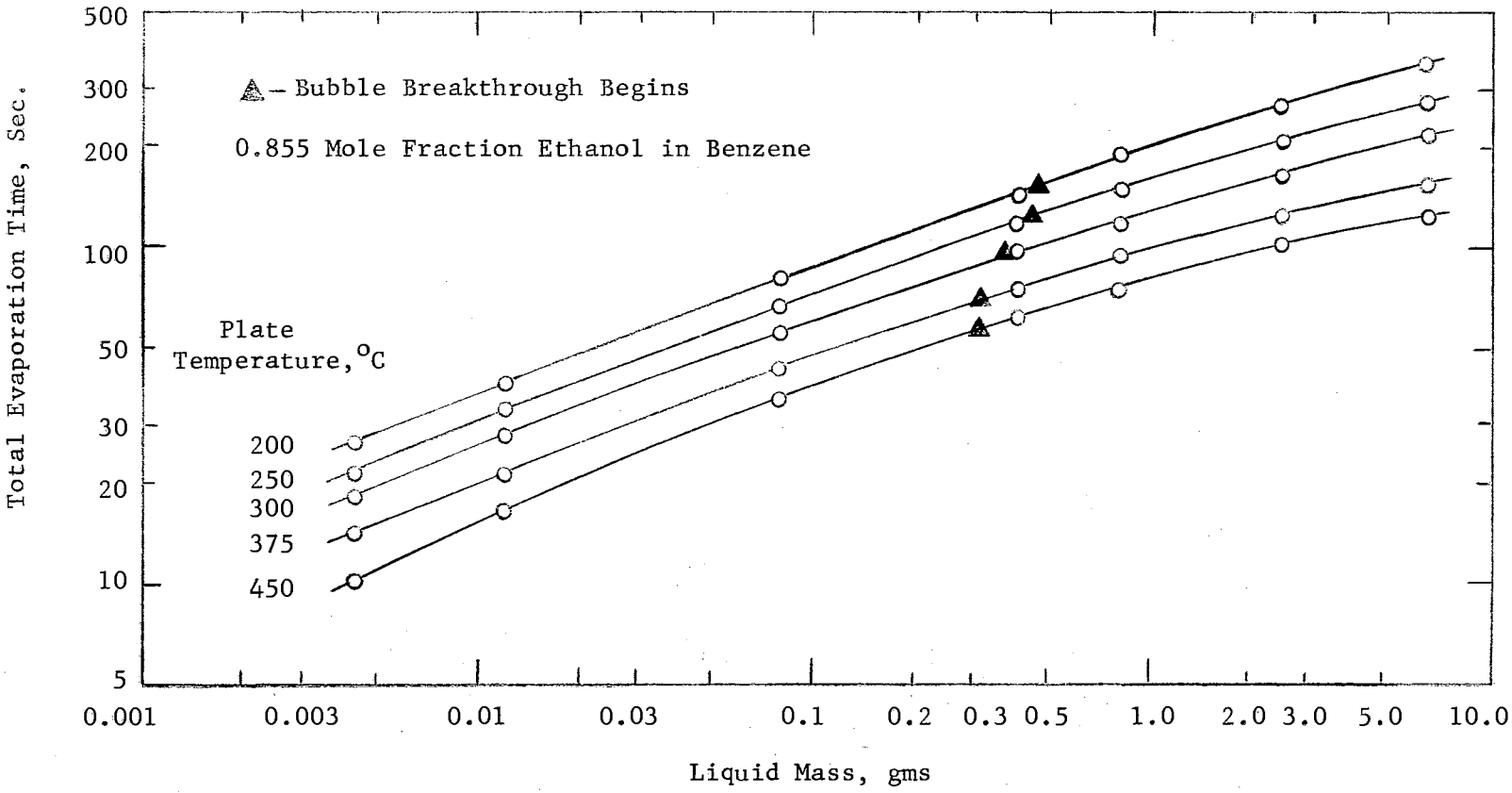

Figure 10. Total Evaporation Time vs. Initial Liquid Mass for the Ethanol-Benzene System

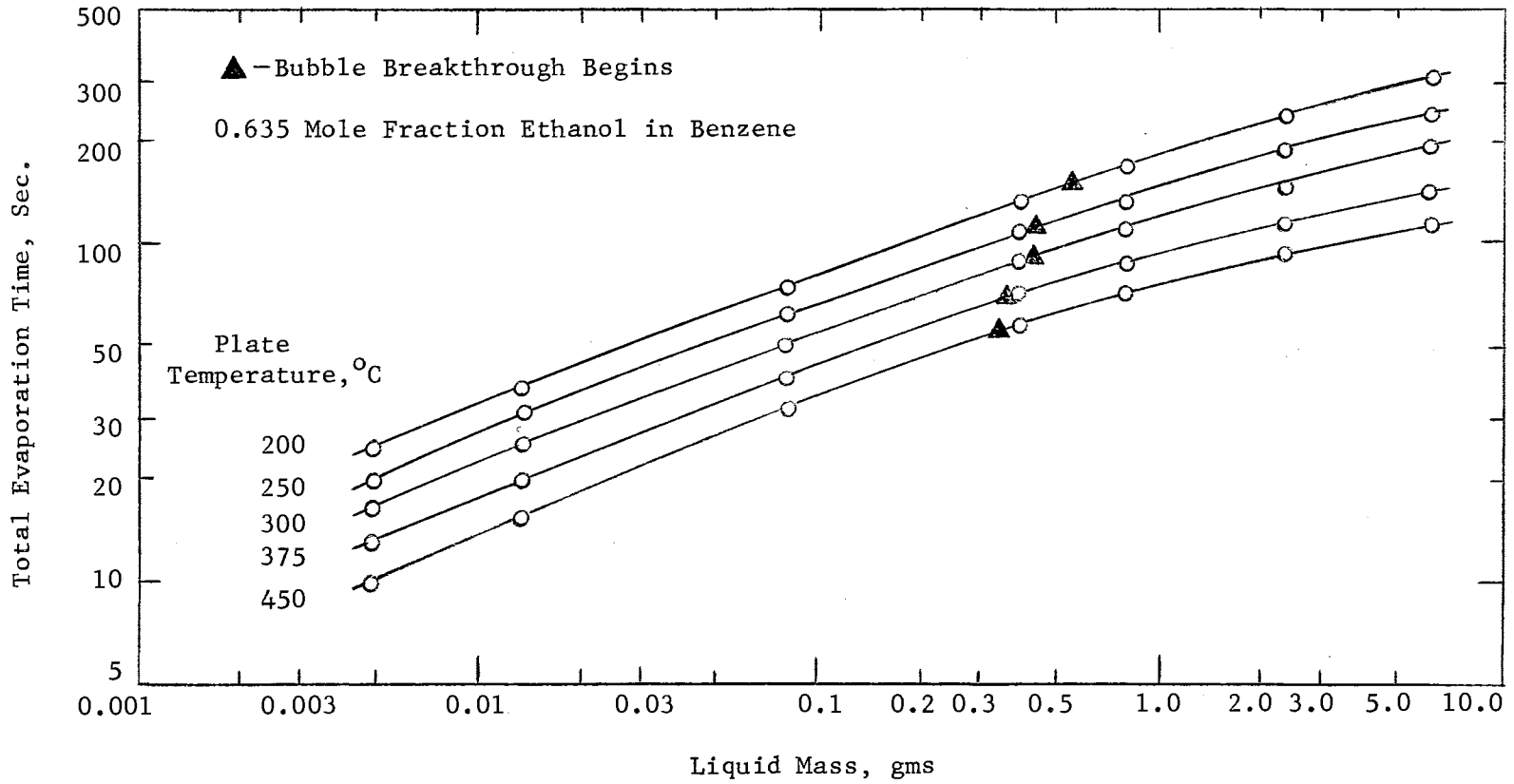

Figure 11. Total Evaporation Time vs. Initial Liquid Mass for the Ethanol-Benzene System

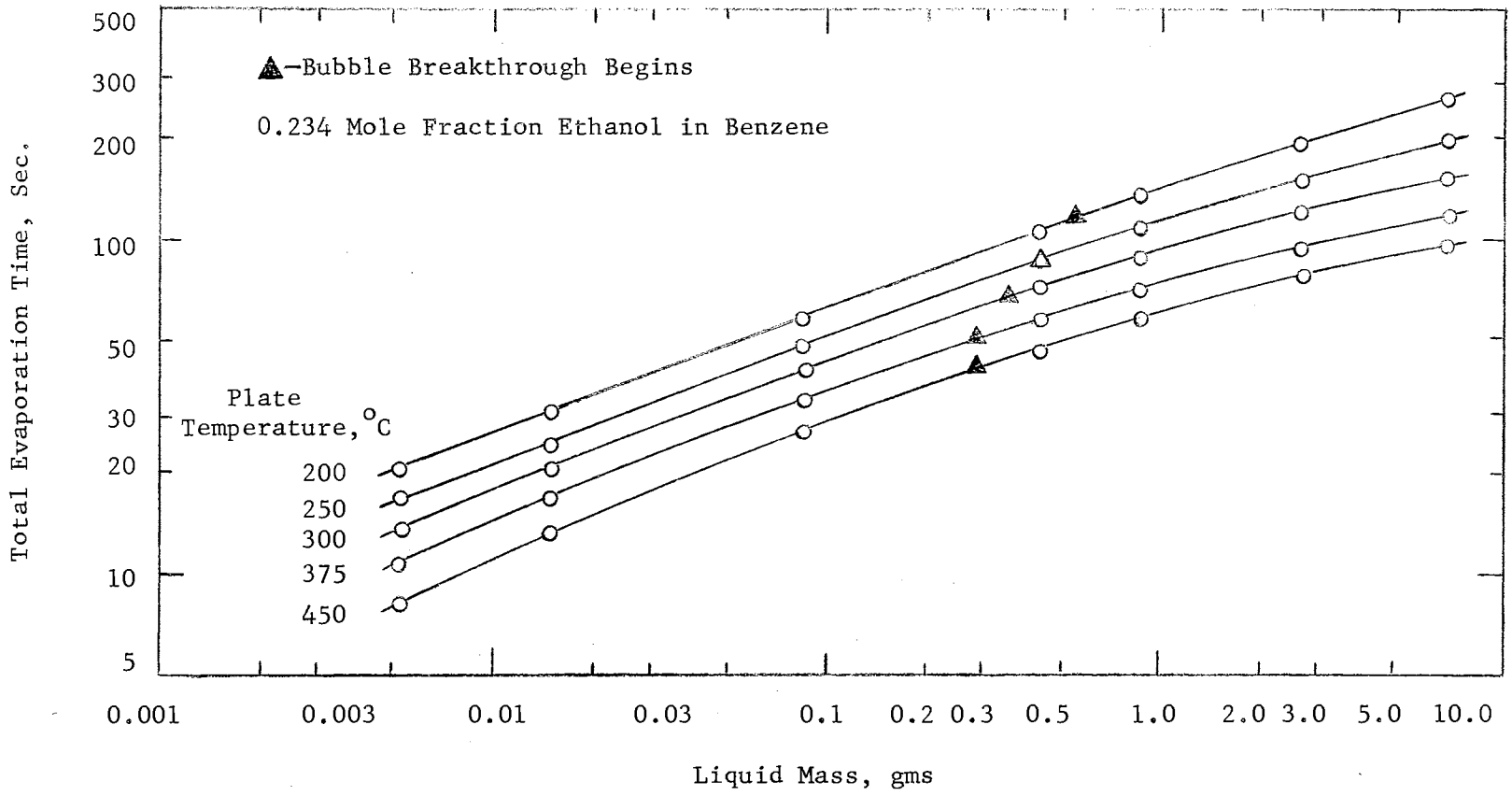

Figure 12. Total Evaporation Time vs. Initial Liquid Mass for the Ethanol-Benzene System

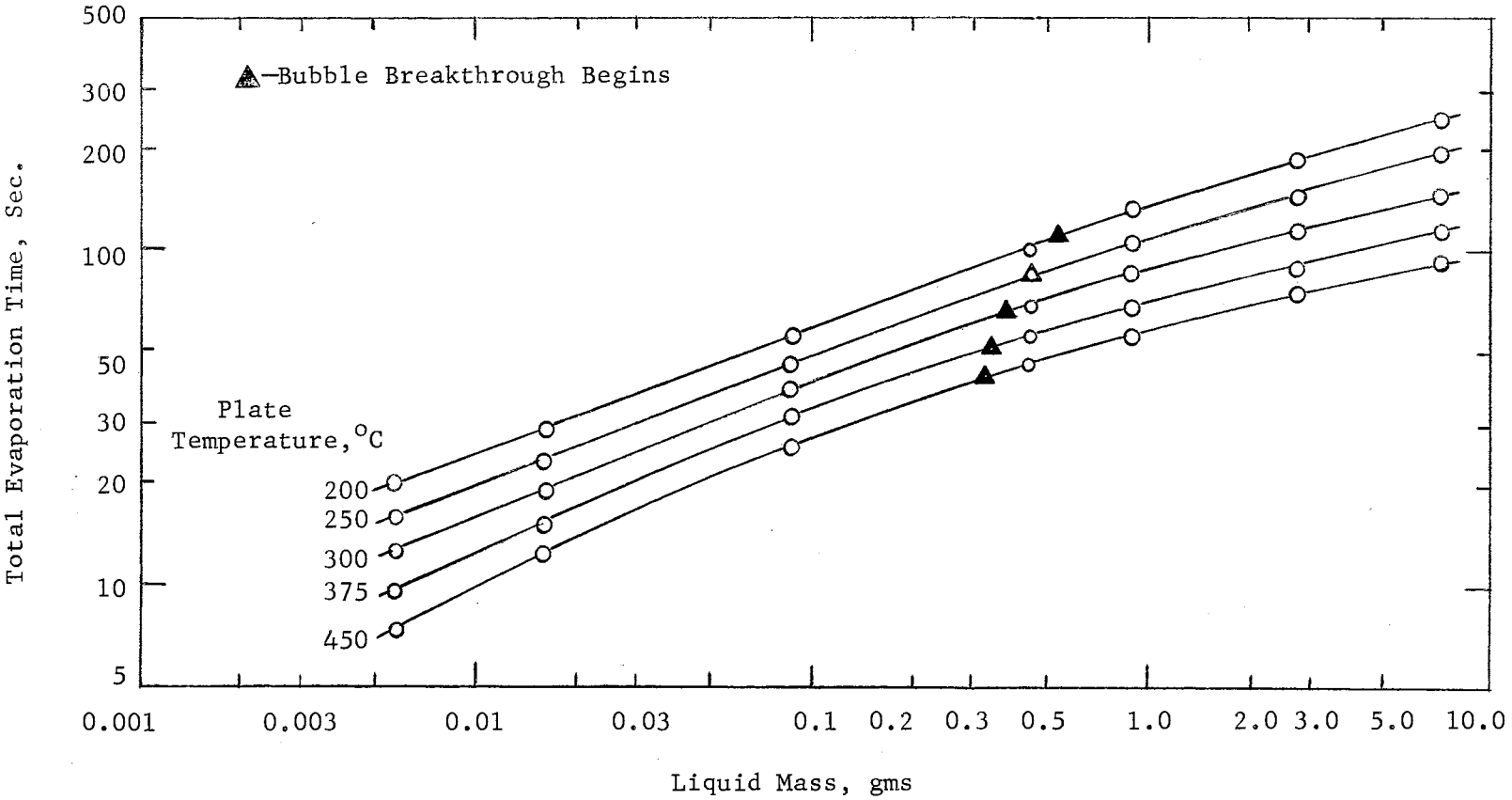

Figure 13. Total Evaporation Time vs. Initial Liquid Mass for Benzene

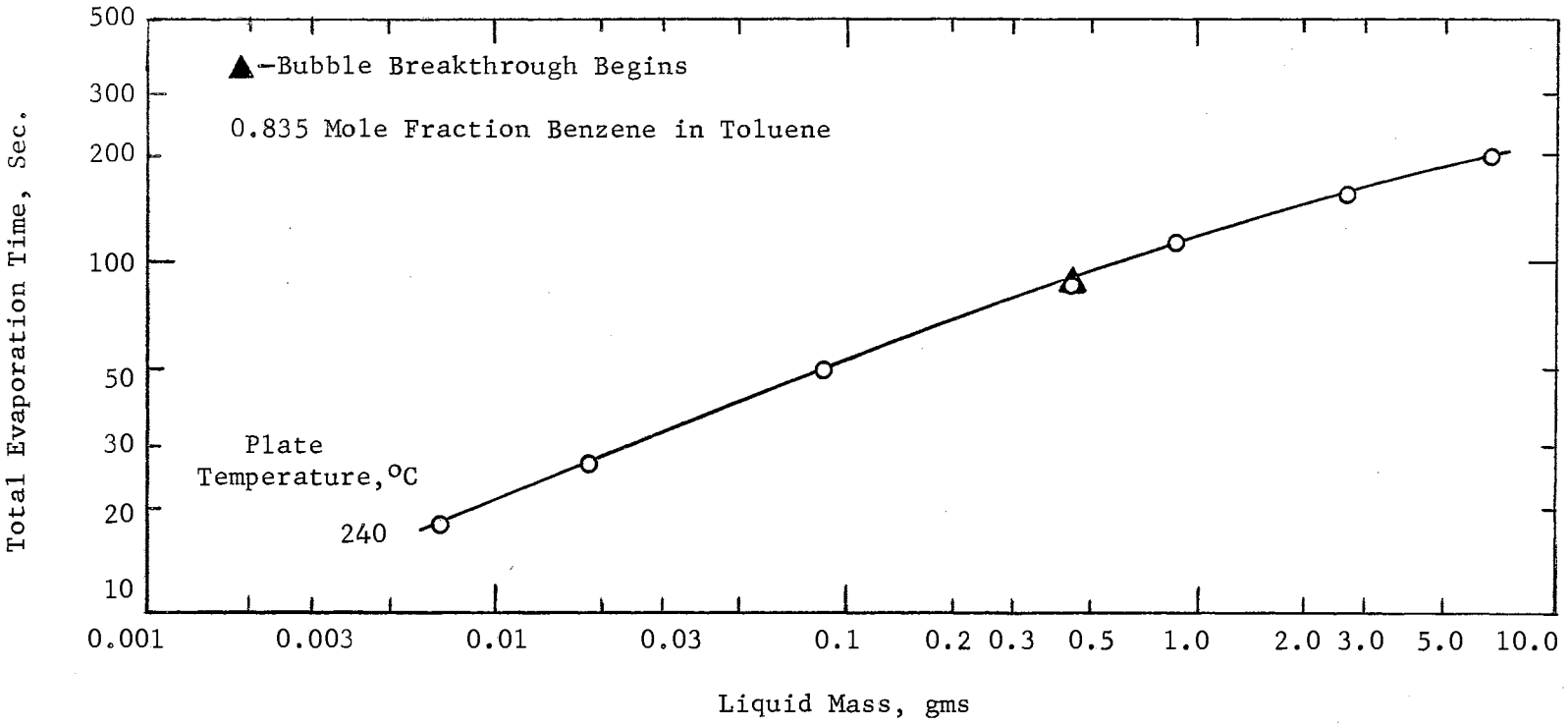

Figure 14. Total Evaporation Time vs. Initial Liquid Mass for the Benzene-Toluene System

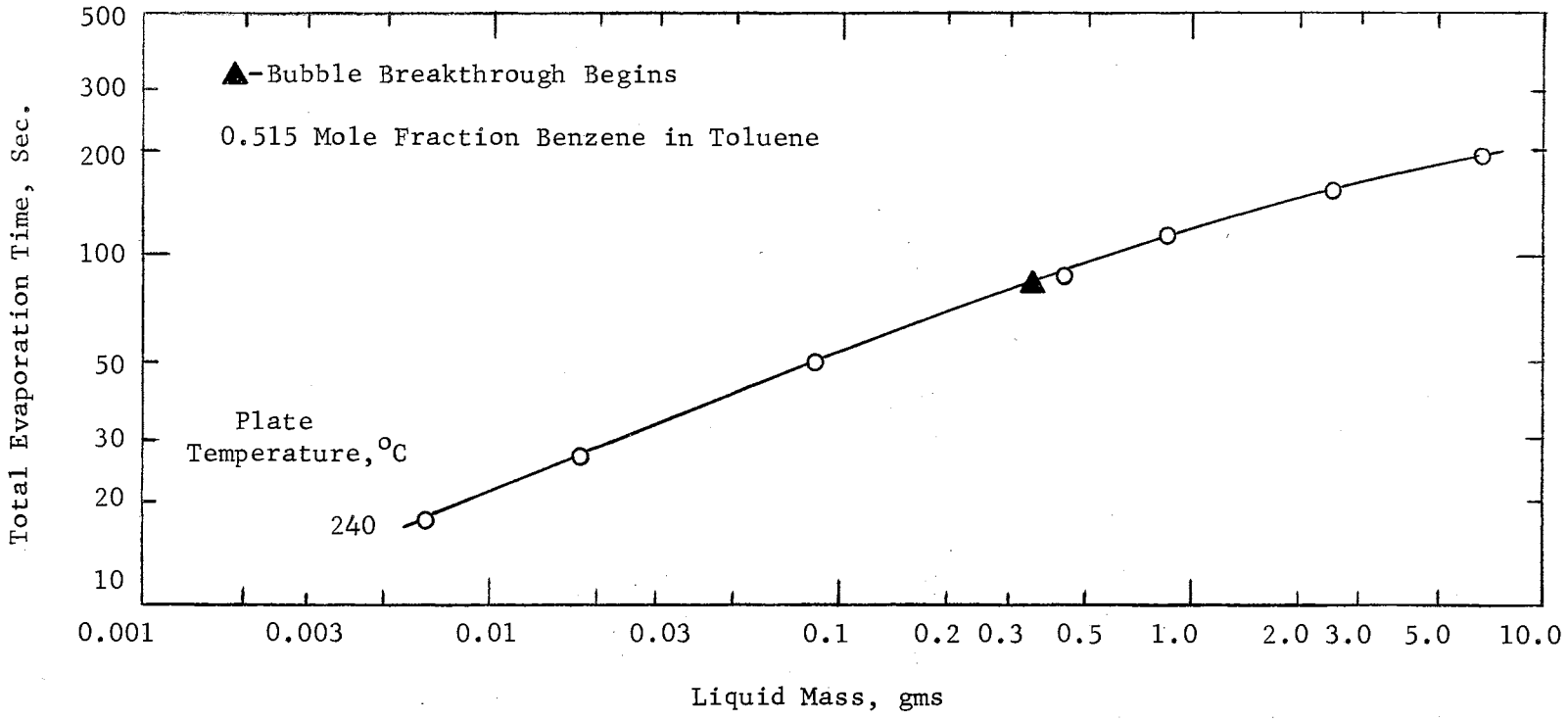

Figure 15. Total Evaporation Time vs. Initial Liquid Mass for the Benzene-Toluene System

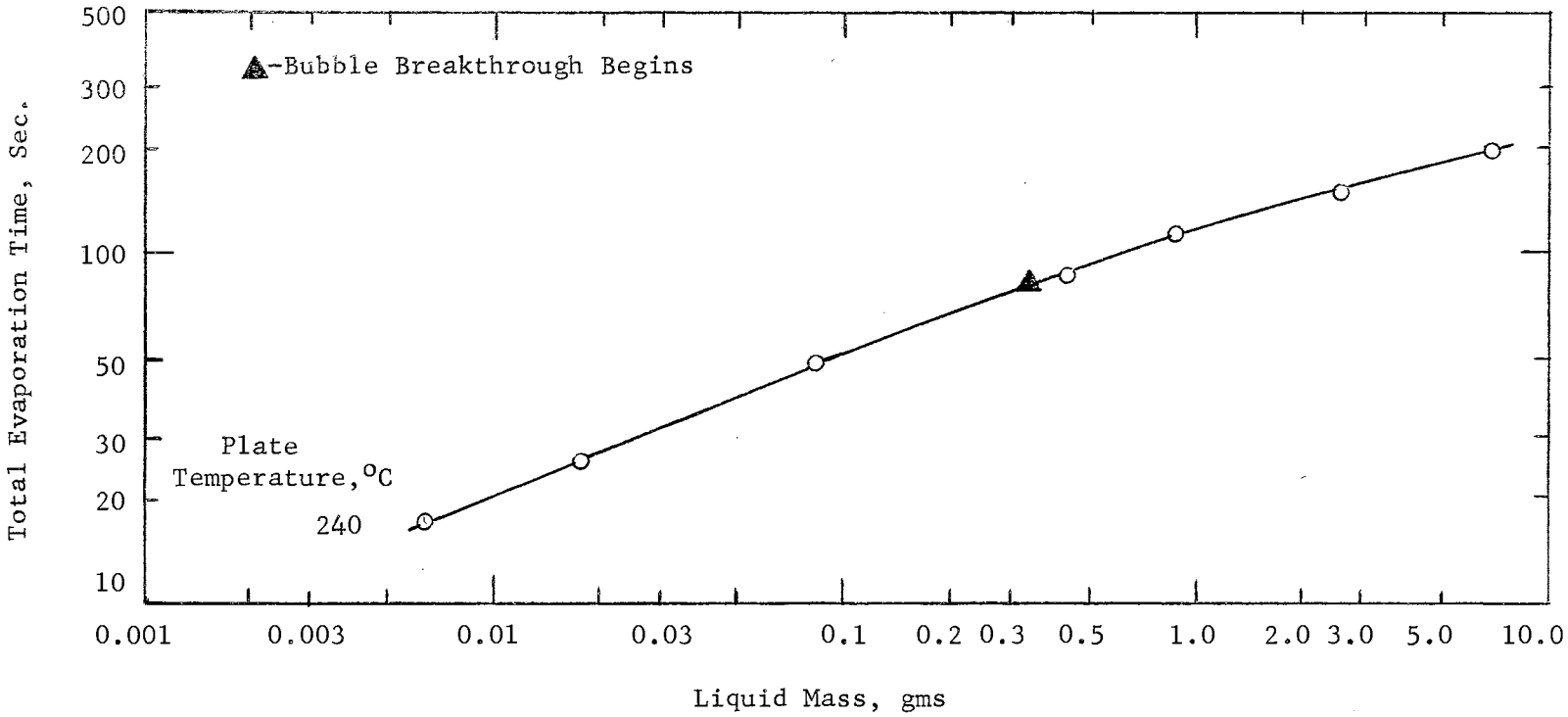

Figure 16. Total Evaporation Time vs. Initial Liquid Mass for Toluene

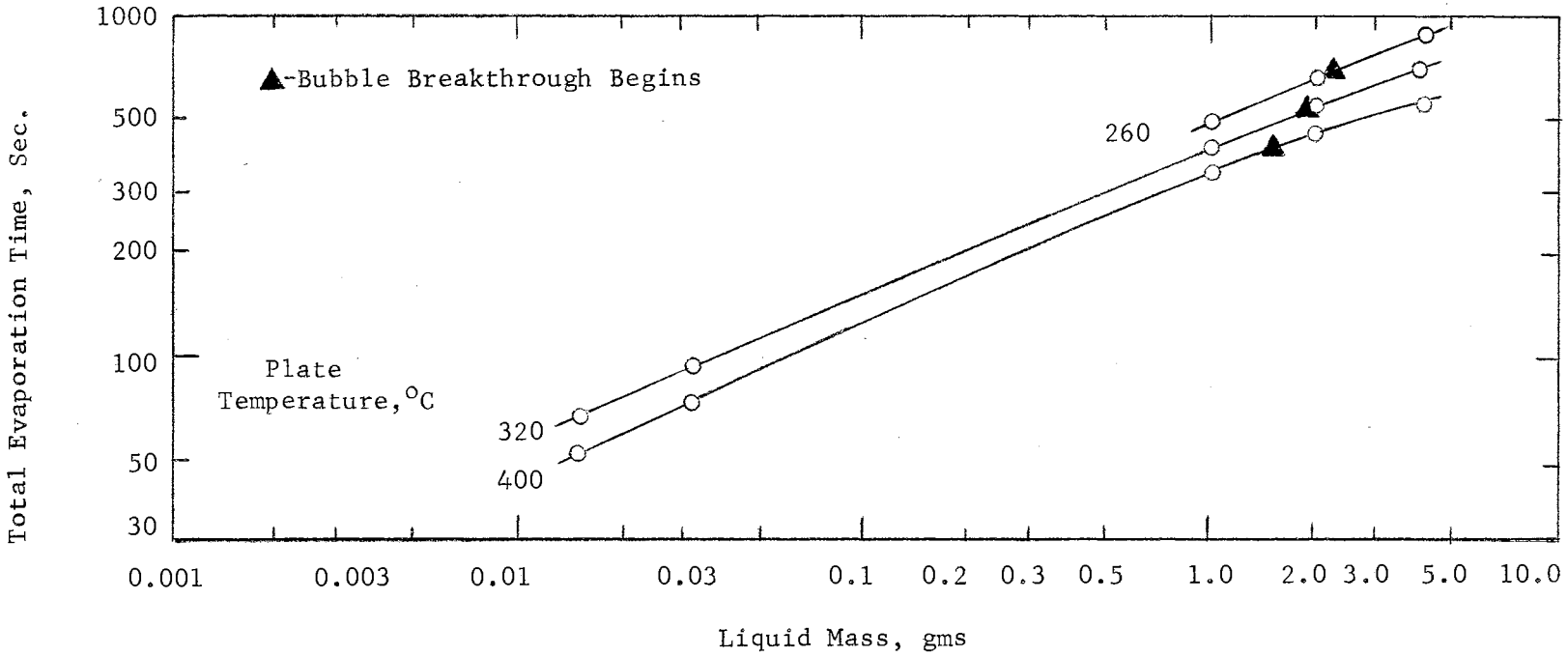

Figure 17. Total Evaporation Time vs. Initial Liquid Mass for Water

range of liquid masses, from small drops to large extended masses with bubble breakthrough and violent surface agitation. Small triangles have been placed on the curves to indicate the mass below which bubble breakthrough does not occur.

The effect of composition on the total evaporation time is shown for the systems ethanol-benzene in Figure 18 and ethanol-water in Figure 19. There is essentially no difference in the total evaporation time for pure benzene and toluene as well as binary solutions of these two liquids. Figure 18 is for a constant plate temperature of 375°C. Figure 19 is for drops of approximately 0.126 gms where the plate temperature varies. Varying the composition from one component of the mixture to the other shifts the entire curve between those for the pure components.

Composition Change

The composition change of a liquid mass experiencing the Leidenfrost Phenomenon was studied to determine if vaporization occurred by: 1) bulk vaporization, where infinitesimal layers of liquid are vaporized as a whole and the overall composition remains constant; 2) diffusional vaporization in which the relative loss of components from the liquid is controlled by molecular diffusion of the vapors through the atmosphere; 3) equilibrium or Rayleigh vaporization in which the instantaneous composition of the vapor produced is in equilibrium with the mixed liquid composition remaining.

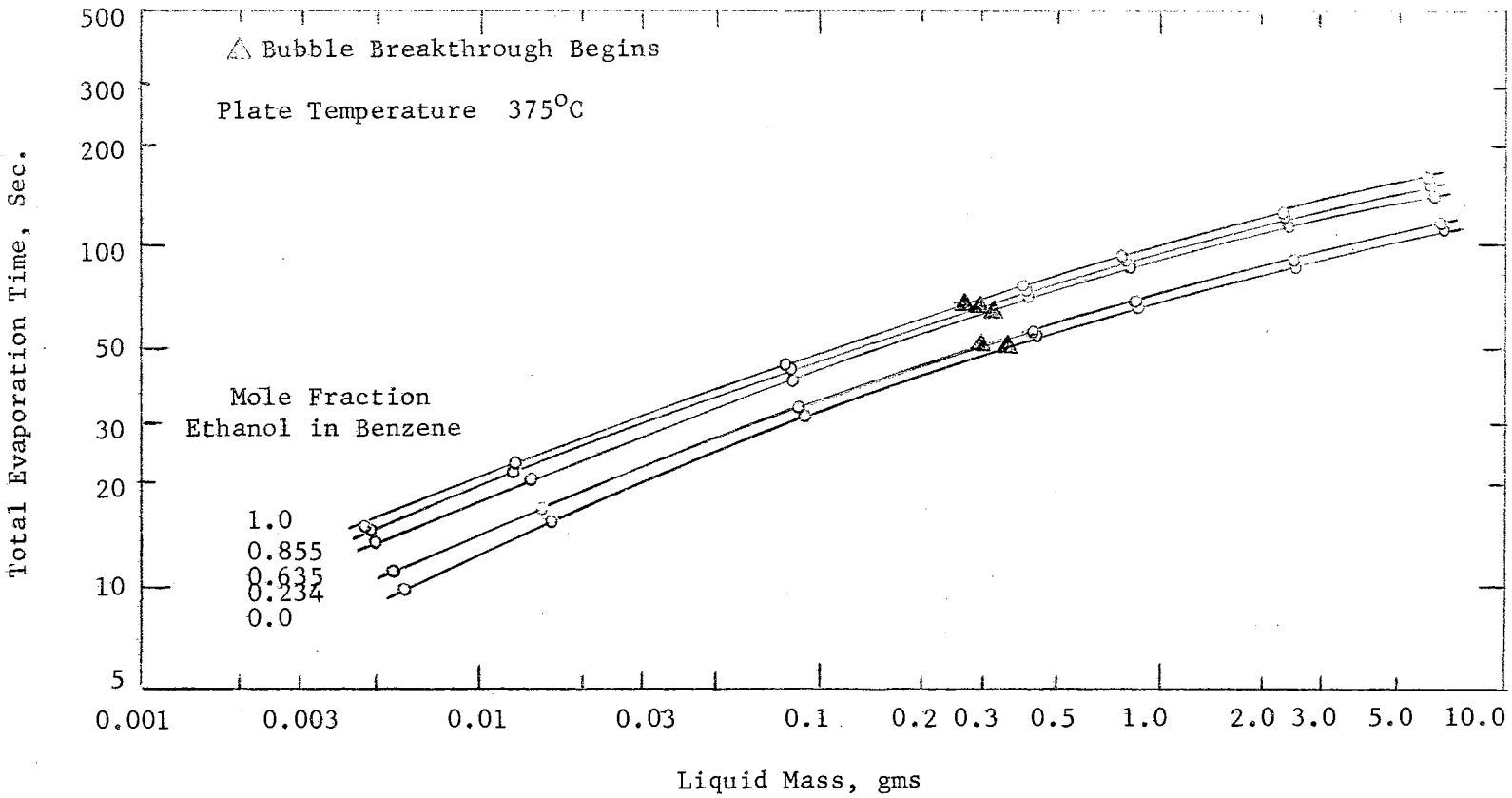

Figure 18. Total Evaporation Time vs. Liquid Mass for the Ethanol-Benzene System

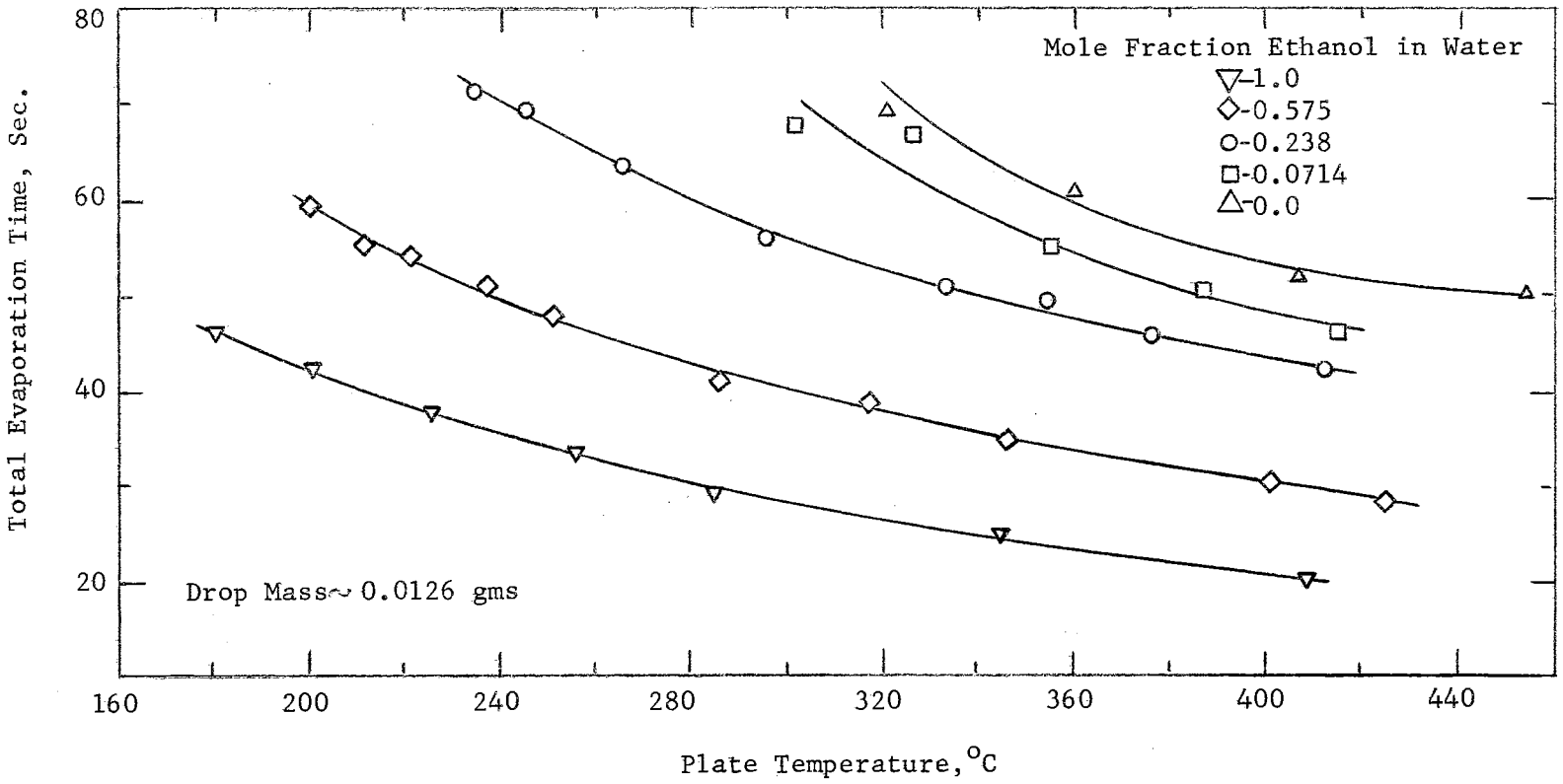

Figure 19. Total Evaporation Time vs. Plate Temperature for the Ethanol-Water System

Figures 20-22 show the theoretical curves for vaporization governed by equilibrium vaporization as well as the experimental data for change in liquid composition with a fraction of the original mass evaporated. The scatter of data is in part due to the difficulty in trying to sample a moving drop on a hot surface. Figure 20 also shows the theoretical curve for diffusional vaporization. The data apparently indicate that evaporation proceeds by equilibrium vaporization though there is an unexplained weak variation with initial mass for the ethanol-benzene system. For the benzene-toluene system the diffusional vaporization curve lies only slightly below the curve for equilibrium vaporization and therefore is not shown in Figures 21 and 22.

Leidenfrost Point

The Leidenfrost temperature was investigated for both pure and binary solutions. The time required for a liquid mass to completely evaporate increases as the plate temperature decreases down to a point where the liquid suddenly vaporizes in from two to five seconds after deposition. This sudden and drastic decrease in total evaporation time marks the transition from film to nucleate or transition boiling. The plate temperature yielding the maximum time for evaporation is the Leidenfrost point for that liquid. Several experimental techniques have been employed, which in some cases result in different values for the Leidenfrost temperature. The experimental data are summarized in Table I.

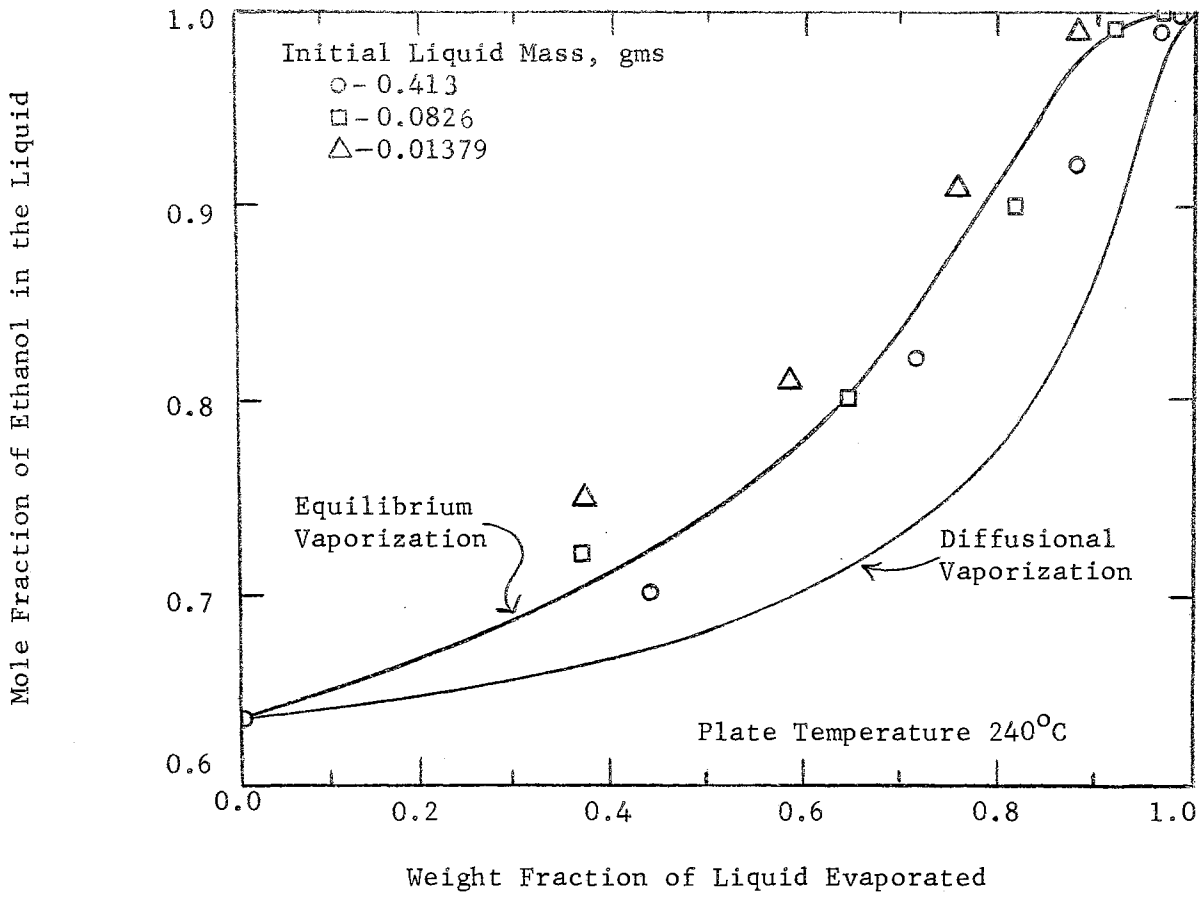

Figure 20. Change in Liquid Composition with Mass for the Ethanol-Benzene System

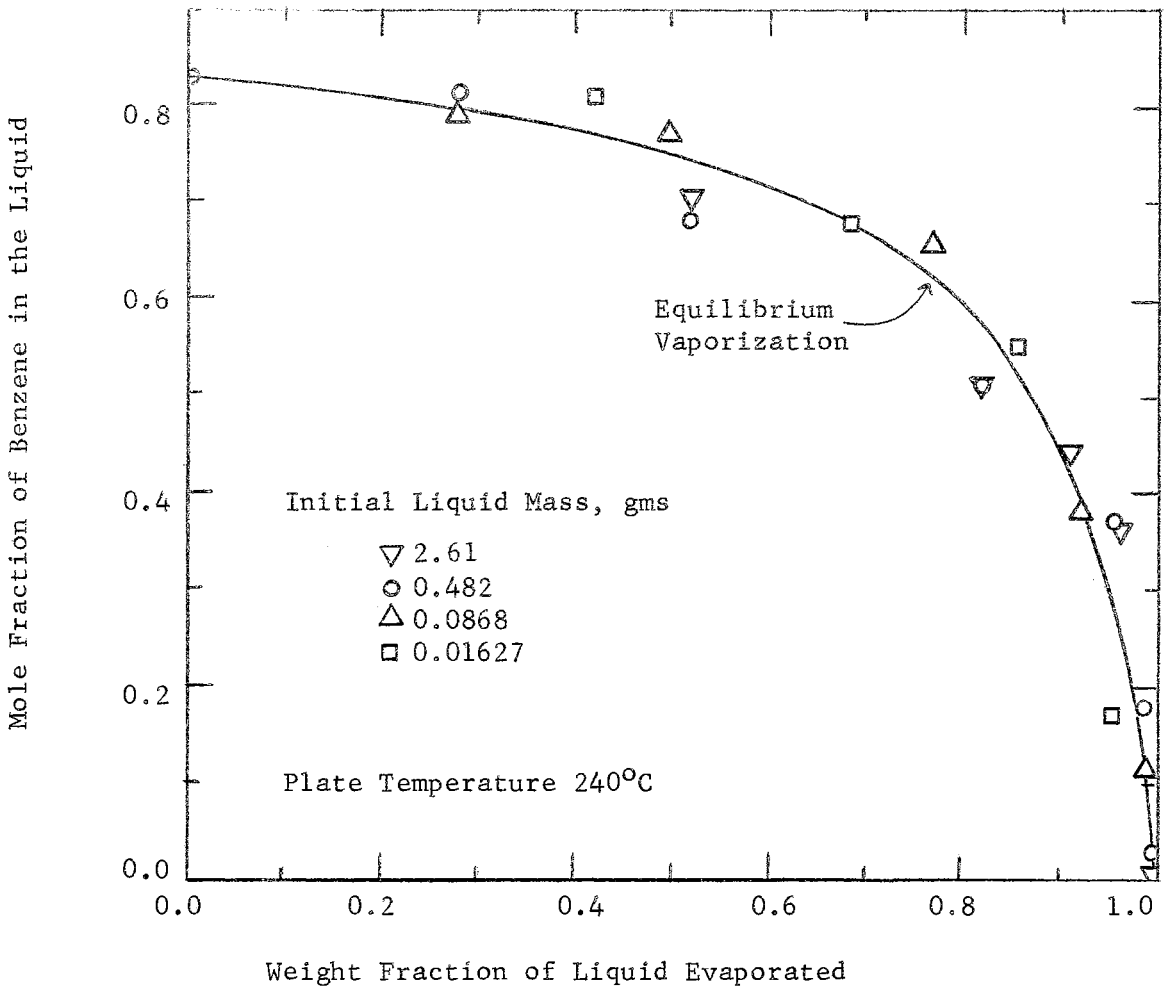

Figure 21. Change in Liquid Composition with Mass for the Benzene-Toluene System

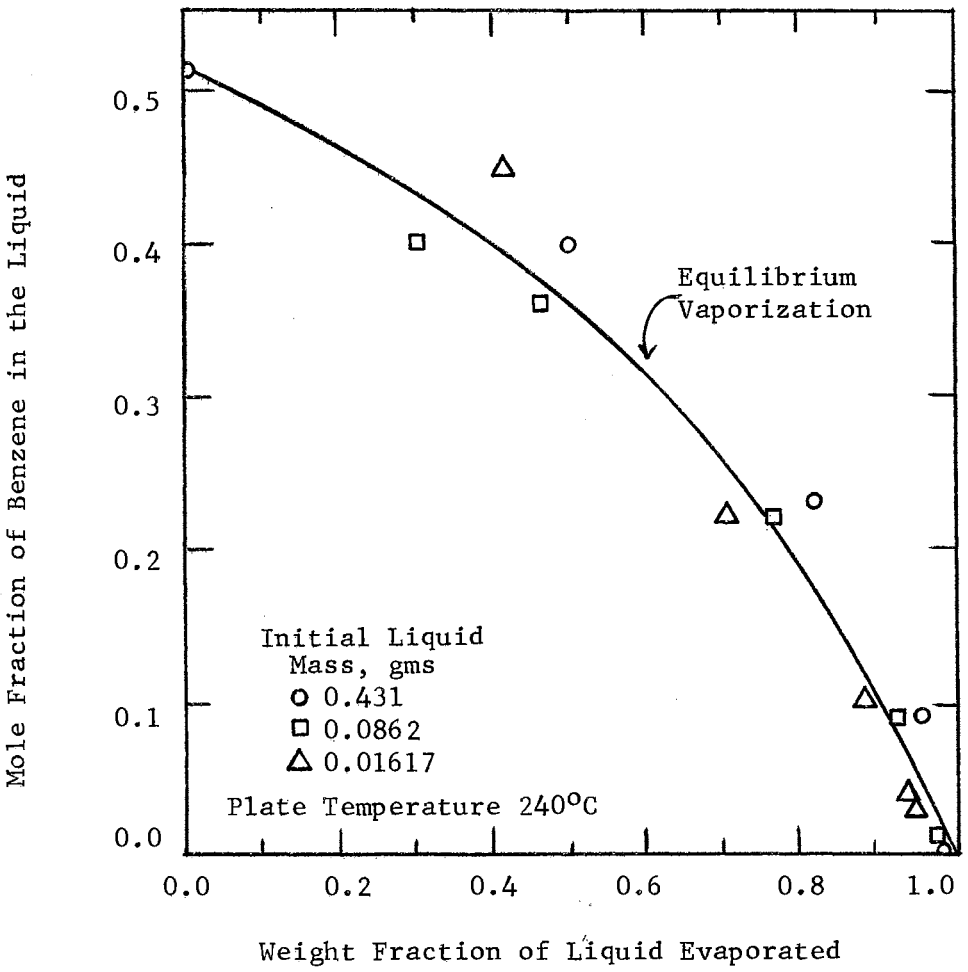

Figure 22. Change in Liquid Composition with Mass for the Benzene-Toluene System

TABLE I

THE LEIDENFROST TEMPERATURE FOR PURE LIQUIDS AND BINARY SOLUTIONS

Solution	Normal Boiling Point, °C	Constant Plate Temperature, °C		Transient Plate Temperature, °C
		Small Drops	Extended Masses	Extended Masses
Ethanol	78.4	175 (97)*	175 (97)*	148 (70)*
Benzene	80.1	180 (100)	180 (100)	154 (74)
Toluene	110.6	210 (100)	-	187 (76)
Water	100.0	320 (220)	264*(164)	161 (61)
Ethanol-Water System				
57.5 Mole % Ethanol	79.3	200 (121)	-	-
23.8	82.6	234 (151)	-	-
7.14	88.6	301 (212)	-	-
Ethanol-Benzene System				
85.5 Mole % Ethanol	70.5	180 (110)	180 (110)	-
63.5	68.2	180 (112)	-	-
44.9	67.9	-	-	150 (82)
23.4	68.3	180 (112)	180 (112)	-
Benzene-Toluene System				
83.5 Mole % Benzene	83.7	-	-	185 (84)
51.5	91.8	202 (110)	-	-

*Numbers in parentheses are the difference between the Leidenfrost temperature and the normal boiling point.
**Liquid poured onto plate.

No experimental difficulty was encountered in determining the Leidenfrost points for either pure or binary solutions of the organic liquids. Water and solutions with a high concentration of water present many problems. Water temporarily goes into transition or nucleate boiling upon initially touching the heated plate at temperatures below 310°C. This causes rapid generation of vapor below the liquid, sometimes resulting in the spattering of the mass into many smaller masses. The remaining liquid then continues to evaporate in film boiling. This results in considerable uncertainty for the Leidenfrost point for water and its solutions. Heating the water to its boiling point before placing it on the plate, in some cases, reduces or even eliminates the initial contact of the liquid with the plate surface. The use of liquids at their boiling point instead of at room temperature did not substantially decrease the total evaporation time. This was substantiated by Gottfried (12) for drops and verified in this work for extended masses. Representative data are presented in Table II.

For the binary system ethanol-water, the higher the concentration of water the closer is the behavior during evaporation to that of pure water. An interesting occurrence accompanies the evaporation of drops with a high water content at plate temperatures near the Leidenfrost point: after the drop has been evaporating for a period of time, it jumps on the plate or in some cases splatters into a fine spray. This phenomenon is reproducible as

indicated in Table III. This drop had a total evaporation time of 65 seconds. The "explosion" occurs after 39 seconds of evaporation, or when the weight fraction of initial liquid that had vaporized was 0.88. The mole fraction of an initial 57.5 mole percent solution of ethanol in water as a function of weight fraction of the original mass evaporated has been calculated, assuming equilibrium vaporization. At weight fractions evaporated greater than 0.86, the concentration of ethanol in the liquid has decreased to a value below 18 mole percent, and drops with such a high concentration of water usually vaporize very rapidly on a 200°C surface.

TABLE II

THE EFFECT OF INITIAL LIQUID TEMPERATURE ON TOTAL EVAPORATION TIME

Solution: Pure Ethanol

Plate Temperature: 300°C

	Total Evaporation Time, Seconds	
Liquid Mass, gms	Liquid Initially at Room Temperature	Liquid Initially at its Boiling Point
6.28	214.0	212.1
2.36	166.0	164.2
0.778	121.8	122.6

TABLE III

DATA FOR A TYPICAL CASE OF DESTRUCTION OF STABLE FILM BOILING DURING EVAPORATION

Initial Composition: 57.5 Mole % Ethanol
42.5 Mole % Water

Plate Temperature: 200°C

Initial Mass: 0.0146 gms

Total Evaporation Time, sec.	Time Drop Remained on Plate Before Splattering, sec.
65.1	39.8
64.8	36.7
65.7	38.0
64.4	41.5
65.0	39.0

The variation of the Leidenfrost point with composition for the ethanol-water, the ethanol-benzene, and the benzene-toluene systems are shown in Figure 23. The Leidenfrost point for binary solutions varies quite regularly between the Leidenfrost values for the pure components.

Leidenfrost points were also determined by a transient plate temperature technique. A mass of liquid was placed on the plate at a plate temperature above the Leidenfrost point. The plate was then cooled while the liquid evaporated. The plate temperature at which the liquid collapsed onto the plate (transition boiling) was considered the transient Leidenfrost point. The average rate of cooling of the plate was 0.1°C per second. The rate of cooling was higher when the liquid was first placed on the plate and lower

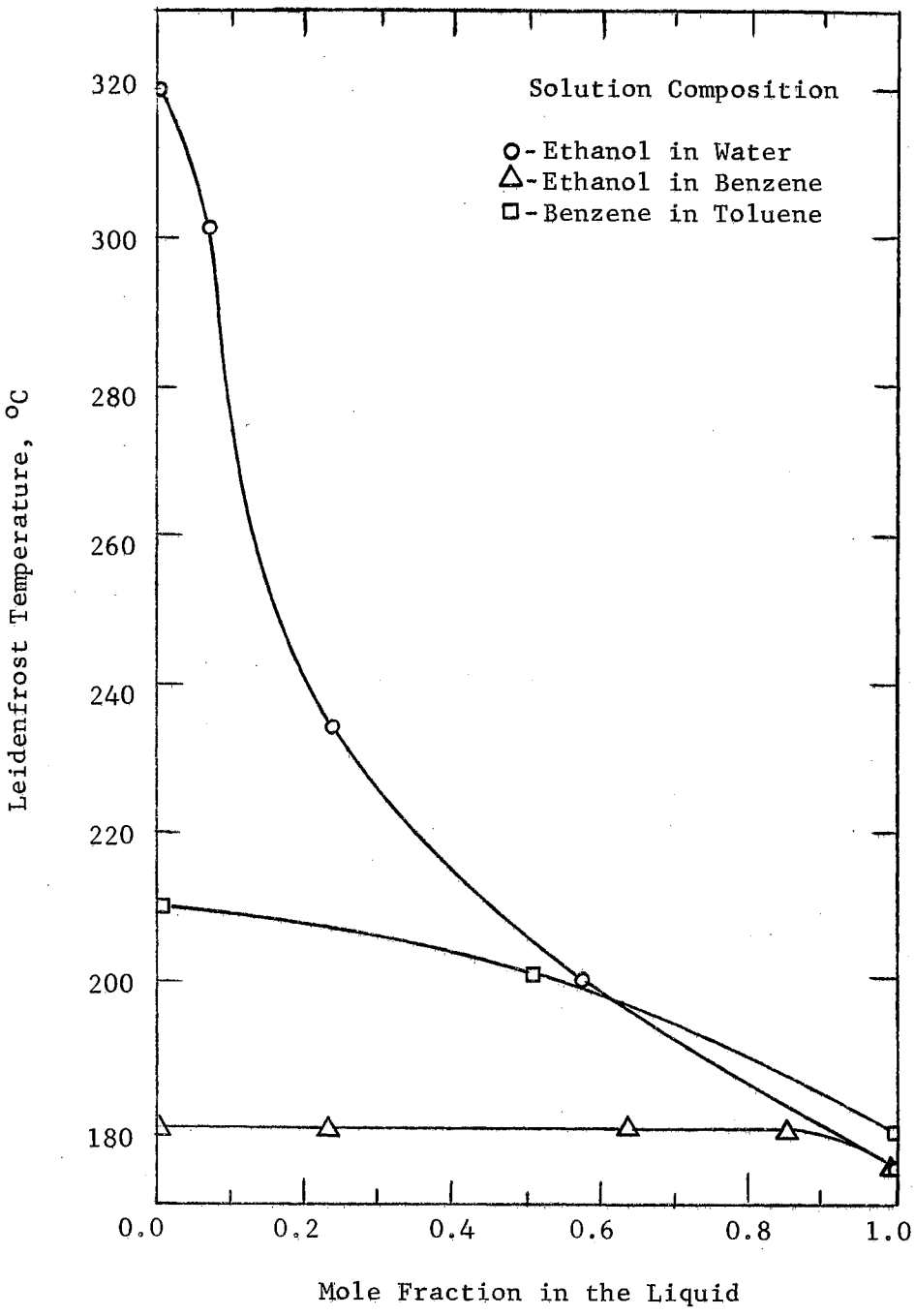

Figure 23. Variation of the Leidenfrost Temperature with Composition

near the Leidenfrost temperature. The results are presented in Table I for comparison with the values obtained by the other method. The Leidenfrost temperatures obtained by this technique are all very much below the values obtained previously.

As the liquid is placed on the heated plate, its lower surface must be heated at least to its boiling point and then sufficient vapor must be generated to prevent contact with the plate and to support the liquid above the surface. This must happen within that fraction of a second before the liquid reaches the plate. Therefore, the Leidenfrost point is the temperature required for the minimum rate of energy transfer to satisfy these requirements. Since the latent heat of vaporization of water is over five times as great as that of benzene or toluene and its specific heat is twice that for these organic liquids, it appears that the difference in behavior of water compared to the organics when placed on a hot surface at low plate temperatures is due to the greater energy requirements in establishing a vapor film to support the mass.

For liquids already supported by their vapor film, as the plate cools, substantially lower temperatures are possible before the liquid touches the plate and goes into transition boiling. Once a vapor film has been established beneath the liquid, the energy requirements are reduced. It is interesting to note that the difference in Leidenfrost points obtained by this technique for benzene and toluene is still 30°C, the value obtained from the steady state technique.

There can be little doubt that the Leidenfrost point depends upon the technique used in its determination. In Table IV a comparison is made of the Leidenfrost points determined by several investigations. References (14) and (22) used techniques consistent with the constant plate temperature experiments in this study and the results are in good agreement. All this suggests that the experiments with transient plate temperatures represent a state of metastable film boiling where small surface disturbances result in regression to transition boiling. In fact, Leidenfrost temperatures lower than those reported in this work have since been attained by Baumeister (3) and Wachters (32).

TABLE IV

COMPARISON OF LEIDENFROST TEMPERATURE OBTAINED BY VARIOUS WORKERS

All Temperatures in ^{o}C

		Drops			Extended Masses		Pool Boiling		
Liquid	Boiling Point	Present Work	Ref. (14)	Tamura & Tanasawa (26)	Present Work	Ref. (22)	Hosler & Westwater (15)	Berenson Theoretical (4)	Transient Plate Temperatures - Present Work
Water	100.0	320	280	302	264	300	258	177	161
Ethanol	78.4	175	178	185	175	183	-	158	148
Benzene	80.1	180	185	195	180	184	-	166	154

Liquid Dynamics During Evaporation

It is apparent that surface disturbances affect the Leidenfrost Phenomenon. For this reason a brief qualitative description of the liquid behavior during evaporation is presented.

1. Evaporation of Drops: Drops of an initial volume of about 0.02 cc when first placed on the plate, are not spherical but have the shape of a slightly flattened sphere. They pulsate between this biscuit shape and a slightly vertically elongated sphere at slow and irregular frequencies of about one per second. As the drop volume decreases, the frequency of these pulsations increases to the point where the outline of the drop is blurred. This is accompanied by violent surface waves and ripples. The drop, much smaller now, becomes almost perfectly spherical and too small for surface disturbances to be observed. Occasionally a vapor bubble formed inside the drop when it first touched the plate. This bubble is swirled violently through the entire volume of the drop. In a few cases, as the drop becomes very small, it starts bouncing on the plate. This bouncing occurs in the last four or five seconds before the drop is totally vaporized and the drop bounces to a height five or six times its diameter. This phenomenon usually increases the total evaporation time by about two seconds. The drops are constantly moving about the plate. These movements are sometimes random but usually follow the circular path about the rim of the plate, at speeds up to 30 cm/sec. It is not unusual for a drop

traveling in one direction to reverse directions. These observations have been made for both pure and binary liquids.

2. Evaporation of Extended Masses: For large initial volumes, the vapor generated beneath the mass is not able to escape from the sides, and so it accumulates into a bubble that eventually breaks through the mass. In some cases, this bubble breakthrough is extremely violent. The entire surface of the mass is covered with ripples and waves. (Reference (22) showed that there is a high degree of order in this apparently chaotic process.) As evaporation proceeds, the bubble breakthrough decreases until only one bubble at a time breaks through the mass. The outline of the mass is now circular and the surface smooth. Further decreases in mass result in the cessation of the bubble breakthrough. The mass starts to oscillate in a regular pattern, and the surface now starts a slow but steadily increasing rotation, usually on the order of 4 cm/sec for a 1 cm diameter water globule ($\sim$1 ml). This rotation increases as the mass decreases until it leads to pulsation and vibration of the drops.

As can be realized from this qualitative discussion of the liquid dynamics during evaporation, the liquid motion is very complex in detail; however, the sequence of events is always followed.

Theoretical Model

An analytical model has been proposed for the Leidenfrost Phenomenon for binary liquid drops. A test of this model is how

well it predicts the experimental data. The analytical equations were solved on an IBM-1410 digital computer. The computer time averaged one minute per ten seconds of drop evaporation time. The experimental total evaporation times for both pure liquids and binary solutions are shown in Figures 24 to 34. The solid curves represent the results obtained from the analytical model. Figures 24, 28, 32, and 34 are for the pure liquids water, ethanol, benzene, and toluene, respectively. The data are well predicted by the theory for the smaller masses. The weakest agreement is for ethanol. For the larger masses, the agreement is poorest for benzene. The theoretical curve is of the right shape but displaced above the data. This is true but to a lesser extent for the other solutions. These theoretical curves are essentially the same as those computed from the analytical model proposed by Gottfried, Lee, and Bell. However, their model is valid only for pure liquids.

Figures 25-27, 29-31, and 33 present the data and theoretically predicted curves for total evaporation time of binary solutions. The data and theoretical curves vary in a regular manner as the composition of the mixture shifts between the pure components.

The total evaporation time data of pure benzene and toluene as well as a 51.5 mole percent solution of benzene in toluene are essentially the same. This is no doubt due to their very similar chemical and physical properties. However, the theoretically predicted curves for these pure components are not the same. They differ in both slope and total evaporation time for a given plate

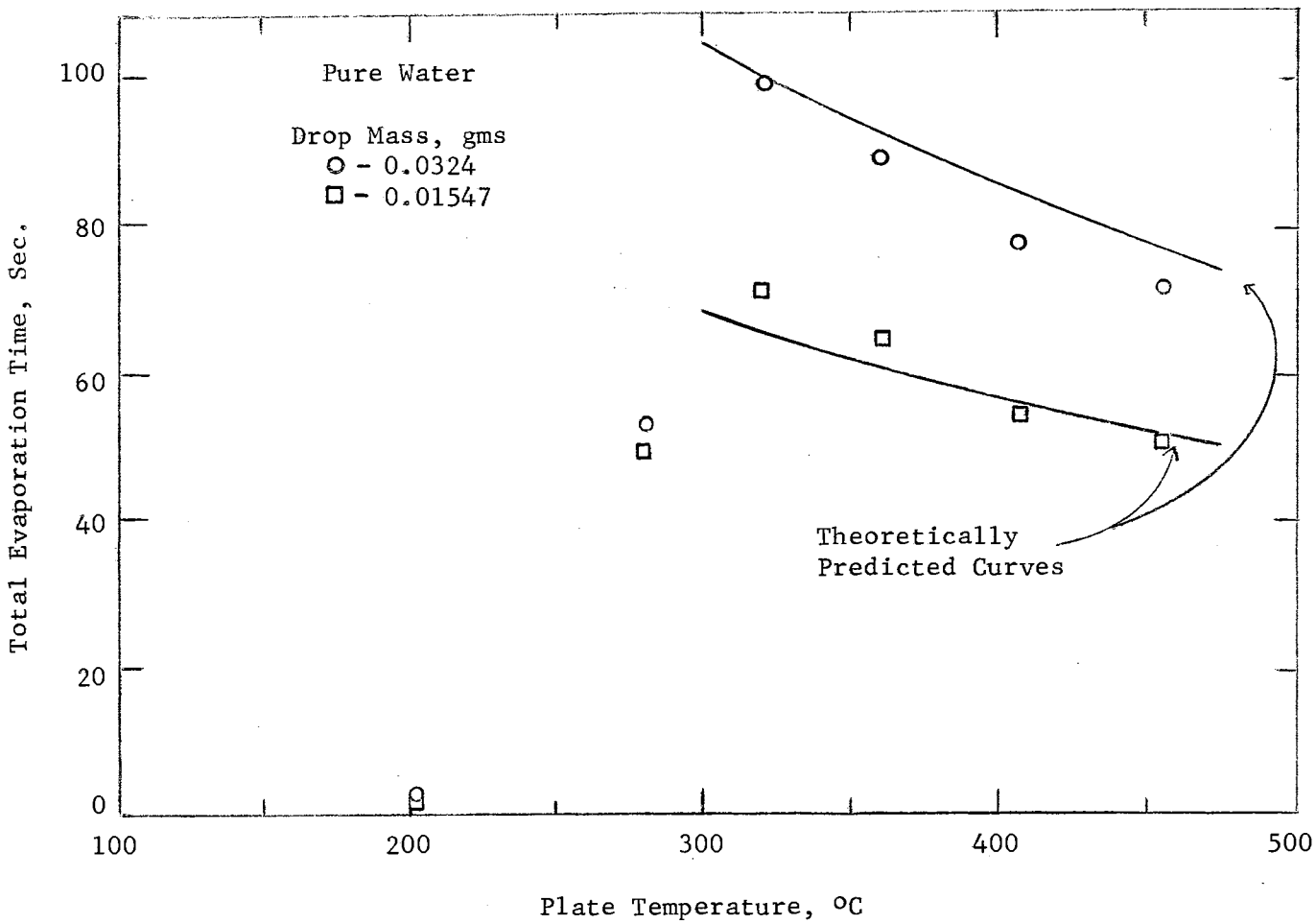

Figure 24. Drop Evaporation Time vs. Plate Temperature for Water

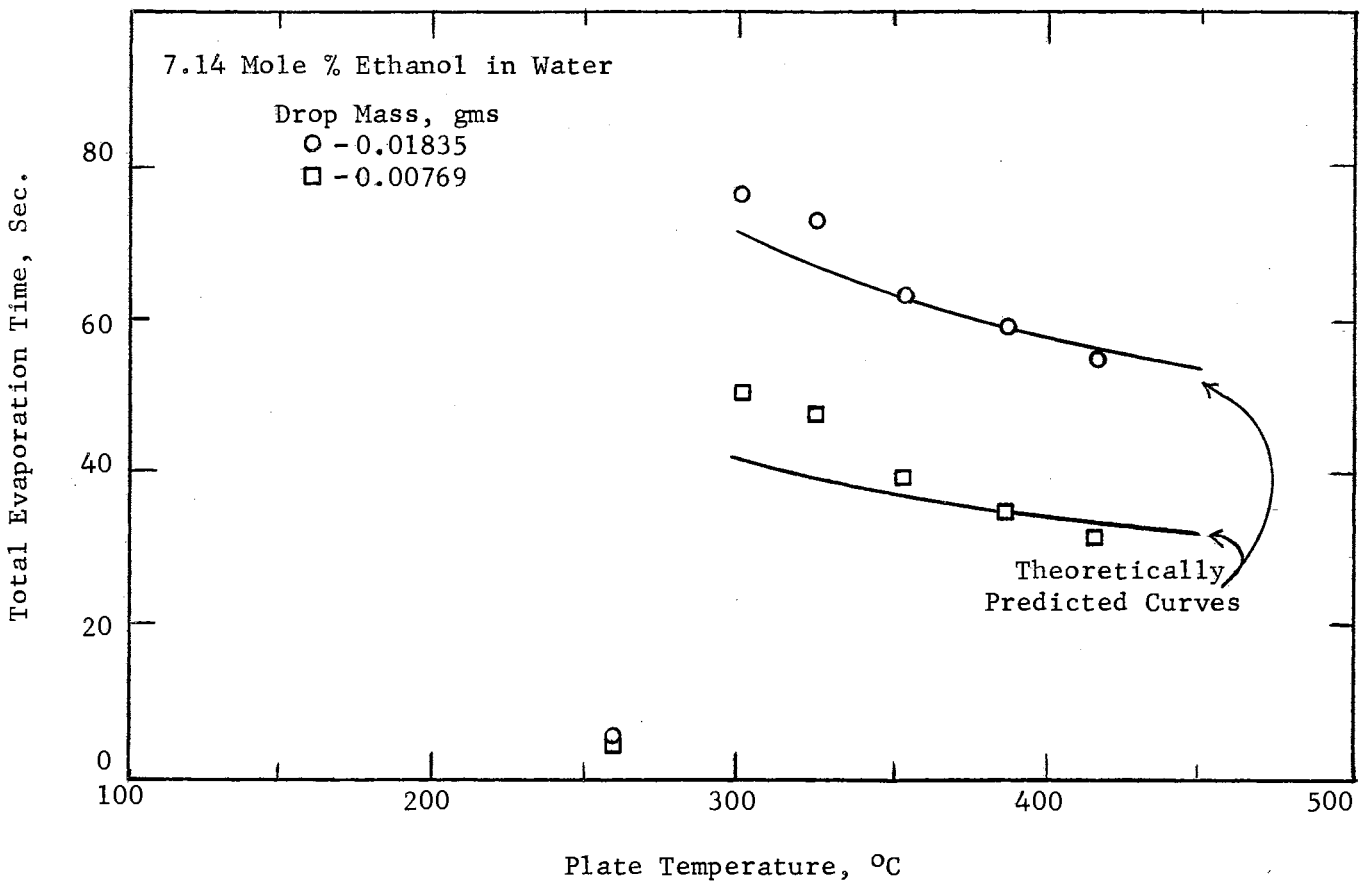

Figure 25. Drop Evaporation Time vs. Plate Temperature for the Ethanol-Water System

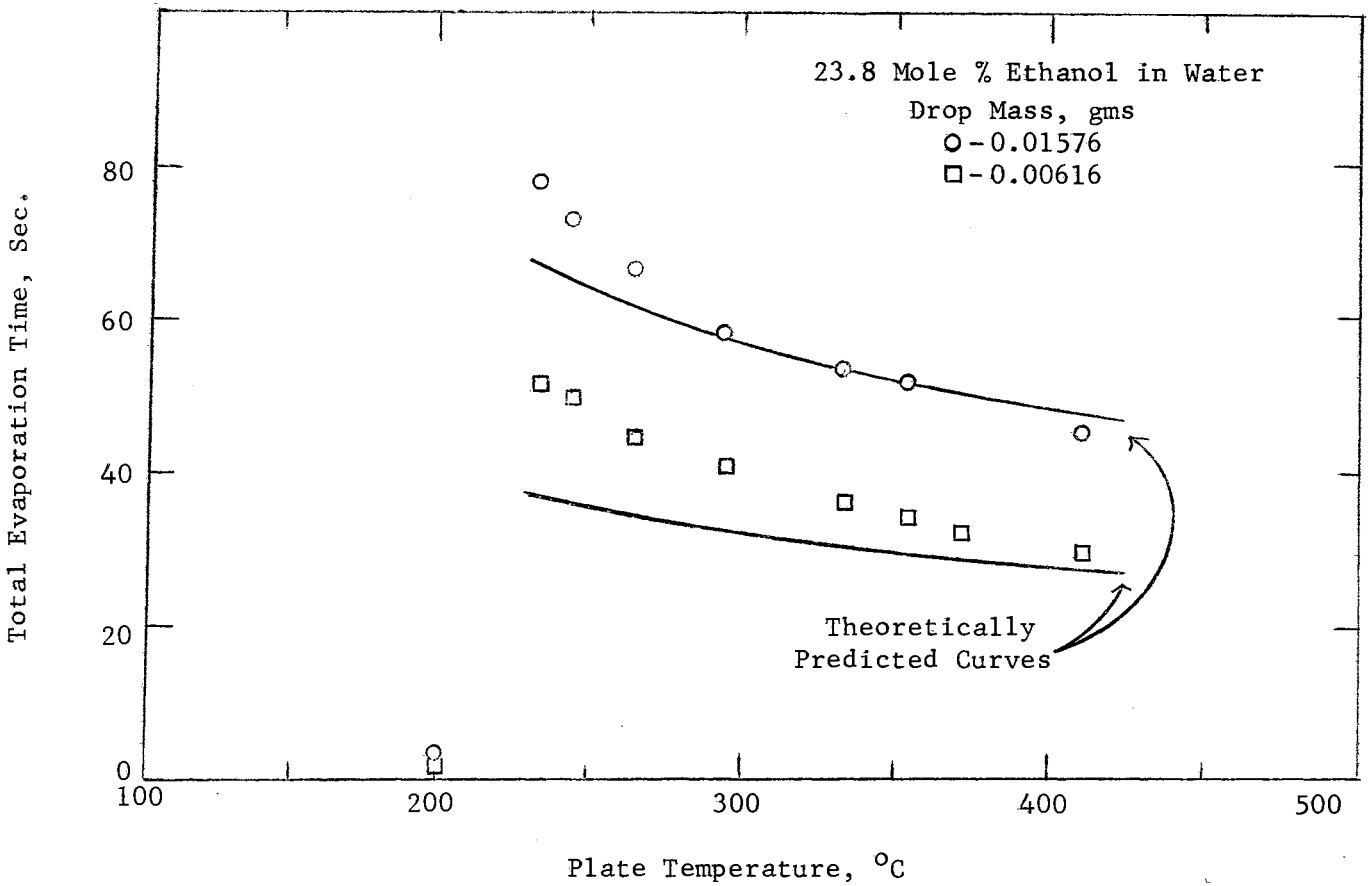

Figure 26. Drop Evaporation Time vs. Plate Temperature for the Ethanol-Water System

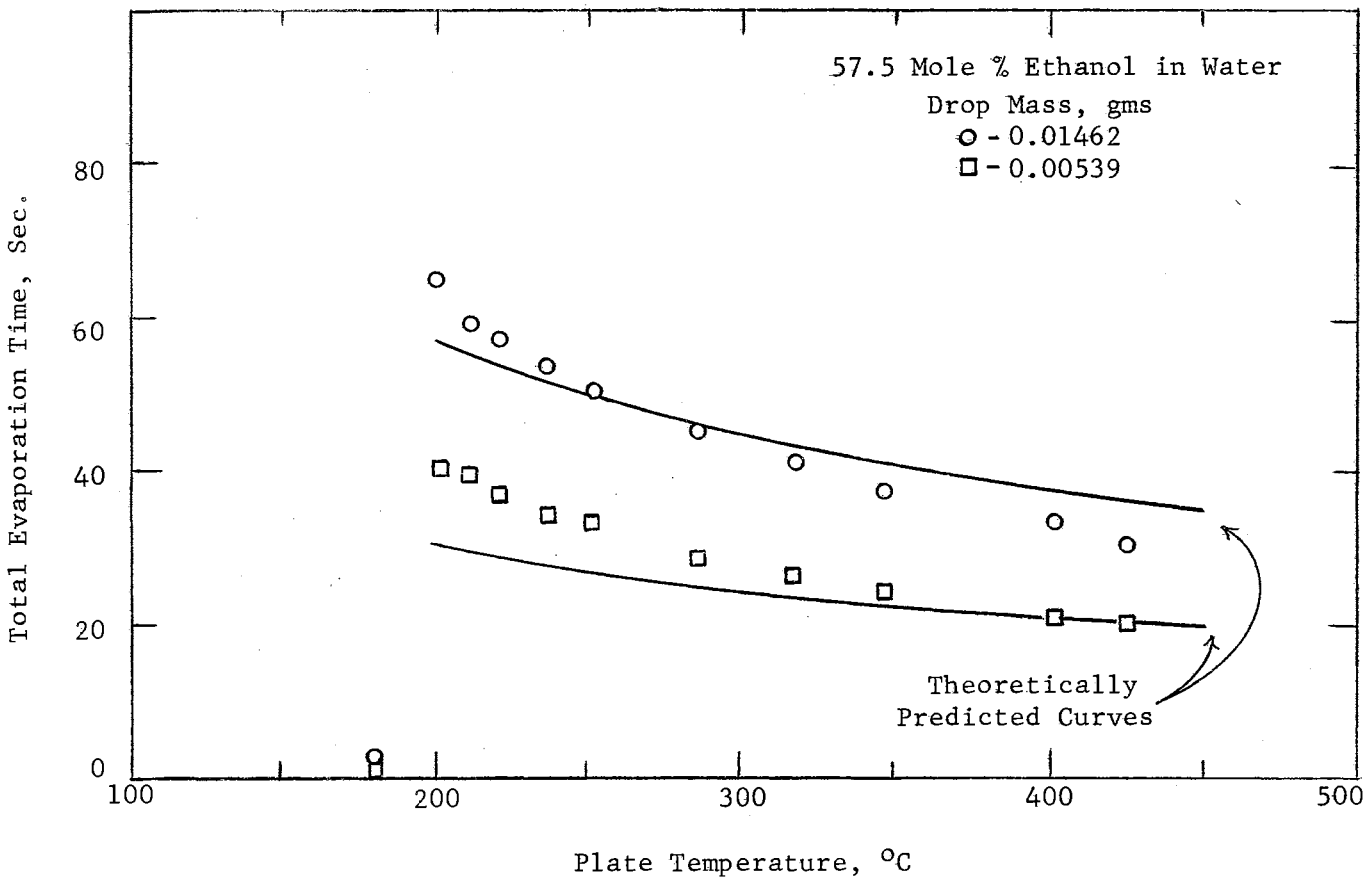

Figure 27. Drop Evaporation Time vs. Plate Temperature for the Ethanol-Water System

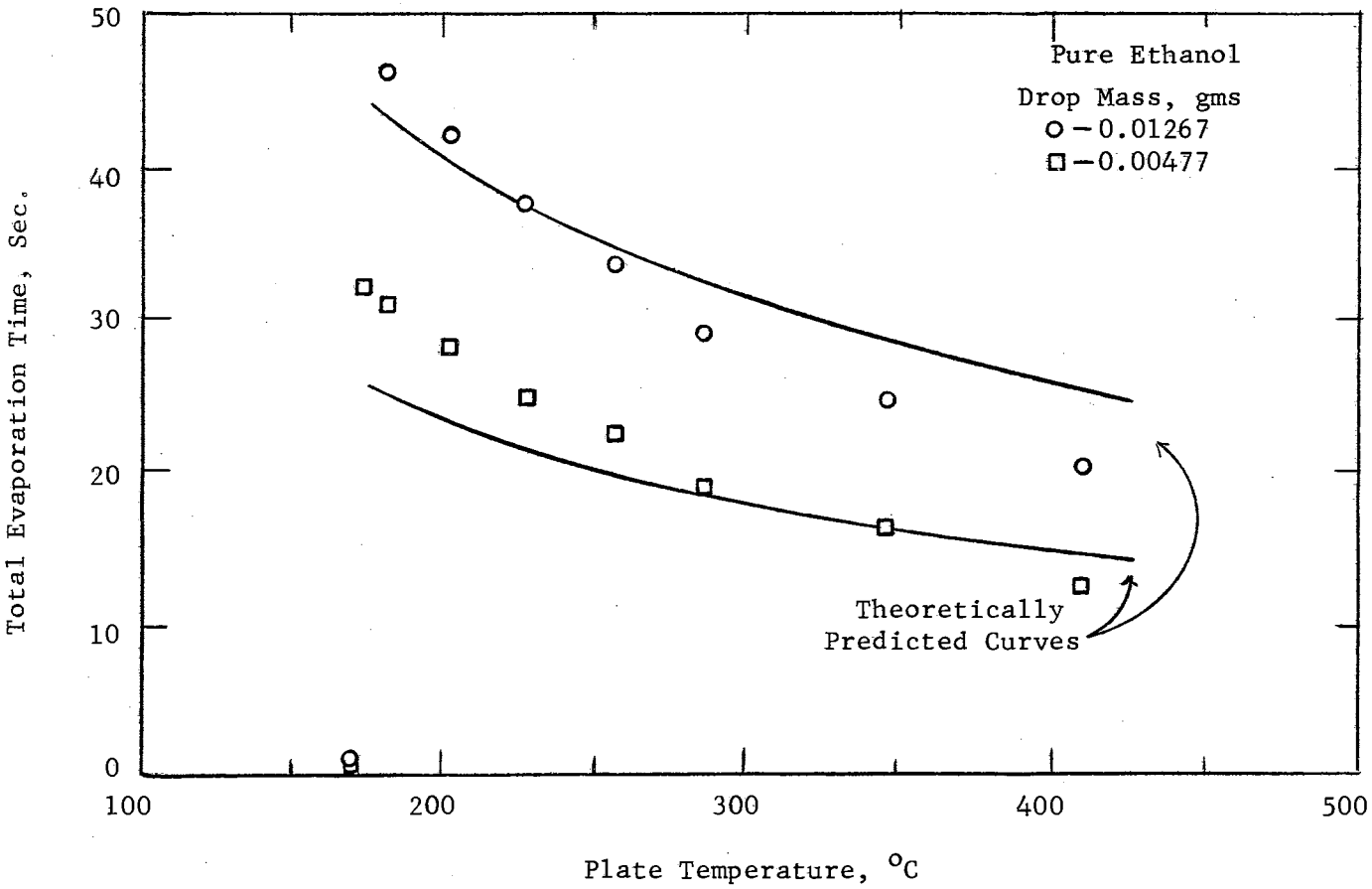

Figure 28. Drop Evaporation Time vs. Plate Temperature for Ethanol

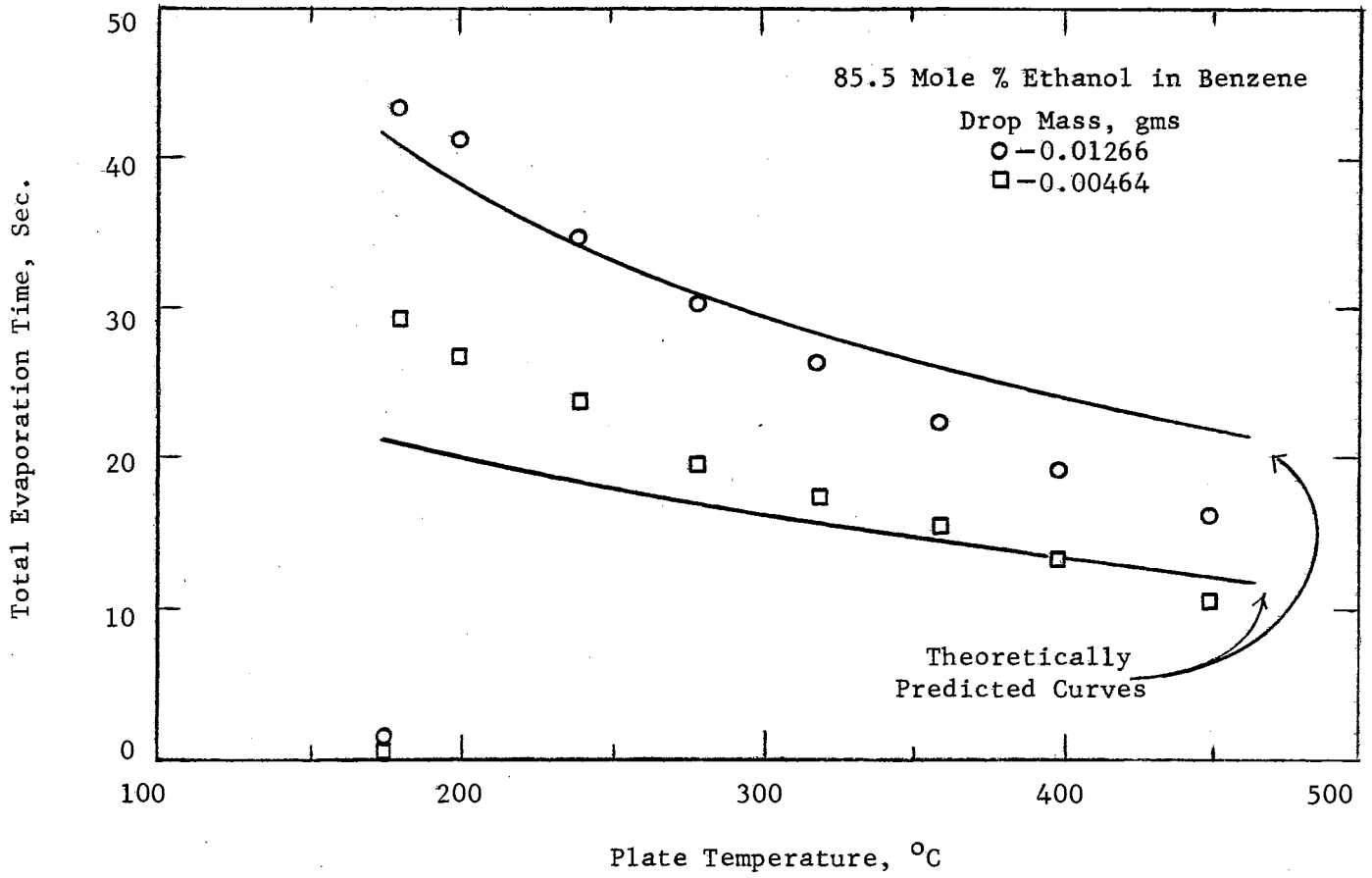

Figure 29. Drop Evaporation Time vs. Plate Temperature for the Ethanol-Benzene System

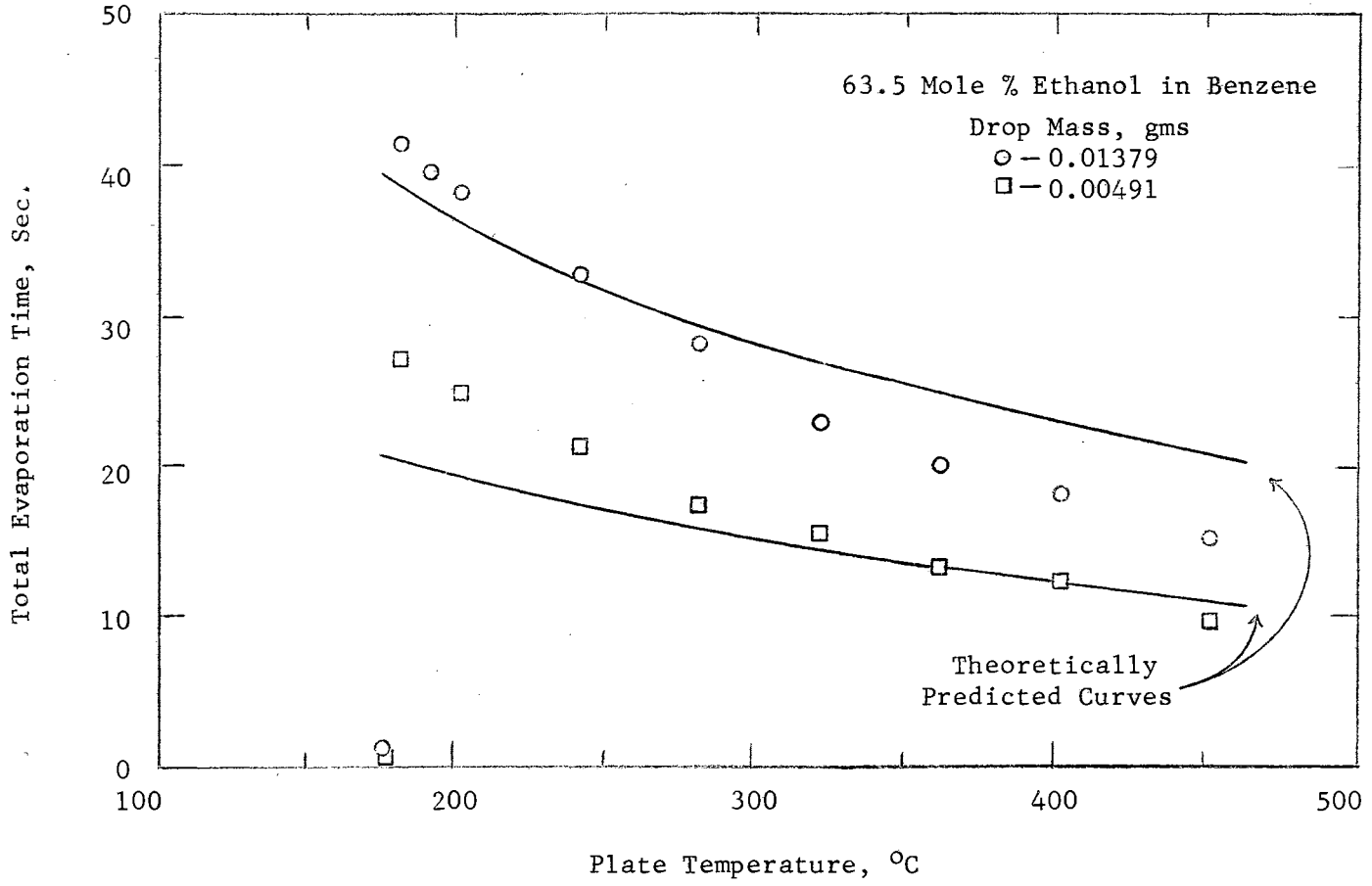

Figure 30. Drop Evaporation Time vs. Plate Temperature for the Ethanol-Benzene System

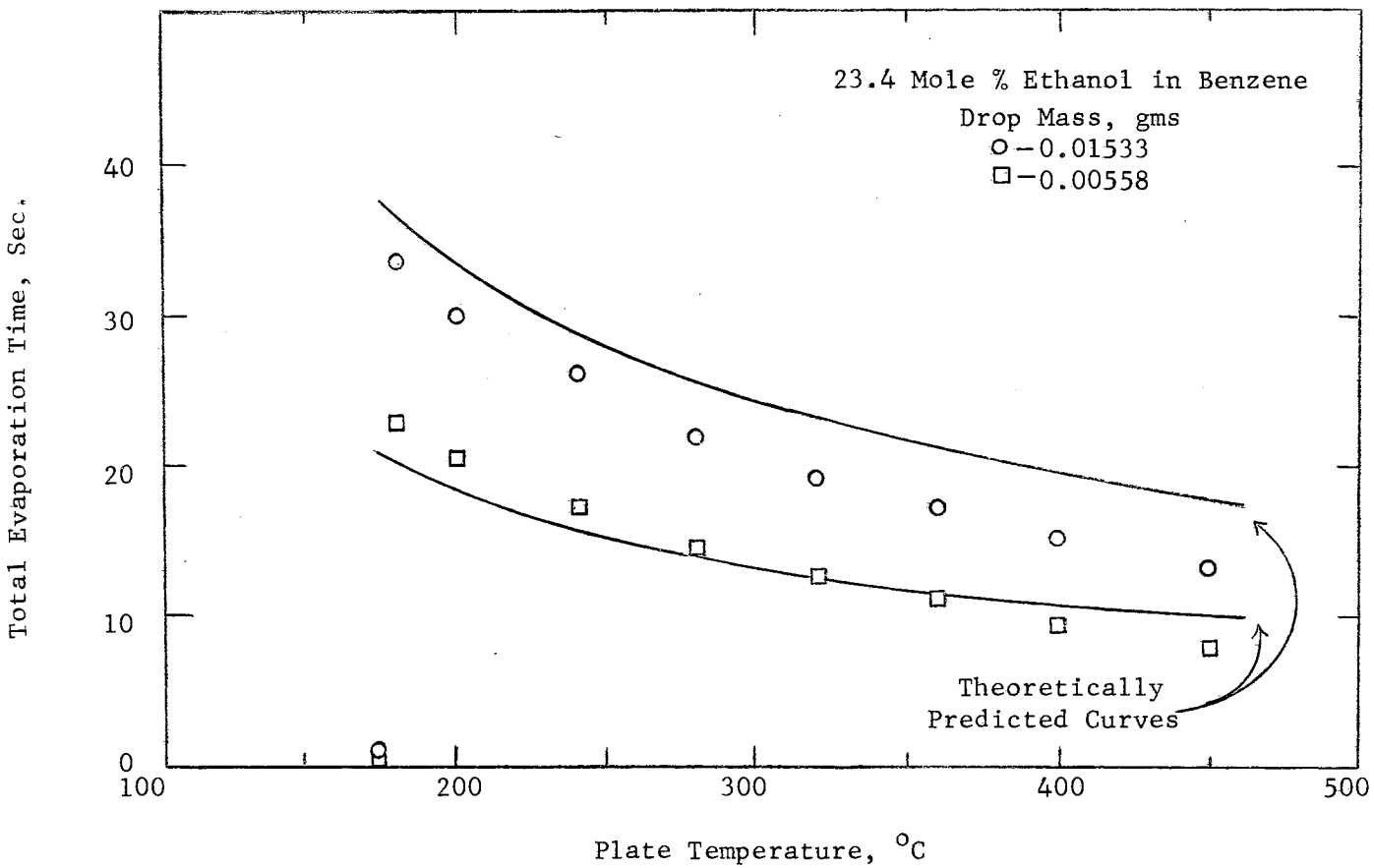

Figure 31. Drop Evaporation Time vs. Plate Temperature for the Ethanol-Benzene System

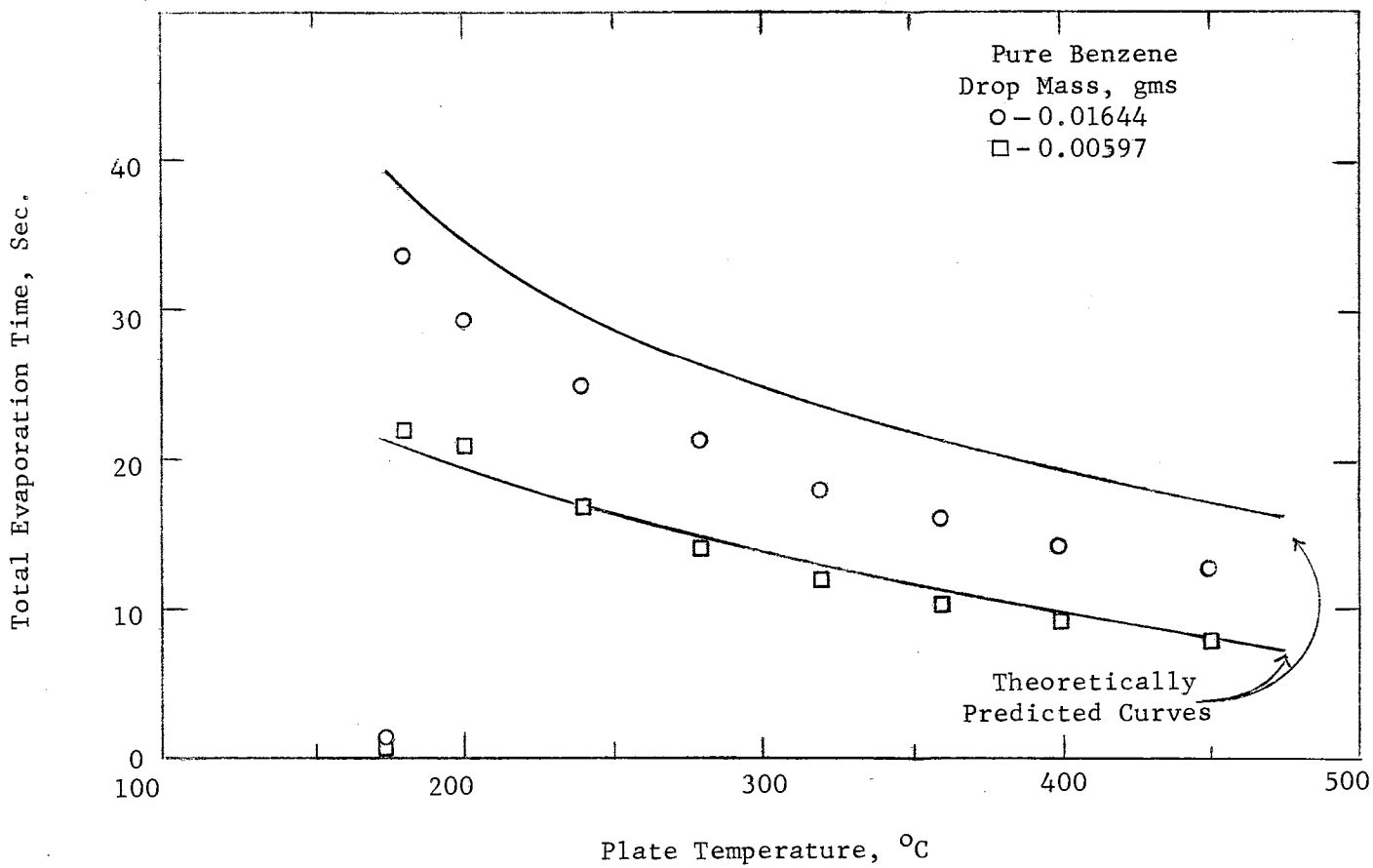

Figure 32. Drop Evaporation Time vs. Plate Temperature for Benzene

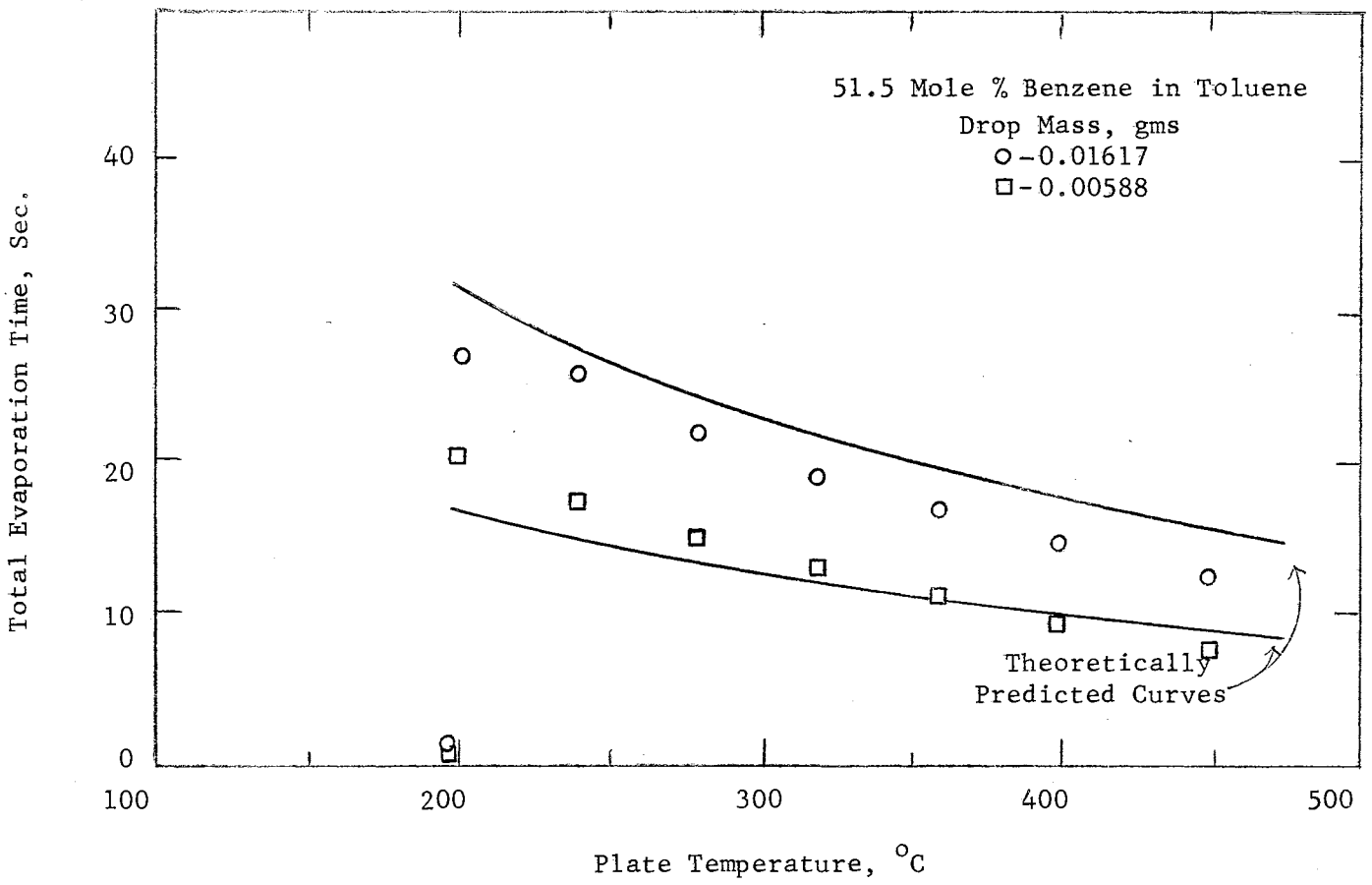

Figure 33. Drop Evaporation Time vs. Plate Temperature for the Benzene-Toluene System

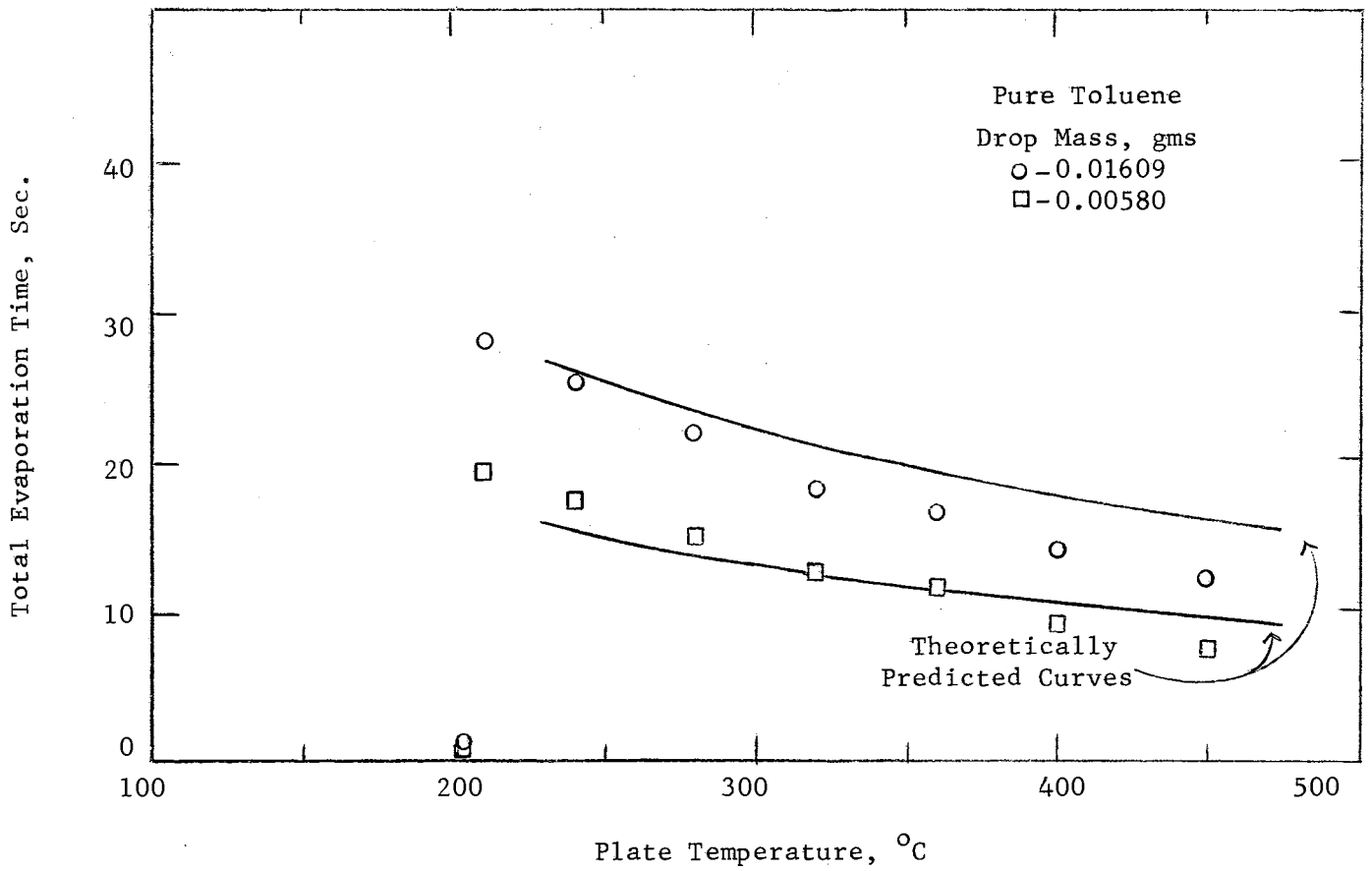

Figure 34. Drop Evaporation Time vs. Plate Temperature for Toluene

temperature. This possibly illustrates how dependent the analytical model is upon the physical properties chosen for the components. A difference in slope could be due to different temperature dependence for the physical properties while the absolute displacement of the curves may be due to inexact values for the same physical property at the same temperature for the two liquids. Considering these limitations, and the fact that no arbitrary constants are introduced into the results, the agreement between experiment and theory is quite good.

The theoretical model assumes that equilibrium vaporization governs the composition change of the liquid. The solution of the theoretical equations therefore coincides with the composition change as predicted by equilibrium vaporization as presented in Figures 20-22. The data are for various initial masses at a constant plate temperature of 240°C but the results should also be independent of plate temperature.

CHAPTER VII

CONCLUSIONS

The following conclusions result from this study:

(1) The Leidenfrost Phenomenon for binary solutions is very similar to that for the pure substances and the phenomena vary in a regular way with composition.

(2) Vaporization of binary solutions apparently occurs by equilibrium vaporization; composition changes are nearly independent of the mass of the liquid.

(3) The Leidenfrost point depends upon the technique used in its determination. The transient technique probably represents the best test of the lower stability limit for film boiling

(4) The Leidenfrost point for a binary solution is intermediate between the values for the pure components.

(5) The theoretical model for predicting the evaporation time of binary liquid solutions is in reasonable agreement with the experimental data.

A SELECTED BIBLIOGRAPHY

1. Anderson, L. B., and Wenzel, L. A., "Introduction to Chemical Engineering," McGraw-Hill Book Company, Inc., New York, (1961).

2. Baumeister, K. J., Hammill, T. D., Schwartz, F. L., and Schoessow, G. J., "Film Boiling Heat Transfer to Water Drops on a Flat Plate," Chem. Eng. Progr. Symposium Ser. No. 64, Vol. 62, 52, (1966).

3. Baumeister, K. J., Hendricks, R. C., and Hammill, T. D., "Metastable Leidenfrost States," NASA TN D-3226, (1966).

4. Berenson, P. J., "Film-Boiling Heat Transfer from a Horizontal Surface," Trans. ASME, 83, 341, (1961).

5. Bird, R. B., Stewart, W. E., and Lightfoot, E. N., "Transport Phenomena," John Wiley and Sons, Inc., New York, (1960).

6. Brown, G. G., et al., "Unit Operations," John Wiley and Sons, Inc., (1950).

7. Carlson, H. C., and Colburn, A. P., "Vapor-Liquid Equilibrium of Non-ideal Solutions," Ind. Eng. Chem. 34, 581, (1942).

8. Craven, P. M., and Lambert, J. D., "The Viscosities of Organic Vapours," Proc. Roy. Soc. (London), A205:439, (1951).

9. Dodge, B. G., "Chemical Engineering Thermodynamics," McGraw-Hill Book Company, Inc., New York, (1944).

10. Eduljee, H. E., and Rao, J. Narasinga, "Correlations of Vapour-Liquid Equilibrium Data - I Ethanol - Water System," Trans. Indian Inst. Chem. Eng. 7, 129, (1954-55).

11. Fuller, E. N., Schettler, P. D., and Giddings, J. C., "A New Method for Prediction of Binary Gas-Phase Diffusion Coefficients," Ind. Eng. Chem. 58, 19, (1966).

12. Gottfried, B. S., "The Evaporation of Small Drops on a Flat Plate in the Film Boiling Regime," Ph.D. Thesis, Case Institute of Technology, Cleveland, Ohio, (1962).

13. Gottfried, B. S., and Bell, K. J., "Film Boiling of Spheroidal Droplets," Ind. Eng. Chem. Fundamentals, 5, 561, (1966).

14. Gottfried, B. S., Lee, C. J., and Bell, K. J., "The Leidenfrost Phenomenon: Film Boiling of Liquid Droplets on a Flat Plate," Intern. J. Heat Mass Transfer, 9, 1167, (1966).

15. Hosler, E. R., and Westwater, J. W., "Film Boiling on a Horizontal Plate," ARS Journal, 32, 553, (1962).

16. Hougen, O. A., Watson, K. M., and Ragatz, R. A., "Chemical Process Principles," Part I, 2nd ed., John Wiley and Sons, Inc., New York, (1954).

17. Keyes, F. G., and Sandell, D. J., Jr., "New Measurements of the Heat Conductivity of Steam and Nitrogen," Trans. Am. Soc. Mech. Engrs. 72, 767, (1950).

18. Kunz, K. S., "Numerical Analysis," McGraw-Hill Book Company, Inc., New York, (1957).

19. Lee, C. J., "The Leidenfrost Phenomenon for Small Droplets," Ph.D. Thesis, Oklahoma State University, Stillwater, Oklahoma, (1965).

20. Lewis, W. L., and Squires, L. "Evaporation of Mixed Lacquer Solvents," Ind. Eng. Chem. 29, 109, (1937).

21. Patel, B. M., "The Leidenfrost Phenomenon for Extended Liquid Masses," Ph.D. Thesis, Oklahoma State University, Stillwater, Oklahoma, (1965).

22. Patel, B. M., and Bell, K. J., "The Leidenfrost Phenomenon for Extended Liquid Masses," Eng. Progr. Symposium Ser. No. 64, Vol. 62, 52, (1966).

23. Perry, J. H. (ed.), "Chemical Engineers' Handbook," 4th ed., McGraw-Hill Book Co., Inc., New York, (1963).

24. Reid, R. C., and Sherwood, "The Properties of Gases and Liquids," McGraw-Hill Book Company, Inc., New York, (1950).

25. Rollet, A. P., Elkaim, G., Tolédano, P., and Sénè, M., "Les Equilibres Liquide Vapeur Du Systeme Binaire Benzenetoluene," Compt. rend. 242, 2560, (1956).

26. Tamura, F., and Tanasawa, Y., "Evaporation and Combustion of a Drop Contacting with a Hot Surface," Seventh International Symposium on Combustion, 509, Butterworths, (1959).

27. Timmermans, J., "Physico-Chemical Constants of Pure Organic Compounds," Elsevier Publishing Company, Amsterdam, (1950).

28. Timmermans, J., "Physico-Chemical Constants of Binary Systems," Vol. I and II, Interscience Publishers, Inc., New York, (1959).

29. Titani, T., "Viscosity of Benzene Vapor," Bull. Chem. Soc. Japan, 8, 255, (1933).

30. Touloukian, Y. S., (ed.), "Retrieval Guide to Thermophysical Properties Research Literature, Data Book Vol. 2," McGraw-Hill Book Company, Inc., New York, (1960).

31. Vargaftik, N. B., and Smirnova, "Temperature Dependence of the Thermal Conductivity of Water Vapor," Zhuv. Tekh. Friz.26, 1251, (1956), (C. A. 50:16329b).

32. Wachters, L. H. J., Bonne, H., and van Nouhuis, H. J., "The Heat Transfer from a Hot Horizontal Plate to Sessile Water Drops in the Spheroidal State," Chem. Engrg. Sci., 21, 923, (1966).

NOMENCLATURE

A_1	surface area of lower half of drop, cm^2
A_2	surface area of upper half of drop, cm^2
A_{12}, A_{21}	constants in the Van Laar equation
A_p	projected area of drop, cm^2
C_p	heat capacity of vapor, cal/gmole,^oK
D	vapor diffusivity, cm/sec
DT	vapor diffusivity corrected for temperature, cm/sec
f	function of one or more variables, dimensionless
g	gravitational acceleration, dm/sec^2
g_c	conversion factor, 980 gm-cm/dyne,sec^2
ΔH	latent heat of vaporization, cal/gm
K	correction factor for vapor thermal conductivity
k	thermal conductivity of vapor, cal/sec,cm,^oK
k_e	effective thermal conductivity of vapor, cal/sec,cm,^oK
M	molecular weight
P	excess pressure beneath drop, $dyne/cm^2$
P_t	external (atmospheric) pressure on system, $dyne/cm^2$
Q_c	heat transferred by conduction through vapor film between plate and drop, cal/sec
Q_{R1}	heat transferred by radiation from plate to lower half of drop, cal/sec
Q_{R2}	heat transferred by radiation from plate to upper half of drop, cal/sec

QW_1 heat required to support the rate of evaporation from the lower half of the drop, cal/sec

QW_2 heat required to support the rate of evaporation from the upper half of the drop, cal/sec

R gas constant

r radius of drop at any time, cm

T absolute temperature, ^oK

T_p plate temperature, ^oC

T_s saturation temperature of liquid, ^oC

t time variable, sec

u radial vapor velocity beneath drop, cm/sec

$\bar{u}$ mean radial vapor velocity beneath drop, cm/sec

V drop volume, cm^3

V_i, V_{i+1} volume variable in the numerical iteration process, cm^3

VP vapor pressure of liquid, mm Hg

W_1 rate of evaporation from lower half of drop, gm/sec

W_2 rate of evaporation from upper half of drop, gm/sec

x mole fraction in liquid

x' radial space variable beneath drop, cm

y mole fraction in vapor

y' axial space variable beneath drop, cm

Greek Letters

γ activity coefficient, dimensionless

δ vertical distance from some point on lower drop surface to plate, cm

δ_1 vertical distance between bottommost part of drop and plate surface, cm

$\bar{\delta}$ mean vapor film thickness, cm

ϵ_L thermal emissivity of liquid, dimensionless

θ angular variable in drop, radians

θ' dummy angular variable in drop, radians

λ heat of vaporization of saturated liquid, cal/g,

λ' $= \lambda + \frac{T_p - T_s}{2} C_p$, cal/gm

μ viscosity of vapor, g/cm,sec (poise)

ρ_L density of liquid, gm/cm^3

ρ_v density of vapor, gm/cm^3

σ Stefen-Boltzman constant, 1.355×10^{-2} $cal/(^oC)^4 cm^2$

ϕ correlation parameter for gas viscosity and thermal conductivity

Subscripts

1 component 1 in the mixture

2 component 2 in the mixture

mix physical property of a mixture

APPENDIX A

PHYSICAL PROPERTIES OF THE LIQUID SOLUTIONS

PHYSICAL PROPERTIES OF THE LIQUID SOLUTIONS

Although this investigation dealt with binary mixtures, it was necessary to determine the behavior of the four pure substances comprising the mixtures as a basis of comparison. The physical properties of the pure substances as well as the mixtures are therefore required. The experimental data taken from the literature on physical properties are not always accurate or in agreement with other investigations. In many cases, such data as are available for mixtures are questionable; where two or more sets of data exist for the same physical property, they often differ significantly. Whenever the physical properties of the pure and binary liquids are used, the literature reference is noted. A summary of these properties as a function of temperature and composition follow.

Four pure substances and three binary mixtures of these substances were investigated. The pure substances consisted of:

Absolute pure ethyl alcohol-U.S.P.-N.F. U.S. Industrial Chemicals Co., New York, New York.

Benzene and Toluene - 'Baker Analyzed' Reagent to meet A.C.S. Specifications, J. T. Baker Chemical Co., Phillipsburg, N.J.

Distilled water - Soil Mechanics Laboratory of the School of Civil Engineering, Oklahoma State University.

The ehtanol, benzene, and toluene were reagent grade with specified purities of 99.99, 99.99, and 99.98 mole percent, respectively.

The three binary mixtures consisted of:

Ethanol-Water
Ethanol-Benzene
Benzene-Toluene

Because the physical properties of mixtures vary with both temperature and composition it was necessary to obtain the physical properties of the pure substances as a function of temperature and to combine the temperature equations to express the variation of the property with composition. Since in most cases the data are given as point values, it was necessary to curve-fit the data over the appropriate temperature range. This was done with a standard regression analysis program on an IBM 1620 computer. The minimum temperature range required was from 65 to 280°C but in most cases the equations are valid for a much wider range.

Gas Viscosity

1. Ethanol - An equation obtained from the available data is presented in reference (30). Its temperature range is from 16 to 371°C with 1 percent deviation.

$$\mu = 4.0061 \times 10^{-2} + 2.80911 \times 10^{-3} T \qquad \text{(A-1a)}$$

2. Benzene - The data of Craven and Lambert (8) and Titani (29) were curve fitted. Since Titani's data extend only to 312.8°C the viscosity curve was extrapolated to 400°C using, as a guide, the viscosity curve of toluene.

$$\mu = 0.296858 + 5.79322 \times 10^{-4} T + 4.44002 \times 10^{-6} T^2 - 3.36164 \times 10^{-9} T^3 \qquad \text{(A-1b)}$$

3. Toluene - Reference (30) gives the best equation representing the available data as the molecular viscosity equation and the Lennard-Jones (6-12) potential. This is equation (6-14) of reference (24). Since this equation contains the collision integral which varies with temperature, the values of viscosity versus temperature obtained from this equation and tabulated in reference (30) were used for the regression analysis. The equation approximates the available data to within 3 percent and the temperature range is from 90 to 450°C.

$$\mu = -0.113299 + 2.90480 \times 10^{-3} T - 6.63910 \times 10^{-7} T^2 \qquad \text{(A-1c)}$$

4. Water - The equation given in reference (30) is good to 4 percent between 100-345°C and to 10 percent above 345°C.

$$\mu = 0.0965 + 2.9347 \times 10^{-3} T + 9.2109 \times 10^{-7} T^2 - 4.166 \times 10^{-10} T^3 \qquad \text{(A-1d)}$$

5. Mixtures - Wilke's equation (24) for binary gas mixtures was used for the change of viscosity with composition.

$$\mu_{mix} = \frac{\mu_1}{1 + \frac{y_2}{y_1} \phi_{12}} + \frac{\mu_2}{1 + \frac{y_1}{y_2} \phi_{21}} \qquad \text{(A-1e)}$$

Since the values of ϕ_{12} and ϕ_{21} varied only slightly over the required temperature range, they were assumed constant at the average value for the mixture.

1	2	ϕ_{12}	ϕ_{21}
Ethanol-Benzene		1.40	0.71
Ethanol-Water		0.57	1.75
Benzene-Toluene		1.14	0.87

Gas Thermal Conductivity

1. Ethanol - The equation presented in reference (30) was obtained from data to 204°C with a deviation of 2.6 percent. However, this equation was used to calculate values of thermal conductivity for temperatures up to 280°C.

$$k = -5.90902 \times 10^{-5} + 3.73294 \times 10^{-7} T - 1.97544 \times 10^{-10} T^2 \qquad \text{(A-2a)}$$

2. Benzene - The equation as presented in reference (30) was used. It can be used to 204°C with an accuracy of 5 percent and supposedly (30) can be extrapolated to 316°C.

$$k = 3.04565 \times 10^{-5} - 1.94679 \times 10^{-7} T + 5.87783 \times 10^{-10} T^2 \qquad \text{(A-2b)}$$

3. Toluene - Values of thermal conductivity versus temperature representing the smoothed curve of the experimental data were obtained from reference (30) from 71 to 371°C. Since no equation was given this data was curve fitted.

$$k = -3.78630 \times 10^{-5} + 2.21903 \times 10^{-7} T + 4.09677 \times 10^{-11} T^2 \qquad \text{(A-2c)}$$

4. Water - The data listed in Perry [(23), p.3-206] are apparently incorrect. Therefore the data of Keyes and Sandell (17) were used. Their values have been confirmed by Vargaftik and Smirnova (31). The equation applies between 0 and 316°C.

$$k = -8.25437 \times 10^{-6} + 1.58789 \times 10^{-7} T + 3.82579 \times 10^{-11} T^2 \qquad \text{(A-2d)}$$

5. Mixtures - The thermal conductivity of gas mixtures was estimated using the method of Mason and Saxena as presented by Bird et al. [(5), p.258] , since it is analogous to Wilke's equation for viscosity. The same values of $\emptyset_{12}$ and $\emptyset_{21}$ as for viscosity were used.

$$k_{mix} = \frac{k_1}{1 + \frac{y_2}{y_1}\emptyset_{12}} + \frac{k_2}{1 + \frac{y_1}{y_2}\emptyset_{21}} \qquad \text{(A-2e)}$$

Vapor Pressure

The vapor pressure of the pure substances as a function of temperature are needed to calculate the boiling point curves of the mixtures. The boiling point range for the mixtures and therefore the vapor pressure range of the pure components is:

Ethanol-Water	78-100°C
Ethanol-Benzene	67-80°C
Benzene-Toluene	80-110°C
Ethanol	67-100°C
Benzene	67-110°C
Toluene	80-110°C
Water	78-100°C

For these narrow temperature ranges, the data are well approximated by an equation of the form:

$$\log VP = A + \frac{B}{T}$$

The data for ethanol, benzene, and toluene were obtained from the following sources as presented in Timmermans (27):

Ethanol - Merriman (1913); Swietoslowski and Zlotowski (1930).
Benzene - Smith (1941); Willingham, Taylor, Pignocco and Rossini (1945).
Toluene - Willingham, Taylor, Pignocco and Rossini (1945).

The data for water are from Perry [(23), p.3-43] .

Ethanol $\log_{10} VP = 8.87867 - \frac{2107.10}{T}$ (A-3a)

Benzene $\log VP = 7.57876 - \frac{1659.00}{T}$ (A-3b)

Toluene $\log VP = 7.69558 - \frac{1846.56}{T}$ (A-3c)

Water $\log VP = 8.71399 - \frac{2175.60}{T}$ (A-3d)

Heat Capacity of Gases

The heat capacities of the substances studied are [(1), p.350] .

Ethanol $C_p = 0.15173 + 8.6262 \times 10^{-4} T - 2.5887 \times 10^{-7} T^2$ (A-4a)

Benzene $C_p = -5.2362 \times 10^{-3} + 9.9374 \times 10^{-4} T - 3.3836 \times 10^{-7} T^2$ (A-4b)

Toluene $C_p = 6.2620 \times 10^{-3} + 1.0148 \times 10^{-3} T - 3.3895 \times 10^{-7} T^2$ (A-4c)

Water $C_p = 0.40266 + 1.2753 \times 10^{-4} T + 1.5705 \times 10^{-8} T^2$ (A-4d)

Heat capacities at the average temperature can be used in place of the mean heat capacity for short temperature ranges [(16), p.239]. The heat capacity of gas mixtures is additive on a mole basis [(23), p.3-220] .

$$C_{p_{mix}} = y_1 C_{p_1} + y_2 C_{p_2} \quad \text{(A-4e)}$$

Density of Gases

At the conditions studied the reduced pressures are so low that the compressibility factors are unity. Amagat's law of additive volumes may be used. The densities are additive on a mole fraction basis.

$$\rho_{mix} = y_1\rho_1 + y_2\rho_2 \qquad \text{(A-5a)}$$

The densities are calculated from the ideal gas law.

$$\rho_1 = \frac{P_t M_1}{RT} = \frac{M_1}{82.06T} \qquad \text{(A-5b)}$$

$R = 82.06$ cc-atm/^{o}K-gmole
$P_t = 1$ atm
M = molecular weight
ρ = Vapor density, g/cc

Liquid Density at the Mixture Boiling Point

Data could not be found for the liquid densities of the mixtures at their normal boiling point as a function of composition. For density versus weight and mole percent, the weight percent gives less curvature and a more symmetrical curve. Therefore, curves were drawn using the density versus weight composition data at temperatures below the boiling point. Essentially the same smooth curve was drawn between the values of the densities of the pure components at their normal boiling point. These values were then curve-fitted on a density versus mole fraction basis. This procedure was used for the ethanol-water and ethanol-benzene mixtures. Since the densities of pure benzene and pure toluene are close and the values of the density

versus mole percent at 28°C fall almost on a straight line, a linear relationship was assumed for the values of the densities between the pure components.

The pure component densities at the normal boiling point for the pure components are:

Ethanol at 78.3°C - 0.7353 g/cc,	Young (1910) as reported in Timmermans (27).
Benzene at 80.1°C - 0.8145,	Young (1900-10) as reported in Timmermans(27).
Toluene at 110.6°C - 0.7795,	Massart (1936) as reported in Timmermans (27).
Water at 100°C - 0.9584,	Perry [(23), p.3-70].

x_1 x_2

$$\text{EtOH - } H_2O \quad \rho_L = 0.959248 - 1.65489 \times 10^{-1} x_1 - 6.02047 \times 10^{-2} x_1^2 \qquad \text{(A-6a)}$$

$$\text{EtOH - } C_6H_6 \quad \rho_L = 0.814349 - 5.82459 \times 10^{-2} x_1 - 2.01268 \times 10^{-2} x_1^2 \qquad \text{(A-6b)}$$

$$C_6H_6 - C_7H_8 \quad \rho_L = 0.7795 + 3.50 \times 10^{-2} x_1 \qquad \text{(A-6c)}$$

Activity Coefficients

The vapor composition in equilibrium with the liquid mixture is determined from the relative volatility of the system. When the liquid mixture is a non-ideal solution, the relative volatility is corrected by the activity coefficients. There are several equations that represent the activity coefficients as a function of liquid composition. The two-suffix Van Laar equations

$$\log_{10} 1 = \frac{A_{12}}{\left[1 + \frac{A_{12} x_1}{A_{21} x_2}\right]^2} \qquad \text{(A-7a)}$$

$$\log_{10} \gamma_2 = \frac{A_{21}}{\left[1 + \frac{A_{21}\, x_2}{A_{12}\, x_1}\right]^2} \qquad \text{(A-7b)}$$

were chosen since they are simple equations and apply to binary systems, particularly the water-alcohol system (7). These equations apply only at constant temperature and pressure, but can be used in this study because of the small boiling point range of the solutions studied. This assumes that the activity coefficients at the solution boiling point do not vary with temperature over the boiling point range.

Ethanol-Water. Rao (10) used the Van Laar equation to correlate isobaric activity coefficient data. He tabulates the vapor-liquid equilibrium data at 760 mm. The activity coefficients calculated from his equation are given below. Since they are at the normal boiling point, these values were used to determine the constants in the Van Laar equation.

at $x_{EtOH} = 0.0$

$$\log_{10} \gamma_{EtOH} = A_{12} = \log_{10} 5.459; \quad A_{12} = 0.737$$

Ethanol-Benzene. For this system, the Van Laar constants evaluated at the normal boiling point are available in the literature [(23), p.13-7] .

$$A_{12} = 0.845$$

$$A_{21} = 0.699$$

Benzene-Toluene. In many cases this system is assumed ideal. However, its relative volatility varies from 2.29 to 2.68. Rollet

and co-workers (25) experimentally determined the activity coefficients of benzene and toluene. Their results, arranged to apply to Van Laar's equations are:

at $x_{C_6H_6} = 0$ $\gamma_{C_7H_8} = 0.9733$

$$\log_{10} \gamma_1 = A_{12} = \log_{10} 0.9733; \quad A_{12} = -0.0596$$

at $x_{C_7H_8} = 0$ $\gamma_{C_7H_8} = 0.9713$

$$\log_{10} \gamma_2 = A_{21} = \log_{10} 0.9713; \quad A_{21} = -0.0639$$

Diffusivity Coefficient

The liquid evaporated from the upper surface of a drop is calculated assuming pure molecular diffusion (Eq.(3), Chapter V). A bulk diffusivity term, D, appears in this equation. This term was calculated by averaging the diffusivities of the pure components in air according to the equilibrium mole fraction of the diffusing components in the vapor film at the liquid-vapor interface:

$$D = D_1 y_1 + D_2 y_2 \qquad \text{(A-8a)}$$

This bulk diffusivity was temperature corrected (11) by

$$DT = D \left(\frac{Ts}{298}\right)^{1.75} \qquad \text{(A-8b)}$$

where D is the bulk diffusivity at 25°C and DT is the bulk diffusivity at the saturation temperature.

The diffusivities for the pure components in air are listed below as from Reid and Sherwood (24) and Fuller et al. (11).

Ethanol	0.135 cm/sec
Benzene	0.0962
Toluene	0.0860
Water	0.260

Latent Heat of Vaporization

The experimental results of this study indicate that evaporation follows the path of differential, not integral vaporization; the vapor is in equilibrium with the liquid. The differential heat of vaporization must be at the normal boiling point of the solution.

The latent heat of vaporization for dissimilar substances changes rapidly upon initial dilution of one substance with another, but varies little through the middle ranges of concentration. Because of the sharp curvature, it was necessary to divide the latent heat versus composition curve into two sections and curve-fit each section separately. The sections covered the concentration range from 0.0 to 0.2 and from 0.2 to 1.0 mole fraction for the components. Since these equations need not be differentiated, the slopes at the point where the two sections joined were not required to be equal. Latent heat versus mole fraction gave a smoother curve than weight fraction.

The latent heats of vaporization for the pure substances are:

	t^oC	$\triangle H$ cal/gm	Reference
Ethanol	78.4	200.3	(27)
Benzene	80.1	94.14	(27)
Toluene	110.6	86.8	(23)
Water	100.0	538.0	(23)

Ethanol-Water. The latent heat of vaporization versus liquid weight fraction was obtained from Brown (6).

$$x_{EtOH} \quad 0.0 - 0.2 \quad \triangle H = 538.34193 - 5591.0043\, x_1 + 42523.523\, x_1^2 - 104841.10\, x_1^3 \qquad \text{(A-9a)}$$

$$x_{EtOH} \quad 0.2 - 1.0 \quad \triangle H = 308.08822 - 156.59691\, x_1 + 181.57748\, x_1^2 - 132.07630\, x_1^3 \qquad \text{(A-9b)}$$

Ethanol-Benzene. For this system the data of Tyrer (1912) as presented by Timmermans (28) was used. The data are at a pressure of 750 mm Hg. No pressure correction was attempted.

$$x_{EtOH} \quad 0.0 - 0.2 \quad \triangle H = 94.421470 + 336.50380\, x_1 - 2846.6579\, x_1^2 + 9010.158\, x_1^3 \qquad \text{(A-9c)}$$

$$x_{EtOH} \quad 0.2 - 1.0 \quad \triangle H = 82.956700 + 292.27055\, x_1 - 631.25069\, x_1^2 + 456.497\, x_1^3 \qquad \text{(A-9d)}$$

Benzene-Toluene. For ideal solutions Dodge [(9), p.392] suggests the following equation for the latent heat of vaporization:

$$\triangle H_{mix} = \triangle H_1 x_1 + \triangle H_2 x_2 \qquad \text{(A-9e)}$$

Since the benzene-toluene system is nearly ideal with similar values for the latent heats, this simple equation was used:

$$x_{C_6H_6} \quad 0.0 - 0.2 \quad \triangle H = 86.80 + 7.34\, x_1 \qquad \text{(A-9f)}$$

$$x_{C_6H_6} \quad 0.2 - 1.0 \quad \triangle H = 86.80 + 7.34\, x_1 \qquad \text{(A-9g)}$$

APPENDIX B

HYPODERMIC NEEDLE CALIBRATION DATA

HYPODERMIC NEEDLE CALIBRATION DATA

All Liquids At Toom Temperature

Needle Gauge Number	Drop Weight, gms	Drop Volume, cc
	Pure Ethanol	
13	0.01267	0.01607
15	0.01055	0.01339
17	0.00941	0.01194
21	0.00612	0.00777
24	0.00477	0.00605
	57.5 Mole % Ethanol in Water	
13	0.01462	0.01729
15	0.01215	0.01437
17	0.01068	0.01263
21	0.00694	0.00820
24	0.00539	0.00637
	23.8 Mole % Ethanol in Water	
13	0.01576	0.01708
15	0.01264	0.01370
17	0.01184	0.01283
21	0.00804	0.00872
24	0.00616	0.00668
	7.14 Mole % Ethanol in Water	
13	0.01835	0.01888
15	0.01550	0.01595
17	0.01254	0.01290
21	0.01007	0.01036
24	0.00769	0.00792

Needle Gauge Number	Drop Weight, gms	Drop Volume, cc
	Pure Water	
13	0.03236	0.03244
15	0.02647	0.02653
17	0.02073	0.02078
21	0.01547	0.01550
24	0.01134	0.01137
	85.5 Mole % Ethanol in Benzene	
13	0.01266	0.01580
15	0.01058	0.01321
17	0.00928	0.01158
21	0.00607	0.00758
24	0.00464	0.00578
	63.5 Mole % Ethanol in Benzene	
13	0.01379	0.01670
15	0.01132	0.01371
17	0.00997	0.01207
21	0.00645	0.00781
24	0.00491	0.00594
	23.4 Mole % Ethanol in Benzene	
13	0.01533	0.01787
15	0.01285	0.01498
17	0.01127	0.01315
21	0.00722	0.00841
24	0.00558	0.00650
	Pure Benzene	
13	0.01644	0.01882
15	0.01369	0.01567
17	0.01212	0.01387
21	0.00786	0.00900
24	0.00597	0.00684

Needle Gauge Number	Drop Weight, gms	Drop Volume, cc
	83.5 Mole % Benzene in Toluene	
13	0.01627	0.01873
15	0.01361	0.01567
17	0.01203	0.01385
21	0.00778	0.00896
24	0.00589	0.00678
	51.5 Mole % Benzene in Toluene	
13	0.01617	0.01875
15	0.01354	0.01570
17	0.01196	0.01387
21	0.00765	0.00887
24	0.00588	0.00682
	Pure Toluene	
13	0.01609	0.01868
15	0.01344	0.01560
17	0.01189	0.01380
21	0.00767	0.00891
24	0.00580	0.00673

APPENDIX C

DROP TOTAL EVAPORATION TIME DATA

DROP TOTAL EVAPORATION TIME DATA, SECONDS

Drop Mass, gms	Plate Temperature °C									
	Pure Ethanol									
	170.0	172.5*	175.0*	180.0	200.5	225.5	255.0	284.5	344.0	408.5
0.01267	1.8	---	---	46.2	42.2	37.5	33.6	29.0	24.6	20.3
0.01055	1.5	---	43.8	43.4	39.5	35.2	31.1	26.9	22.8	18.6
0.00941	1.2	---	41.7	41.1	37.7	33.3	29.2	25.3	21.3	17.9
0.00612	1.2	35.4	35.8	34.2	31.3	28.3	25.1	21.7	18.0	14.4
0.00477	1.1	32.4	31.9	31.1	28.3	25.0	22.5	18.9	16.4	12.4

	57.5 Mole % Ethanol in Water											
	180.0	200.0*	211.0	221.0	236.0	238.0	251.0	286.0	317.0	346.0	401.0	424.5
0.01462	3.7	65.0	59.8	57.4	54.3	53.4	51.1	45.2	41.5	37.6	33.2	30.5
0.01215	3.2	59.3	55.2	54.3	49.3	49.0	47.8	41.0	38.9	34.7	30.8	28.5
0.01068	2.9	55.1	52.2	50.0	47.2	46.2	45.2	39.7	36.1	32.9	29.2	27.0
0.00694	2.8	46.4	43.4	42.4	39.3	38.9	38.4	32.2	30.4	27.6	24.2	22.4
0.00539	2.8	40.5	39.8	37.4	34.9	34.9	33.7	28.9	26.7	24.4	21.4	20.1

*Leidenfrost Temperature

DROP TOTAL EVAPORATION TIME, SECONDS

Drop Mass, gms	Plate Temperature °C								
	23.8 Mole % Ethanol in Water								
	200	234*	245	265	295	333	354	376	412
0.01576	3.5	77.8	72.9	66.4	58.0	53.9	51.7	---	44.8
0.01264	3.2	71.7	69.6	63.6	56.1	50.6	49.4	45.6	42.5
0.01184	2.9	69.3	65.0	59.9	54.3	47.6	46.1	43.5	40.0
0.00804	2.5	56.7	54.2	50.9	46.1	40.1	38.1	36.0	33.1
0.00616	2.6	51.6	49.7	44.4	40.6	36.1	34.3	32.0	29.7
	7.14 Mole % Ethanol in Water								
	260	301*	326	355	387	415			
0.01835	5.4	77.0	73.5	63.8	59.6	55.4			
0.01550	5.2	74.0	70.7	58.9	54.8	51.7			
0.01254	4.8	68.0	67.3	55.0	50.6	46.0			
0.01007	4.9	54.3	52.2	44.0	40.2	37.3			
0.00769	4.6	51.0	48.1	39.8	35.0	32.0			

* Leidenfrost Temperature

DROP TOTAL EVAPORATION TIME, SECONDS

Drop Mass, gms	Plate Temperature °C					
	Pure Water					
	200	280	320*	360	407	455
0.03236	2.7	52.7	99.4	89.0	77.3	71.6
0.02647	2.1	49.7	90.0	80.8	69.4	64.7
0.02073	1.9	45.7	84.0	74.6	64.8	60.7
0.01547	1.7	49.2	69.8	62.6	54.3	50.4

	85.5 Mole % Ethanol in Benzene								
	175	180*	200	240	280	320	360	400	450
0.01266	1.7	43.5	41.4	34.8	30.4	26.5	22.4	19.3	16.3
0.01058	1.2	41.7	38.1	33.1	28.8	24.6	21.0	18.2	15.2
0.00928	0.9	39.5	36.1	31.7	27.4	23.2	20.4	17.4	14.3
0.00607	1.1	32.9	30.0	25.9	22.4	19.1	16.9	14.7	11.8
0.00464	0.8	29.5	27.0	23.8	19.7	17.5	15.3	13.3	10.5

* Leidenfrost Temperature

DROP TOTAL EVAPORATION TIME, SECONDS

Drop Mass, gms	Plate Temperature °C								
63.5 Mole % Ethanol in Benzene									
	175	180*	200	240	280	320	360	400	450
0.01379	1.3	41.7	38.5	33.1	28.5	23.2	20.1	18.5	15.4
0.01132	1.1	38.9	35.3	31.2	26.6	21.6	18.2	16.8	14.6
0.00997	0.8	36.5	33.7	29.0	25.1	20.4	17.6	15.8	13.4
0.00645	0.7	31.0	28.2	24.2	21.1	17.4	14.6	13.5	11.5
0.00491	0.5	27.5	25.3	21.6	17.7	15.8	13.4	12.4	9.6
23.4 Mole % Ethanol in Benzene									
	175	180*	200	240	280	320	360	400	450
0.01533	1.7	33.8	30.1	26.4	21.9	19.4	17.4	15.2	13.3
0.01285	1.8	31.8	27.7	25.4	20.5	17.8	16.2	14.1	12.2
0.01127	1.2	30.2	25.5	23.2	19.0	16.9	15.3	13.2	11.5
0.00722	1.0	25.9	23.5	19.6	17.1	14.1	12.3	11.2	9.7
0.00558	0.8	23.0	20.7	17.5	14.7	12.8	11.4	9.6	8.0

* Leidenfrost Temperature

DROP TOTAL EVAPORATION TIME, SECONDS

Drop Mass, gms	Plate Temperature °C								
	Pure Benzene								
	175	180*	200	240	280	320	360	400	450
0.01644	1.8	34.0	29.4	25.0	21.4	18.1	16.2	14.4	12.9
0.01369	1.5	31.7	27.7	23.5	20.6	17.4	14.8	13.4	11.5
0.01212	1.1	27.8	26.3	22.2	19.0	15.8	13.7	12.0	10.8
0.00786	1.0	24.1	22.1	18.3	15.5	13.2	12.0	10.3	8.6
0.00597	0.6	22.2	21.1	17.0	14.0	12.0	10.3	9.2	7.6
	51.5 Mole % Benzene in Toluene								
	195	202*	240	280	320	360	400	450	
0.01617	1.2	27.0	26.1	22.1	19.2	17.0	14.8	12.6	
0.01354	1.0	26.9	24.4	20.9	18.0	15.5	13.6	11.5	
0.01196	0.8	26.5	22.8	19.4	16.9	14.4	12.4	10.8	
0.00765	0.9	22.3	19.6	17.3	14.3	12.4	10.5	8.9	
0.00588	0.7	20.7	17.5	15.1	13.1	11.3	9.3	7.8	

* Leidenfrost Temperature

DROP TOTAL EVAPORATION TIME, SECONDS

Drop Mass, gms	Plate Temperature °C							
	Pure Toluene							
	205	210*	240	280	320	360	400	450
0.01609	1.3	28.1	25.4	21.9	18.1	16.7	14.2	12.0
0.01344	---	---	24.1	20.4	17.2	14.8	13.2	11.6
0.01189	---	---	22.5	19.1	16.3	14.4	12.4	10.5
0.00767	---	---	19.1	16.1	14.1	12.4	10.3	8.5
0.00580	0.7	19.4	17.4	14.9	12.6	11.5	9.0	7.4

83.5 Mole % Benzene in Toluene

	240
0.01627	26.7
0.01361	25.5
0.01203	23.3
0.00778	19.8
0.00589	17.7

* Leidenfrost Temperature

APPENDIX D

EXTENDED MASS TOTAL EVAPORATION TIME DATA

EXTENDED MASS TOTAL EVAPORATION TIME DATA, SECONDS

Mass, gms	Plate Temperature °C						
	Pure Ethanol						
	160	175	200	250	300	375	450
6.28	14.0	396.7(205)*	349.8(190)	270.8(148)	214.0(120)	161.0(88)	126.9(69)
2.36	11.8	298.2(112)	267.9(108)	215.1(91)	169.1(72)	127.4(55)	101.0(44)
0.788	8.7	211.7(27)	193.5(38)	152.8(28)	123.5(28)	95.4(25)	79.6(20)
0.394	6.3	165.2	152.0	121.9	101.4	77.8(7)	64.8(10)
0.0788	2.0	91.7	80.4	68.5	55.8	45.5	36.4
	85.5 Mole % Ethanol in Benzene						
	160	180	200	250	300	375	450
6.41	21.2	353.2(178)	344.1(186)	268.5(142)	210.4(103)	155.0(84)	124.5(66)
2.40	12.6	287.1(105)	261.4(97)	206.6(83)	162.2(70)	122.3(52)	100.4(42)
0.801	6.2	204.5(35)	190.1(31)	149.6(29)	115.1(25)	94.0(23)	75.2(20)
0.401	6.5	----	144.8	118.7	97.3	75.9(7)	62.7(10)
0.0801	2.7	----	79.8	67.2	55.2	43.5	35.5

* Numbers in parentheses are length of time in seconds that bubble breakthrough occurs

EXTENDED MASS TOTAL EVAPORATION TIME, SECONDS

Mass, gms	Plate Temperature ^{o}C						
	160	180	200	250	300	375	450
			63.5 Mole % Ethanol in Benzene				
6.61	17.5	335.1(180)*	318.7(164)	250.4(128)	200.3(100)	142.6(76)	116.9(59)
2.48	12.1	261.7(95)	247.8(92)	193.2(75)	150.3(58)	115.5(46)	93.9(37)
0.826	9.9	193.5(30)	173.8(27)	138.6(27)	110.5(18)	88.7(22)	71.6(16)
0.413	5.6	141.9	134.1	111.2	90.3	71.7(7)	57.8(6)
0.0826	3.9	90.0	75.2	62.6	49.4	39.9	33.3
			23.4 Mole % Ethanol in Benzene				
6.86	17.6	268.1(140)	255.0(138)	190.7(106)	149.0(82)	114.6(64)	94.2(53)
2.57	13.7	211.0(77)	192.8(77)	147.8(68)	118.6(51)	90.2(39)	76.2(33)
0.858	7.0	152.4(26)	136.8(22)	108.0(23)	87.8(20)	70.3(19)	57.2(14)
0.429	5.3	111.8	102.9	86.8	70.7	56.2	46.7(6)
0.0858	3.3	62.1	56.9	48.0	40.7	33.2	26.7

* Numbers in parentheses are length of time in seconds that bubble breakthrough occurs

EXTENDED MASS TOTAL EVAPORATION TIME, SECONDS

Mass, gms	Plate Temperature °C						
	Pure Benzene						
	160	180	200	250	300	375	450
6.99	19.2	266.7(136)*	239.4(131)	190.0(105)	145.7(80)	113.0(60)	92.5(49)
2.62	13.6	195.1(72)	181.5(69)	143.1(63)	116.2(52)	89.8(39)	75.1(31)
0.874	9.1	137.2(13)	132.5(20)	103.9(18)	86.7(22)	67.9(17)	55.8(14)
0.437	7.7	104.8	99.6	85.3	69.3	55.7	45.9(5)
0.0874	3.8	63.4	55.6	47.7	39.4	32.5	26.5
	Pure Water						
	230	264	300	400			
3.99	28.6	829.0(130)	712.2(145)	535.2(140)			
2.00	22.5	631.7	557.8(4)	446.7(30)			
0.998	12.1	470.6	424.2	351.0			

* Numbers in parentheses are length of time in seconds that bubble breakthrough occurs

EXTENDED MASS TOTAL EVAPORATION TIME, SECONDS

Plate Temperature 240°C

Mass, gms	Time	Bubble Breakthrough
	83.5 Mole % Benzene in Toluene	
6.95	198.2	114
2.61	155.2	67
0.868	114.3	28
0.434	86.3	
0.0868	49.3	
	51.5 Mole % Benzene in Toluene	
6.90	192.8	112
2.59	153.9	71
0.862	114.0	29
0.431	87.2	
0.0862	48.6	
	Pure Toluene	
6.89	192.2	110
2.59	144.0	66
0.862	111.9	30
0.431	85.5	
0.0862	48.2	

APPENDIX E

CHANGE IN LIQUID COMPOSITION

DURING EVAPORATION DATA

CHANGE IN LIQUID COMPOSITION DURING EVAPORATION DATA

Plate Temperature 240°C

Liquid Mass, gms	Evaporation Time, Sec	Composition Mole Fraction	Mass Fraction Evaporated
	Ethanol in Benzene		
0.413	0	0.635	0.0
0.234	20	0.70	0.433
0.120	40	0.82	0.709
0.0525	60	0.92	0.873
0.0158	80	0.99	0.962
0.0128	83	1.0	0.969
0.0	115.5	-	1.0
0.0826	0	0.635	0.0
0.0528	10	0.72	0.361
0.0301	20	0.80	0.636
0.0158	30	0.90	0.809
0.0073	40	0.99	0.912
0.0026	50	1.0	0.970
0.0	65	-	1.0
0.01379	0	0.635	0.0
0.00880	5	0.75	0.362
0.00585	10	0.81	0.576
0.00345	15	0.91	0.750
0.00175	20	0.99	0.873
0.0	32.7	-	1.0
	Benzene in Toluene		
2.61	0	0.835	0.0
1.27	30	0.70	0.513
0.480	60	0.51	0.816
0.245	80	0.44	0.906
0.105	100	0.36	0.960
0.0275	120	0.10	0.990
0.0093	140	0.0	0.996
0.0	153	-	1.0

COMPOSITION CHANGE DURING EVAPORATION

Plate Temperature 240°C

Liquid Mass, gms	Evaporation Time, Sec	Composition Mole Fraction	Mass Fraction Evaporated
	Benzene in Toluene		
0.482	0	0.835	0.0
0.348	10	0.815	0.278
0.235	20	0.68	0.512
0.0880	40	0.51	0.817
0.0212	60	0.37	0.956
0.00780	70	0.18	0.984
0.00178	80	0.03	0.996
0.0	90	-	1.0
0.0868	0	0.835	0.0
0.0630	5	0.79	0.274
0.0440	10	0.77	0.493
0.0205	20	0.66	0.763
0.0072	30	0.38	0.917
0.0015	40	0.11	0.983
0.0	49.3	-	1.0
0.01627	0	0.835	0.0
0.00950	5	0.81	0.416
0.00520	10	0.68	0.680
0.00240	15	0.55	0.852
0.00077	20	0.17	0.950
0.0	26.7	-	1.0
0.431	0	0.515	0.0
0.215	20	0.40	0.501
0.0780	40	0.23	0.819
0.0180	60	0.09	0.958
0.0057	70	0.0	0.987
0.0	87.2	-	1.0

COMPOSITION CHANGE DURING EVAPORATION

Plate Temperature 240°C

Liquid Mass, gms	Evaporation Time, Sec	Composition Mole Fraction	Mass Fraction Evaporated
	Benzene in Toluene		
0.0862	0	0.515	0.0
0.0600	6	0.40	0.304
0.0460	10	0.36	0.466
0.0205	20	0.22	0.762
0.0065	30	0.09	0.923
0.0010	40	0.01	0.988
0.0	48.6	-	1.0
0.01617	0	0.515	0.0
0.00950	5	0.45	0.412
0.00480	10	0.22	0.703
0.00192	15	0.10	0.881
0.00114	18	0.04	0.938
0.00090	19	0.03	0.944
0.0	26.1	-	1.0

APPENDIX F

FORTRAN PROGRAM AND SAMPLE PRINTOUT

```
    PROGRAM LEIDEN
    LEIDENFROST PHENOMENON FOR BINARY LIQUID SOLUTIONS     12/15/65
1010FORMAT(15X,18HINITIAL CONDITIONS,3X,3HVO=E15.8,2X,3HXO=F7.4,2X,4 H
   4MW1=F7.2,2X,4HMW2=F7.2,2X,3HTP=F8.2)
1020FORMAT(33X,6HDELAT=F6.2,2X,6HDELTT=F5.2,2X,6HVCONV=F10.7,2X, 6HXCO
   4NV=F6.3///)
1030FORMAT(5X,2HW1,10X,2HW2,9X,3HQR1,9X,3HQR2,10X,2HQC,8X,5HDELTA,7X,5
   4HAVDEL,8X,3HQW1,9X,3HQW2,9X,4HRADK/)
1040FORMAT(10X,16HVOLUME INCERMENT,I3,2X,2HV=,E15.8,2X,3HX1=,F7.4,2X ,
   43HY1=,F7.4,2X,3HTS=,F8.2,2X,3HTV=,F8.2,2X,5HTIME=,F8.2/)
1050FORMAT(4X,13HK CONVERGENCE,3X,2HI=,I3,2X,3HZ1=,E12.5,2X,5HRADK=, F
   47.4)
1060FORMAT(4X,15HVOL CONVERGENCE,3X,2HJ=,I3,2X,3HZ2=,E12.5,2X,2HV=, E1
   42.5,2X,3HV2=,E12.5,2X,3HV3=,E12.5//////)
1070FORMAT(6X,16HFINAL CONDITIONS,3X,2HV=,E15.8,2X,3HX1=,E13.6,2X, 3HY
   41=,E13.6,2X,5HTIME=,F8.2,2X,6HDELAT=,F6.2)
108 FORMAT(10E12.5)
109 FORMAT(10E12.5/)
 10 CONTINUE
    READ 0,V0,X0,WMW1,WMW2,TP,DELAT,DELTT,VCONV,XCONV
    READ 0,EPSL,GAMA,GAMB,PH1,PH2,RHOLA,RHOLB,RHOLC
    READ 0,VP1A,VP1B,VP2A,VP2B,VIS1A,VIS1B
    READ 0,VIS1C,VIS1D,VIS2A,VIS2B,VIS2C,VIS2D
    READ 0,CON1A,CON1B,CON1C,CON2A,CON2B,CON2C
    READ 0,VAPHA,VAPHB,VAPHC,VAPHD,VAPHE,VAPHF
    READ 0,CP1A,CP1B,CP1C,CP2A,CP2B,CP2C
    READ 0,VAPHG,VAPHH,D1,D2
    PRINT 101,V0,X0,WMW1,WMW2,TP
    PRINT 102,DELAT,DELTT,VCONV,XCONV
    PRINT 103
    V=V0
    V1=V0
    X1=X0
    X2=1.-X1
    K=1
    TIME=0.
    RADK=0.
    INCR=0
    DELLT=DELAT
    I=0
    TS=340.
 20 L=1
    J=0
    IF(X2)122,122,111
111 AGAM1=GAMA/(1.0+GAMA*X1/(GAMB*X2))**2
    GO TO 114
112 AGAM1=0.
    GO TO 114
114 IF(X1)116,116,115
115 AGAM2=GAMB/(1.0+GAMB*X2/(GAMA*X1))**2
    GO TO 118
```

```
116 AGAM2=0.
118 IF(AGAM1)22,25,25
 22 AGAM1=-AGAM1
    GAM1=10.0**AGAM1
    GAM1=1.0/GAM1
    GO TO 26
 25 GAM1=10.0**AGAM1
 26 IF(AGAM2)177,27,27
177 AGAM2=-AGAM2
    GAM2=10.0**AGAM2
    GAM2=1.0/GAM2
    GO TO 29
 27 GAM2=10.0**AGAM2
 29 T=TS/100.
 21 AVP1=VP1A+VP1B/T
    AVP2=VP2A+VP2B/T
    VP1=10.0**AVP1
    VP2=10.0**AVP2
    TOTL=0.
    TOTL=GAM1*VP1*X1+GAM2*VP2*X2
    ERROR=760.0-TOTL
    IF(ABS(ERROR)-0.1)24,174,174
174 T=(1.0+ERROR/6000.0)*T
    GO TO 21
 24 TS=T*100.0
    Y1=GAM1*VP1*X1/TOTL
    Y2=1.0-Y1
    TV=(TS+TP)/2.0
    VISC1=VIS1A+(VIS1B+(VIS1C+VIS1D*TV)*TV)*TV
    VISC2=VIS2A+(VIS2B+(VIS2C+VIS2D*TV)*TV)*TV
    COND1=CON1A+(CON1B+CON1C*TV)*TV
    COND2=CON2A+(CON2B+CON2C*TV)*TV
    IF(Y1)122,122,172
172 IF(Y2)124,124,175
175 VISC=(VISC1/(1.0+Y2/Y1*PH1)+VISC2/(1.0+Y1/Y2*PH2))*0.0001
    COND=(COND1/(1.0+Y2/Y1*PH1)+COND2/(1.0+Y1/Y2*PH2))*0.00001
    GO TO 126
122 VISC=VISC2*0.0001
    COND=COND2*0.00001
    GO TO 126
124 VISC=VISC1*0.0001
    COND=COND1*0.00001
126 CP1=CP1A+(CP1B+CP1C*TV)*TV
    CP2=CP2A+(CP2B+CP2C*TV)*TV
    CP=Y1*CP1+Y2*CP2
    RHOV1=WMW1/(82.06*TV)
    RHOV2=WMW2/(82.06*TV)
    RHOV=Y1*RHOV1+Y2*RHOV2
    RHOL=RHOLA+(RHOLB+RHOLC*X1)*X1
    IF(X1-0.2)178,28,28
178 VAPH=VAPHA+(VAPHB+(VAPHC+VAPHD*X1)*X1)*X1
```

```
    GO TO 23
 28 VAPH=VAPHE+(VAPHF+(VAPHG+VAPHH*X1)*X1)*X1
 23 WMW=WMW1*Y1+WMW2*Y2
    CPP=VAPH+(TV-TS)*CP
    D=D1*Y1+D2*Y2
    DF=D*(TS/298.0)**1.75
    EMB1=18.0*VISC*COND*(TP-TS)/(980.0*RHOV*((RHOL-RHOV)*CPP))
    EW2=WMW*DF/(82.06*TS)
    BOLZ=1.355*((TP/1000.0)**4-(TS/1000.0)**4)
    EQR1=BOLZ/(1.0/0.682+1.0/EPSL-1.0)
    EQR2=BOLZ/(1.0/0.318+1.0/EPSL-1.0)
    PRINT 104,INCR,V,X1,Y1,TS,TV,TIME
 30 IF(V1)60,60,130
130 R=(.23873241*V1)**.33333333
    A=12.566371*R**2
    W2=EW2*(0.5*A)/R
    QW2=W2*VAPH
    QR1=EQR1*0.5*A
 37 S33=R**3/(EMB1*(1.0+RADK))
    S3=ALOG(S33)
    THIK=-1.383204+S3*(S3*(0.0003547*S3-0.010403)-0.398007)
    IF(THIK+4.9627)133,133,33
133 S1=-0.8321+0.97464*(-THIK)
    GO TO 34
 33 S1=0.3874+THIK*(THIK*(0.0087*THIK+0.1328)-0.2835)
 34 W1=6.283185*COND*(TP-TS)*(1.0+RADK)*(R*S1)/CPP
    QW1=W1*CPP
    QR2=EQR2*0.5*A
    DELTA=EXP(THIK)*R
    AVDEL=1.0/(2.0*(DELTA+R)/R**2*ALOG((DELTA+R)/DELTA)-2.0/R)
    QC=COND*(TP-TS)*A/(4.0*AVDEL)
    GO TO (31,35),K
 31 K=2
    RADK=QR1/QC
    WAIT0=V0*RHOL
    WAIT3=WAIT0
    GO TO 37
 35 Q1=QR1+QR2+QC
    Q2=QW1+QW2
    Z1=ABS((Q2-Q1)/Q2)
    IF(Z1-0.01)40,40,140
140 I=I+1
    IF(I-30)141,141,39
141 RADNK=((Q1+Q2)/2.0-QW2)/QC-1.0
    IF(RADNK)171,71,71
171 RADNK=0.
 71 RADVK=(RADK+RADNK)/(2.0*RADK)
    IF(RADVK-1.)182,72,72
182 RADK=RADK*(1.0-RADVK/100.0)
    GO TO 73
```

```
 72 RADK=RADK*(1.0+RADVK/100.0)
 73 EQR2=QW2/(0.5*A)
    GO TO 37
 39 PRINT 105,I,Z1,RADK
 40 GO TO (51,41),L
 51 WAIT=V*RHOL
    RATE=(WAIT3-WAIT)/DELLT
    WTFR=(WAIT0-WAIT)/WAIT0
  1 PRINT 109,W1,W2,QR1,QR2,QC,DELTA,AVDEL,QW1,QW2,RADK
    PRINT 108,WAIT,WTFR,R,A,VP1,VP2,RATE
  3 PRINT 109,VISC,COND,CP,RHOV,RHOL,VAPH,DF,GAM1,GAM2
 41 L=2
    I=0
    IF(J-1)47,42,43
 47 FUN1=(W1+W2)/RHOL
    V2=V-DELAT*FUN1
    J=J+1
    V1=V2
    GO TO 30
 42 FUN2=(W1+W2)/RHOL
    V2=V-DELAT*FUN2
    J=J+1
    V1=V2
    GO TO 30
 43 FUN3=(W1+W2)/RHOL
    V3=V-0.5*DELAT*(FUN2+FUN3)
    Z2=ABS((ABS(V3)-ABS(V2))/ABS(V3))
    IF(Z2-VCONV)45,45,143
143 J=J+1
    IF(J-30)44,44,144
144 PRINT 106,J,Z2,V,V2,V3
    GO TO 45
 44 V2=V3
    V1=V3
    GO TO 30
 45 IF(V3)60,60,160
160 WAIT3=WAIT
    DELLT=DELAT
    TIME=TIME+DELAT
    WY1=Y1*WMW1/(Y1*WMW1+Y2*WMW2)
    DELV=V-V3
    RHOLV=RHOLA+(RHOLB+RHOLC*Y1)*Y1
    WTV1=RHOLV*DELV*WY1
    WTV2=RHOLV*DELV-WTV1
    WX1=X1*WMW1/(X1*WMW1+X2*WMW2)
    WTL1=RHOL*V*WX1
    WTL2=RHOL*V-WTL1
    RWTL1=WTL1-WTV1
    RWTL2=WTL2-WTV2
    RX1=RWTL1/WMW1/(RWTL1/WMW1+RWTL2/WMW2)
    DELX=ABS(X1-RX1)
```

```
    DELX=ABS(X1-RX1)
    IF(DELX-XCONV)54,54,162
162 IF(DELAT-DELTT)54,54,164
164 DELAT=DELAT/2.
 54 X1=RX1
    IF(X1-0.0001)55,155,155
155 IF(X1-0.9999)156,156,56
156 GO TO 57
 55 X1=0.
    GO TO 57
 56 X1=1.
 57 X2=1.0-X1
    INCR=INCR+1
    V=V3
    V1=V3
    GO TO 20
 60 PRINT 107,V1,X1,Y1,TIME,DELAT
    GO TO 10
    END
```

SAMPLE PRINTOUT FOR COMPUTER PROGRAM*

INITIAL CONDITIONS VO= 0.59410000E-02 XO= 0.6350 MW1= 46.07 MW2= 78.11 TP= 473.0
DELAT= 1.00 DELTT= 0.10 XCONV= 0.050

W1	W2	QR1	QR2	QC
QW1	QW2	DELTA	AVDEL	RADK

VOLUME INCREMENT 0 V= .005941 X1= 0.6350 Y1= 0.4940 TS= 340.14 TV= 531.57 TIME= 0.0

.5302E-03	.2290E-03	.1904E-01	.2998E-01	.9972E-01
.1183E-00	.2998E-01	.6880E-03	.1359E-01	.1859

VOLUME INCREMENT 1 V= .005023 X1= 0.6589 Y1= 0.5012 TS= 340.26 TV= 531.63 TIME= 1.0

.4871E-03	.2163E-03	.1703E-01	.2857E-01	.9240E-01
.1093E-00	.2857E-01	.7064E-03	.1310E-01	.1828

VOLUME INCREMENT 2 V= .004178 X1= 0.6883 Y1= 0.5118 TS= 340.44 TV= 531.72 TIME= 2.0

.4422E-03	.2031E-03	.1506E-01	.2721E-01	.8493E-01
.1001E-00	.2721E-01	.7270E-03	.1259E-01	.1798

FINAL CONDITIONS V= -.416053E-05 X1= .100000E 01 Y1= .100000E 01 TIME= 11.0

* See Nomenclature for definition of symbols. Additional symbols are: RADK - K; DELTA - δ; AVDEL - $\bar{\delta}$; TV - $1/2(T_p + T_s)$, °K; DELAT - initial size of time increment, sec; DELTT - lower limit of size of time increment; XCONV - maximum allowable change in liquid composition during any time increment.

VITA

Edward S. Godleski

Candidate for the Degree of

Doctor of Philosophy

Thesis: THE LEIDENFROST PHENOMENON FOR BINARY LIQUID SOLUTIONS

Major Field: Chemical Engineering

Biographical:

Personal Data: Born in Passaic, New Jersey, November, 16, 1936, the son of Stanley E. and Elsie Borant Godleski.

Education: Attended public school in Lodi, New Jersey; graduated from Lodi High School in 1954; received the Bachelor of Science in Chemical Engineering degree from Lehigh University in June, 1958; received the Master of Science degree from Cornell University in February, 1961, with a major in Chemical Engineering and a minor in Physical Chemistry; completed requirements for the Doctor of Philosophy degree in May, 1967.

Professional Experience: Served as a research assistant in the summer of 1960 working on the Cornell Process for Saline Water Conversion; joined the staff of the Chemical Engineering Department of the Cleveland State University (then called Fenn College) as an instructor, January, 1961; took a two year leave of absence to pursue graduate work in September, 1962; was promoted to the rank of Assistant Professor, September, 1964.